LOAN DOCUMENT

PHOTOGRAPH THIS SHEET

DTIC ACCESSION NUMBER

LEVEL

INVENTORY 1

291 - 1995

DOCUMENT IDENTIFICATION

sep 1995

DISTRIBUTION STATEMENT A

Approved for public release;
Distribution Unlimited

DISTRIBUTION STATEMENT

ACCESSION FOR

NTIS GRA&I ☒

DTIC TRAC ☐

UNANNOUNCED

JUSTIFICATION

BY

DISTRIBUTION/

AVAILABILITY CODES

DISTRIBUTION	AVAILABILITY AND/OR SPECIAL
A-1	

DISTRIBUTION STAMP

DATE ACCESSIONED

DATE RETURNED

19980731 117

DATE RECEIVED IN DTIC

REGISTERED OR CERTIFIED NUMBER

PHOTOGRAPH THIS SHEET AND RETURN TO DTIC-FDAC

DTIC FORM 70A JUN 90

DOCUMENT PROCESSING SHEET

PREVIOUS EDITIONS MAY BE USED UNTIL STOCK IS EXHAUSTED.

LOAN DOCUMENT

HANDLE WITH CARE

STRATEGIC ENVIRONMENTAL RESEARCH AND DEVELOPMENT PROGRAM

PROJECT TITLE: IN SITU IMMOBILIZATION OF HEAVY METALS IN APATITE MINERAL FORMULATIONS

MILESTONE FIVE REPORT: SEPTEMBER 1995

APATITE MINERAL FORMULATIONS AND EMPLACEMENT OPTIONS

PACIFIC NORTHWEST LABORATORY

Judith V. Wright, Ph.D., Staff Scientist, PNL
Loni M. Peurrung, Ph.D., Research Engineer, PNL
T.E. Moody, Ph.D., Science Specialist, Bechtel Hanford, Inc.
James L. Conca, Ph.D., Associate Scientist, WSU Tri-Cities
Xiaobing Chen, Ph.D., AWU-NW Postdoctoral Fellow, PNL
Paul P. Didzerekis, AWU-NW Research Assistant, PNL
Eric Wyse, M.S., Senior Research Scientist, PNL

REPORT DOCUMENTATION PAGE

Form Approved
OMB No. 074-0188

1. AGENCY USE ONLY (Leave blank)	2. REPORT DATE	3. REPORT TYPE AND DATES COVERED
	September 1995	Milestone Five Report, September 1995

4. TITLE AND SUBTITLE
In Situ Immobilization of Heavy Metals in Apatite Mineral Formulations

5. FUNDING NUMBERS
N/A

6. AUTHOR(S)
Judith V. Wright, Loni M. Peurrung, T.E. Moody, James L. Conca, Xiaobing Chen, Paul P. Didzerekis, and Eric Wyse.

7. PERFORMING ORGANIZATION NAME(S) AND ADDRESS(ES)
Pacific Northwest Laboratory
Richland, WA

8. PERFORMING ORGANIZATION REPORT NUMBER
N/A

9. SPONSORING / MONITORING AGENCY NAME(S) AND ADDRESS(ES)
SERDP
901 North Stuart St. Suite 303
Arlington, VA 22203

10. SPONSORING / MONITORING AGENCY REPORT NUMBER
N/A

11. SUPPLEMENTARY NOTES
This work was supported in part by SERDP.

12a. DISTRIBUTION / AVAILABILITY STATEMENT
Approved for public release: distribution is unlimited

12b. DISTRIBUTION CODE
A

13. ABSTRACT ***(Maximum 200 Words)***

The sorption and selectivity of aqueous Pb, Cd, and Zn onto a mineral apatite from North Carolina were investigated in relation to a wide range of pH. The heavy metals were applied as single species and multiple species. The sorption of aqueous Pb was primarily through a process of the dissolution of apatite followed by the precipitation of variable pyromorphite-type minerals. Hydrocerussite [$Pb_3(CO_3)_2(OH)_2$ or $Pb(OH)_2 \cdot 2PbCO_3$] and lead oxide fluoride (Pb_2OF_2) formed only under extremely alkaline condition.

14. SUBJECT TERMS
apatite mineral formulation, heavy metals, North Carolina, pyromorphite-type minerals, Hydrocerussite, lead oxide fluoride, SERDP

15. NUMBER OF PAGES
154

16. PRICE CODE
N/A

17. SECURITY CLASSIFICATION OF REPORT	18. SECURITY CLASSIFICATION OF THIS PAGE	19. SECURITY CLASSIFICATION OF ABSTRACT	20. LIMITATION OF ABSTRACT
unclass	unclass	unclass	UL

NSN 7540-01-280-5500

Standard Form 298 (Rev. 2-89)
Prescribed by ANSI Std. Z39-18
298-102

TABLE OF CONTENTS

EXECUTIVE SUMMARY

The objective of this project is to demonstrate that the incorporation of reactive phosphate materials into contaminated soils stabilizes lead and other heavy metals, preventing leaching into the groundwater. Phosphatic solids, solutions, and slurries react with lead and other heavy metals in contaminated soils and groundwater and cause the precipitation of metal-substituted apatite minerals. Heavy metals sequestered in apatites have great durability and leach resistance that significantly exceeds other chemically stabilized waste forms because the apatite mineral structure is very stable over a wide range of environmental conditions for geologically-long time periods. The results of this project and of previous work by the authors demonstrate that stabilization of contaminated soils and groundwater by apatite has the potential to be an extremely successful and widely applicable remediation strategy for heavy metals and radionuclides.

In the Milestone One Report, we reported the characteristics of various lead-contaminated soils, phosphate-containing materials, and groundwaters to be used in this project, including samples from Keesler Air Force Base, the demonstration site originally intended for this technology, and the Bunker Hill Mining District of Idaho. Lead concentrations in the Keesler samples were found to be relatively low, with soil levels at roughly 100 mg kg^{-1} (ppm) and groundwater in the μg kg^{-1} (ppb) range. Bunker Hill mine tailings and soils contain 1000-4000 mg kg^{-1} (ppm) lead. These soils were selected for subsequent project work.

The Milestone Two Report established the baseline leaching rates of metals from untreated Bunker Hill soils and included some studies of Keesler AFB soils. Without the addition of phosphate, metal concentrations in the leachates from the Bunker Hill soils were in the mg kg^{-1} (ppm) range, well in excess of EPA standards.

The Milestone Three Report showed that in flow-through experiments, the addition of small amounts of a North Carolina apatite to soils reduces the leachate concentrations of lead and other heavy metals to less than 1 μg kg^{-1} (ppb), the detection limit of our analytical tools. Leaching of lead was reduced by three orders of magnitude or more, resulting in leachate samples well below the EPA drinking water standard for lead. Similar results were obtained for cadmium and zinc.

In Milestone Four, adsorption isotherm experiments using varying amounts of different apatites and a 10:1 water to soil ratio were used in combination with a thermodynamic model to determine the amount of apatite necessary to treat a given soil. These experiments suggested that soils may be remediated by extrapolating from the isotherm experiments, which equates to 10-50 kg of apatite per treated ton of soil, or less than 1% by weight. By comparison, grouting techniques can require as much as 30% to 50% by weight, depending upon the porosity of the soil. The Milestone Four report also evaluated various apatite formulations that could be used in the field for

treating contaminated soils. As part of the project, we have tested chemically synthesized and biogenic apatite, mined apatite from deposits in Florida and North Carolina, and the effect of grinding the apatite from a coarse sand consistency to a fine powder. We have treated soils in the laboratory simply by adding dry apatite material to them; however, field emplacement may require the use of solutions or slurries. The report discussed the physical properties of apatite that are relevant to emplacement, including data on the flow characteristics of apatite slurries. Several candidate emplacement strategies, their applicability, and their advantages and disadvantages were also discussed. Finally, treatment costs were estimated for various emplacement scenarios.

In this milestone report, the sorption and selectivity of aqueous Pb, Cd, and Zn onto a mineral apatite from North Carolina were investigated in relation to a wide range of pH. The heavy metals were applied as single species and multiple species. The sorption of aqueous Pb was primarily through a process of the dissolution of apatite followed by the precipitation of variable pyromorphite-type minerals. Hydrocerussite [$Pb_3(CO_3)_2(OH)_2$ or $Pb(OH)_2 \cdot 2PbCO_3$] and lead oxide fluoride (Pb_2OF_2) formed only under extremely alkaline condition. Otavite ($CdCO_3$) and cadmium hydroxide [$Cd(OH)_2$], and zincite (ZnO) were formed in the Cd or Zn system, respectively, especially under alkaline conditions, while hopeite [$Zn_3(PO_4)_2 \cdot 4H_2O$] only precipitated under acidic conditions. Alternative sorption mechanisms other than precipitation were important in reducing Cd and Zn concentrations in the presence of the apatite. The selectivity order of heavy metal sorption onto apatite was also pH-dependent. The selectivity order at pH below 7 was Pb > Cd > Zn; but it was Pb > Zn > Cd at higher pH. These sorption experiments indicate that the removal of heavy metals is nearly pH-independent for Pb but pH-dependent for Cd and Zn.

This milestone report also investigated the heavy metals sorption on and desorption from North Carolina mineral apatite, specifically for Pb, Cd, and Zn from aqueous solutions and a contaminated soil from Bunker Hill Superfund site. The sorption results showed that the mineral apatite was very effective in retaining aqueous Pb and was moderately effective in attenuating aqueous Cd and Zn.

Specific highlights of the project to date are:

- All of the concentrations of lead, cadmium, and zinc in the leachate effluents of the flow-through experiments of apatite-treated Bunker Hill soils are below USEPA regulatory limits and most of them are below the detection limits of ICP/MS.

- The change of residence time has no effect on the leaching behaviors of the metals after apatite treatment.

- Using the MINTEQ-A2 geochemical model, thermodynamic predictions for the formations of pyromorphytes (lead apatites) and Hopeite ($Zn_3(PO_4)_2\ 4H_2O$) at less than 1% addition of apatite confirm the molar ratio calculation scenario of $Pb:PO_4$ for pyromorphytes and also confirm the precipitation of Pb and Zn at less than 1% apatite in the adsorption isotherms.

- The kinetics of formation for lead, zinc, and cadmium phosphate complexes are 24 hours or less.

- While lead almost always precipitates as a phosphate phase, other metals precipitate as oxyhydroxides or carbonates because of the buffering of the system by the apatite. In this way, otavite ($CdCO_3$), cadmium hydroxide [$Cd(OH)_2$], and zincite (ZnO) are formed in the apatite-treated soils. The stability of these phases depends upon the buffering capacity of the apatite. If enough apatite is added, then the system will be stable for geologically long time periods.

1.0 INTRODUCTION

The objective of this project is to develop and demonstrate that phosphatic granules, solutions, and slurries will react with lead and other heavy metals in contaminated soils, causing the precipitation of metal-substituted apatite minerals. Metals sequestered in apatites have great durability and leach resistance that significantly exceeds other chemically stabilized waste forms. Metal-apatite mineral structures are highly insoluble, stable over a wide range of environmental conditions for geologically-long time periods. This is applied research that will lead to advanced technology development that can be implemented to remediate metal and radiologically contaminated soils and groundwater at DoD sites. Potential demonstration sites include Keesler Air Force Base (AFB), Vandenburg AFB, and Kahoolawe Naval Base as well as DOE sites and industrial sites where metal contamination of soils and groundwater is a pervasive problem.

Over 300 apatite (calcium phosphate) minerals exist, incorporating elements from the entire periodic table to replace calcium, phosphate, or hydroxide in the fundamental apatite crystal structure. For instance, the major inorganic constituent of teeth and bones is hydroxyapatite, $Ca_5(PO_4)_3OH$. Fluoridation of drinking water causes fluoride substitution into the hydroxyapatite, producing a less soluble mineral and thereby preventing tooth decay.

Using apatite minerals as a remediation strategy puts to use long recognized geochemical principles. Apatite minerals form naturally and are stable across a wide range of geologic conditions for hundreds of millions of years (Nriagu, 1974; Wright 1990). Wright et al. (1987) investigated the trace element composition of apatite in fossil teeth and bones and in sedimentary phosphorite deposits through geologic time. They found that apatite deposited in seawater adsorbs metals and radionuclides from the seawater to millions of times the ambient concentration. The metals were locked into the apatite structure for up to a billion years with no subsequent desorption, leaching, or exchange, even in the face of subsequent diagenetic changes in the porewater chemistry, pH, or temperatures up to 1000° C.

Apatites are therefore natural concentrators of heavy metals and radionuclides. Apatite deposits in Florida, for example, are known to have accumulated large amounts of uranium, resulting in elevated levels of radon in some homes in that area. These deposits have even been considered as a commercial source of uranium (Eisenbud, 1987). A younger apatite deposit in the U.S. is located in North Carolina, which is mined primarily for fertilizer. Young deposits have had less exposure to metals in the environment and are therefore more reactive because they are more highly carbonated.

Introduction of apatite into a soil that contains mobile metal and other inorganic contaminants provides reactants and nucleating sites, where the metal-enriched apatites precipitate as very insoluble minerals. In this way, water passing through the unsaturated zone or through the water table is purified when it passes by the apatite, which acts like a chemical filter.

The leachability of metals sequestered in apatite is insensitive to pH changes over the range of 2 to 12, and the bioavailability of ingested metals is also limited (Davis et al, 1992; Ruby et al, 1992). The reaction between the apatite and metals is rapid (Ma et al, 1993), and so the treatment is effective immediately, requiring no time for the material to "set up." This project has shown that as little as 1% by weight of apatite could remediate soils.

Addition of apatite would not preclude treatment of other contaminants (volatile organic compounds, etc.). For applications in which both chemical stabilization and physical solidification are desired (in landfills, for example), investigations are underway to combine phosphate and grout or to develop a grout of phosphatic composition for improved stabilization performance.

1.1 MILESTONE ONE

The Milestone One goal was to establish the chemical and mineralogical contents of soils, waters, and phosphatic materials that would subsequently be used in leaching-retardation and sorption-desorption studies from contaminated sites. Chemical analyses of the cationic and anionic compositions and soil and metal mineral speciation were performed on contaminated soils from the following sites: 1) Keesler AFB, Mississippi, a tetraethyl lead (TEL) sludge pit; 2) Keesler AFB, a lead and zinc contaminated landfill; 3) three composite soils with varying levels of metal contamination from the Bunker Hill mining area, Idaho; and 4) two Montana soils with varying levels of metal contamination that serve as National Institute of Standards and Technology (NIST) chemical standards. Chemical analyses were also made on water downgradient from the TEL sludge pit at Keesler AFB. Chemical and mineralogical analyses of several types of phosphatic materials including synthetic hydroxyapatite, natural carbonate fluorapatite from phosphorites, fish and shark teeth, and fish cannery wastes were also performed. The data from the chemical and mineralogical speciation studies were used in the geochemical code MINTEQ to determine the stability relationships of soil minerals under varying conditions.

Lead concentrations in the Keesler AFB samples were found to be relatively low, much lower than expected, with soil levels at roughly 100 mg kg^{-1} (parts per million=ppm) and groundwater in the $\mu g\ kg^{-1}$ (parts per billion=ppb) range. These low water concentrations already challenge the detection limits of available analytical methods, Ion Chromatography (IC) for anions and Inductively Coupled Plasma Mass

Spectrometry (ICP/MS) for cations. We anticipate that incorporation of the apatite materials would reduce those concentrations several orders of magnitude, which we would not be able to quantify using the Keesler materials. Therefore, to be able to demonstrate the effectiveness of the remediation technique, we chose to continue our studies using the Bunker Hill mine tailings and soils, which contain 1000-4000 mg kg^{-1} (ppm) of lead.

1.2 MILESTONE TWO

Milestone Two established the baseline contaminant leaching rates from untreated Bunker Hill soils so that comparisons could be made to apatite-treated soils in the Milestone Three Report. Two types of laboratory experiments were performed. In the desorption studies, water was added to small soil samples in centrifuge tubes. The water to soil ratio of 10:1 was selected according to established testing protocols and was useful for studying the basic thermodynamics of the soil system. The concentration of contaminants in solution was monitored over time for up to 336 hours. In the flow-through tests, samples were packed into soil columns or in the Unsaturated Flow Apparatus (the UFA), a new instrument for rapid characterization of unsaturated soils. Water was introduced at the top of the sample, and leachates were collected as a function of the number of pore volumes of solution added.

The results reported for Milestone Two showed that the soil column/UFA leachates from the Bunker Hill soils were in the hundreds of mg kg^{-1} (ppm) range, well in excess of the drinking water standard for lead of 15 μg kg^{-1} (ppb).

1.3 MILESTONE THREE

The Milestone Three Report established that treatment with apatite reduces leaching of metals from soils. Adsorption isotherm tests and flow-through tests were performed, with small amounts of various apatites added. The results of the adsorption isotherm tests, coupled with modelling by MINTEQ, suggest that these contaminated soils can be remediated by adding as little as 1-5 wt. % apatite. Leachate concentrations for most metals from the flow-through tests were consistently below detection limits of 1 μg kg^{-1} (ppb). In particular, these experiments demonstrated that apatite can reduce lead leaching by a factor of one thousand, bringing waters that have percolated through soils with 0.4% lead by weight down to below the drinking water standard. Zinc and cadmium, two other hazardous pollutants, are also effectively treated.

1.4 MILESTONE FOUR

This report focuses on apatite formulations that could be used for soil remediation and potential emplacement strategies. Over the course of the project, we have tested mined, chemically synthesized, and several types of biogenic apatite and the effect of grinding the apatite from a coarse sand consistency to a fine powder. In the laboratory, we have incorporated apatite into the treated samples simply by adding dry material to them; however, field emplacement may require the use of solutions or slurries. This report discusses the physical properties of apatite that are relevant to emplacement, including data on the flow characteristics of apatite slurries. Several candidate emplacement strategies are explained, including injection, auguring, horizontal drilling, and excavation and backfilling. Apatite may be placed directly into a contaminated region or downgradient from it, forming a permeable, reactive barrier. The applicability of these various emplacement options and their advantages and disadvantages are discussed. Moreover, the cost of treatment with apatite will vary depending on the emplacement method required. We have included rough estimates of treatment costs in section 5.4, below.

The methodologies used for each type of analytical and experimental procedure and the results of each group of analyses are detailed in the following sections of the report. Information from the Milestone One Report pertaining to the Bunker Hill or Keesler soils is referenced in the text and included in the Appendix. Much of the text of the Milestone Three Report has been included as sections 2.0 (the adsorption tests) and 3.0 (the flow-through tests) for completeness. The conclusions of these tests are summarized in section 4.0. The new material on formulations and emplacement can be found in section 5.0.

1.5 MILESTONE FIVE

In this milestone report, the sorption and selectivity of aqueous Pb, Cd, and Zn onto a mineral apatite from North Carolina were investigated in relation to a wide range of pH. The effects of pH on solid phase precipitation were particularly emphasized. The heavy metals were applied as single species and multiple species. The results of these sorption tests indicated that a change in pH leads to a change of the sorption mechanism of these heavy metals on apatite and a change of new solid reaction products. The sorption of aqueous Pb was primarily through a process of the dissolution of apatite followed by the precipitation of variable pyromorphite-type minerals under acidic condition or of hydrocerussite [$Pb_3(CO_3)_2(OH)_2$ or $Pb(OH)_2 \cdot 2PbCO_3$] and lead oxide fluoride (Pb_2OF_2) under alkaline condition. Otavite ($CdCO_3$) and cadmium hydroxide [$Cd(OH)_2$], and zincite (ZnO) were formed in the Cd or Zn system, respectively, especially under alkaline condition; while hopeite [$Zn_3(PO_4)_2 \cdot 4H_2O$] might only precipitate under very acidic condition. Alternative sorption mechanisms other than precipitation were important in reducing Cd and Zn

concentrations in the presence of the apatite. The selectivity order of heavy metal sorption onto apatite was also pH-dependent. The selectivity order at pH below 7 was Pb > Cd > Zn; but it was Pb > Zn > Cd at higher pH. These sorption experiments indicate that the removal of heavy metals is nearly pH-independent for Pb but pH-dependent for Cd and Zn. The removal capacities were about 151 mg of Pb, 55-148 mg of Cd, and 39-143 mg of Zn/g of apatite, representing removal of 99.9%, 37-99.9%, and 27-99.9% of heavy metals from solution, respectively.

This milestone report also investigated the heavy metals sorption on and desorption from North Carolina mineral apatite, specifically for Pb, Cd, and Zn from aqueous solutions and a contaminated soil from Bunker Hill Superfund site. Aqueous solutions of Pb, Cd and Zn were reacted with the apatite, followed by desorption experiments under a wide variety of pH conditions ranging from 3 to 12, including the extraction fluids used in the Toxicity Characteristic Leaching Procedure (TCLP) of the United States Environmental Protection Agency (US EPA). The sorption results showed that the mineral apatite was very effective in retaining aqueous Pb and was moderately effective in attenuating aqueous Cd and Zn. Approximately 100% of the Pb applied was removed from solutions, representing a capacity of 151 mg of Pb/g of apatite, while 49% Cd and 29% Zn added were attenuated, with removal capacities of 73 and 41 mg/g, respectively. The desorption experiments showed that the sorbed Pb stayed intact where only 14-23% and 7-14% of the sorbed Cd and Zn, respectively, were mobilized by the TCLP solutions.

The mineral apatite was also effective in removing dissolved Pb, Cd, and Zn leached from the contaminated soil using pH3-12 solutions by 62.3-99.9, 20-97.9, and 28.6-98.7%, respectively. In particular, the mineral apatite was able to reduce the metal concentrations in the TCLP-extracted soil leachates to below US EPA maximum allowable levels, suggesting mineral apatite could be used as a cost-effective option to remediating metal-contaminated soils, wastes, and/or water.

The sorption mechanisms are variable in the reactions between the apatite mineral and dissolved Pb, Cd, and Zn from aqueous solutions and the contaminated soil. The Pb removals primarily resulted from the dissolution of the mineral apatite followed by the precipitation of hydroxyl fluoropyromorphite. Minor otavite precipitation was observed in the interaction of the apatite with aqueous Cd, but other sorption mechanisms, such as surface complexation, ion exchange, and the formation of amorphous solids, are primarily responsible for the removal of aqueous Zn and Cd.

2.0 ADSORPTION ISOTHERMS: NORTH CAROLINA APATITE INDUCED PRECIPITATION OF Pb, Zn, Mn AND Cd DESORBED FROM THE BUNKER HILL 4000 SOIL

Adsorption is most often described in terms of isotherms which show the relationship between the bulk activity, or effective concentration in solution, of the species being adsorbed and the actual amount adsorbed at a constant temperature. When plotted, the shape and mathematical expression of the isotherm provide a great deal of information concerning the chemistry and sorption mechanisms within the system.

Although current research demonstrates the successful precipitation of soluble heavy metals when hydroxyapatites are added to a contaminated medium (Misra and Bowen, 1981; Ma, et al. 1993; Xu and Schwartz, 1994), very little attention has been paid to the precise calculation of hydroxyapatite needed to affect precipitation or complexation of metals from contaminated mediums. In this report, the amounts of hydroxyapatite (as North Carolina apatite) calculated to precipitate soluble metals relative to the molar ratios of the precipitated metal-PO_4 complexes will be illustrated as sharp deviations from linearity of the adsorption isotherms, as predicted by MINTEQ-A2, a thermodynamic speciation model. The amounts of apatite required for precipitating the metals in solution can then be extrapolated and scaled for field remediation.

2.1 PRECIPITATION OF SOLUBLE METALS BASED ON MOLAR RATIOS OF METAL-PO_4 COMPOUNDS

The Bunker Hill 4000 soil (BH 4000), so named because of its 4000 ppm lead concentration, was used to demonstrate the precipitation and metal-PO_4 stabilization potential of the North Carolina apatite (NC apatite). A two-week desorption experiment on the BH 4000 resulted in soluble Pb, Zn, Cd and Mn concentrations presented in graphic and tabular format in Figure 1 and Table 1 and described in greater detail in the Milestone II report.

Of particular interest is the type and amount of metals leaching from the BH 4000 soil as a function of time. Particular metals of interest are those that are regulated by federal agencies relative to health impacts. Metals that are regulated in groundwater and drinking water by the United States Environmental Protection Agency (USEPA) have been correlated to the ICP/MS metal analysis data. Those contaminants that have desorbed from the Bunker Hill 4000 soil that are of USEPA regulatory concern are Pb, Zn, Cd and Mn. These contaminants, which desorb in detectable amounts over the two-week test duration will be the focus of this study.

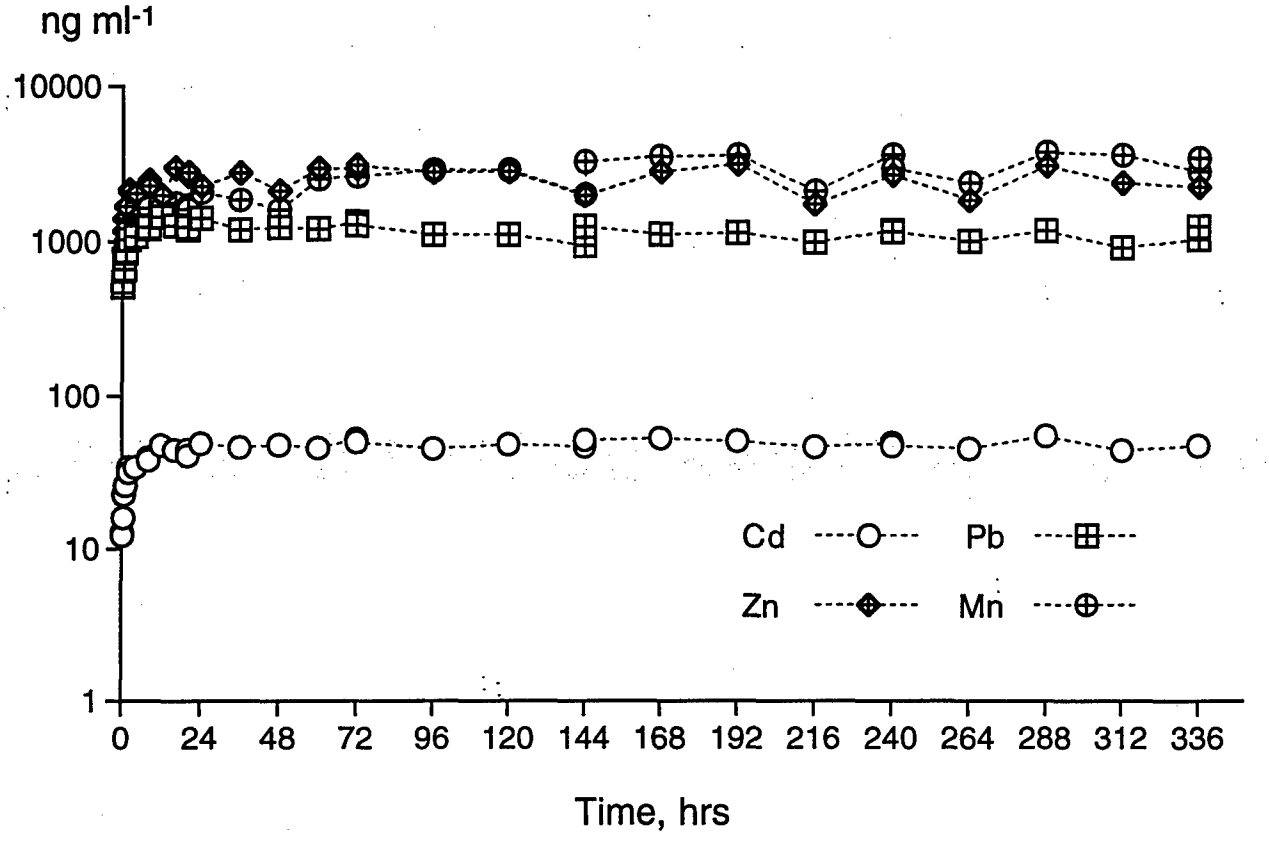

Figure 1. Desorption of Pb, Zn, Mn and Cd From the BH4000 Soil During a two Week Period.

Table 1. Percent Metal Desorption in the BH4000 Soil After 24 Hours.

Element	Total amount mg kg^{-1}	Amount Desorbed mg kg^{-1}	% Desorbed
Mn	1031	37.6	3.65
Zn	1087	30.8	2.83
Pb	4170	14.4	0.35
Ba	808	4	0.5
Sr	120	1.96	1.63
Cd	17	0.52	3.06
Al	79,000	3.75	0.0047

Figure 1 graphically represents the desorption of Pb, Zn, Mn and Cd from the BH 4000 soil during a two-week desorption period. Figure 1 illustrates that the maximum amount of metal desorption occurs within the first 24 hours of desorption.

By adding PO_4 to a solution containing one or more metals, one can induce precipitation/formation of minerals containing the PO_4 and the metal(s). By knowing the type and concentration of a particular metal and the mineral it will form when PO_4 is added, the precise amount of PO_4 to be added can be calculated. Using Pb as an example, stoichiometric amounts of PO_4 (from NC apatite), determined from the molar ratios of the precipitated minerals, can be added to induce the precipitation. In the case of Pb, molar ratios from minerals known as pyromorphytes will be used.

Chloropyromorphyte and hydroxypyromorphyte are the two most likely Pb-PO_4 minerals to form under the given conditions. These two minerals exhibit the fastest kinetic rate of formation (Nriagu, 1974). Although the two minerals are different by chemical formula, they both have the same Pb/PO_4 ratios. The following is the calculation for the molar ratio:

Chemical formula for pyromorphytes $Pb_5(PO_4)_3(OH, Cl)$
(Nriagu, 1972,1973)

Pb: 5@ 207.2 g/mol = 1,036. g/mol
PO_4: 3@94.93 g/mol = 284.79 g/mol
Molar ratio of Pb:PO_4 in pyromorphytes = 3.64

The lead leachate concentration of 1400 µg/kg is equivalent to 6.76×10^{-6} mol/L (M).Therefore,

6.76×10^{-6} M lead / 3.64 moles lead per mole phosphate = 1.86×10^{-6} M,

the concentration of PO_4 needed to drop out the lead, or equivalently,

1.86×10^{-6} M x 94.93 g PO_4/mol = 1.78×10^{-4} g L^{-1} = 0.18 µg PO_4 ml^{-1}.

To convert 0.18 µg PO_4 ml^{-1} to the amount of NC apatite added to cause precipitation, we use the fact that 46.84% by weight of the apatite is PO_4 and assume complete dissolution of the NC apatite. Thus, for example, a .01% addition of NC apatite to the 3 g of BH 4000 soil and 30 ml of water used in these experiments will yield:

0.01% NC apatite = 0.0003g NC apatite = 0.00014 g PO_4/30 ml H_2O=3.3 µg ml^{-1} .

From a proportional calculation, to obtain the concentration of 0.18 µg PO_4 ml^{-1} required for the formation of pyromorphytes, only 0.0005% NC apatite must be added.

It is obvious the resulting concentration of only 0.18 µg PO_4 ml^{-1} required for the formation of a pyromorphyte is substantially less than a 1% addition of NC apatite to the 3 g of contaminated BH 4000 soil. It also must be considered that there are many other metals in the BH 4000 supernatant that will complex with PO_4, which will reduce the overall concentration of PO_4 in solution. It is hypothesized that if metal-PO_4 minerals are to form under these conditions, amounts of up to 1% added NC apatite should cause reductions in most or all of the desorbed metal concentrations.

The formation of pyromorphytes calculated from the molar ratios, shown as such by the reduction of desorbed Pb in the adsorption isotherms, is confirmed by the thermodynamic modeling discussed below. Confirmation of the pyromorphyte formation by this experimental system suggests that PO_4 from the addition of up to 1% NC apatite will also complex with Zn, Mn, and Cd to form stable minerals.

2.2 NC APATITE ADSORPTION ISOTHERM - 24 HOURS REACTION TIME

Using the molar ratio of the pyromorphyte mineral as a beginning concentration range, an adsorption isotherm was conducted to observe the adsorption characteristics of the NC apatite on the desorbed metals from the BH 4000 soil. The nature of the curve, especially the departure from linearity and/or asymptotic characteristics, will determine the NC apatite concentration that induces precipitation of the desorbed metals.

2.2.1 EXPERIMENTAL

Adsorption isotherm tests (Beckwith, 1964), using the NC apatite, were performed on the Bunker Hill 4000 soil. For a 24-hour NC apatite adsorption study, 3 grams of the BH 4000, ground to pass through a 170 mesh screen and weighed to three decimal places, were combined with 1%, 5%, 10% and 20% NC apatite. Thirty ml of deionized water were added to the mixture in 40 ml polycarbonate centrifuge tubes . The polycarbonate tubes containing the 3 grams of BH 4000 soil, incremental percentages of NC apatite and 30 ml of deionized water were shaken continuously for 24 hours. At the end of 24 hours, the samples were taken from the shaker and centrifuged. The supernatant was filtered at 0.2μ, then analyzed for pH, metals, and anions as described in the elemental analysis section of this report. The data for this analysis is presented in Table 2.

Table 2. Metal Analysis for the 24 Hour NC Apatite Adsorption Isotherm for the BH4000 Soil (ng/ml).

% NC Apatite	Pb	Sr	Ba	Al	Fe	Cd	Zn	Mn
0	1600	179	486	68	38	53.6	2760	1740
1	154	157	152	124	41	8.98	536	875
5	220	303	151	304	185	4.3	165	598
10	86	435	130	123	1	2.1	86.1	490
20	23.3	674	137	25	1	1.7	10	359

2.2.2 RESULTS

A number of metals desorbed from the BH 2000 soil, as described in the Milestone 2 report. For brevity, this report will focus on the precipitation of metals that desorbed above their regulatory limits, namely Pb, Zn, Mn, and Cd. Their desorption curves are shown in Figure 1.

2.2.2.1 Pb PRECIPITATION

Figure 2 represents the reduction of desorbed Pb with the addition of 1%, 5%, 10% and 20% NC apatite. At 0% NC apatite, the desorbed amount of Pb in the 24 hour period (control sample) is 1600 ng ml^{-1}. The greatest reduction in Pb occurs with 1% addition of NC apatite, which is a 90% reduction of the desorbed Pb to 154 ng ml^{-1}.Increasing the NC apatite concentration to 5, 10 and 20% show no significant decrease in the desorbed Pb. Therefore, the precipitation of Pb by the addition of NC apatite occurs at 1% or less.

2.2.2.2 Zn PRECIPITATION

Figure 3 represents the reduction of desorbed Zn with the addition of 1%, 5%, 10% and 20% NC apatite. At 0% NC apatite, the desorbed amount of Zn in the 24-hour period (control sample) is 2760 ng ml^{-1}. The greatest reduction in Zn occurs with 1% addition of NC apatite, which is an 81% reduction of the desorbed Zn to 536 ng ml^{-1}. Increasing the NC apatite concentration to 5% decreases the desorbed Zn amount by 13%. Additions of 10 and 20% show no significant decrease in the desorbed Zn. Therefore, the major % of precipitation of Zn by the addition of NC apatite occurs at 1% or less.

2.2.2.3 Mn PRECIPITATION

Figure 4 represents the reduction of desorbed Mn with the addition of 1%, 5%, 10% and 20% NC apatite. At 0% NC apatite, the desorbed amount of Mn in the 24-hour period (control sample) is 1740 ng ml^{-1}. The greatest reduction in Mn occurs with 1% addition of NC apatite, although not as great a reduction as Pb and Zn. The reduction at 1% addition of NC apatite is 50%, with a Mn concentration of 536 ng ml^{-1}. Increasing the NC apatite concentration to 5% decreases the desorbed Mn amount by 16%. Additions of 10 and 20% reduce the desorbed Mn by 6% and 8%, respectively. Therefore, the precipitation of Mn by the addition of NC apatite appears to be greatest at 1% addition of NC apatite, with slight decreases with each incremental addition of the NC apatite.

2.2.2.4 Cd PRECIPITATION

Figure 5 represents the reduction of desorbed Cd with the addition of 1%, 5%, 10% and 20% NC apatite. At 0% NC apatite, the desorbed amount of Cd in the 24 hour period (control sample) is 54 ng ml^{-1}. The greatest reduction in Cd occurs with 1% addition of NC apatite, which is an 83% reduction of the desorbed Cd to 9 ng ml^{-1}. Increasing the NC apatite concentration to 5% decreases the desorbed Cd amount by 8.7%. Additions of 10 and 20% show no significant decrease in the desorbed Cd. Therefore, the major % of precipitation of Cd by the addition of NC apatite occurs at 1% or less.

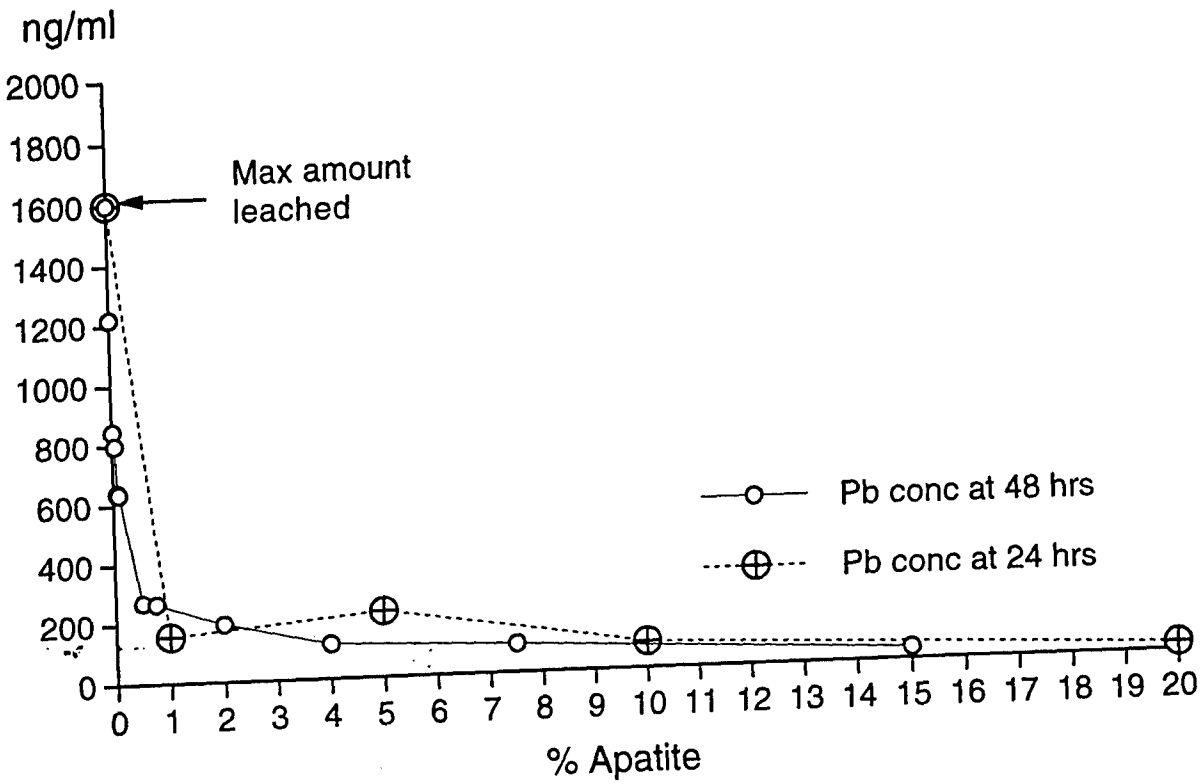

Figure 2. The Reduction of Desorbed Pb by NC Apatite Depicted by 24 and 48 Hour Adsorption Isotherms.

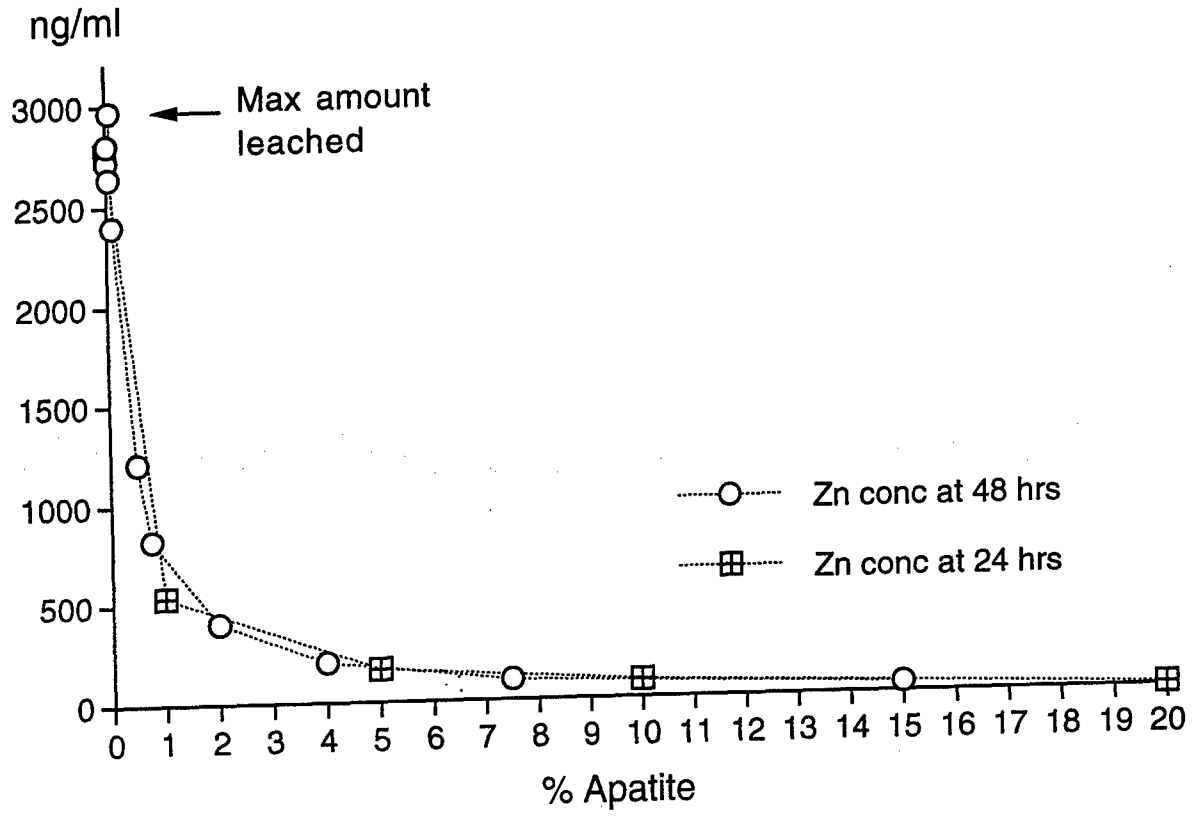

Figure 3. The Reduction of Desorbed Zn by NC Apatite Depicted by 24 and 48 Hour Adsorption Isotherms.

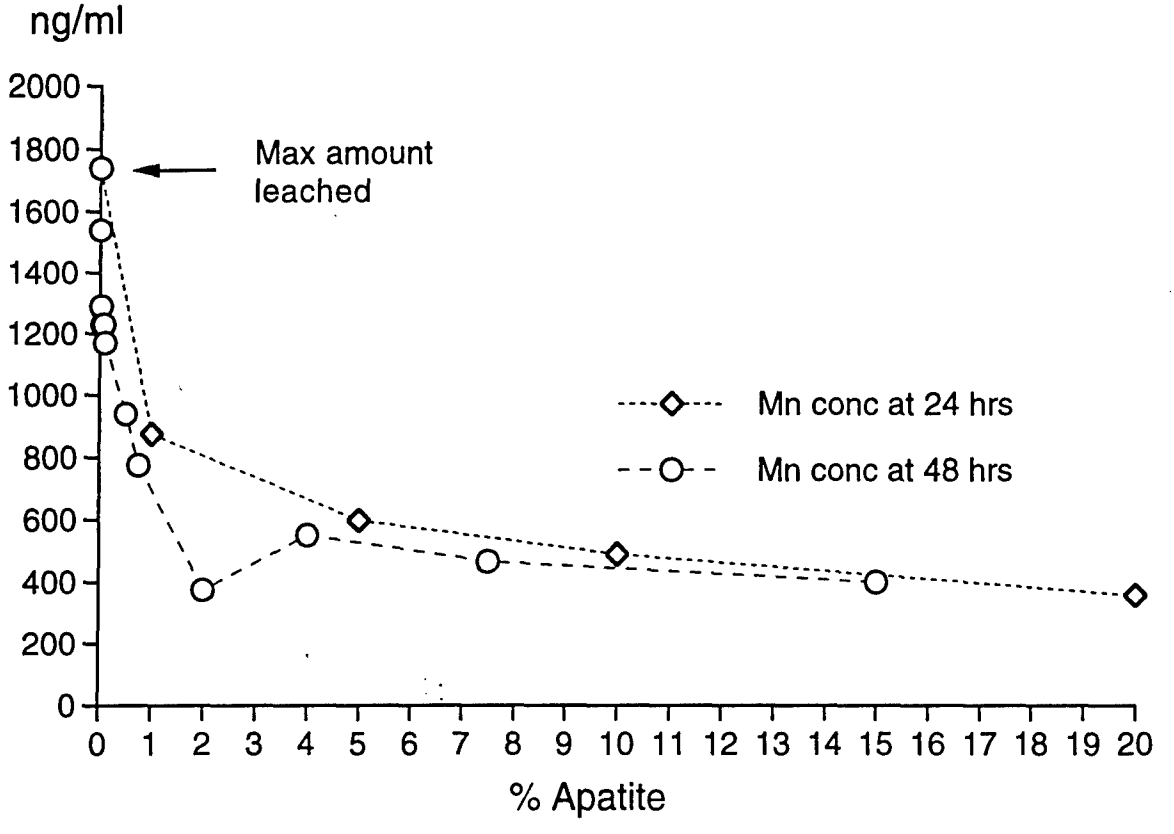

Figure 4. The Reduction of Desorbed Mn by NC Apatite Depicted by 24 and 48 hour Adsorption Isotherms.

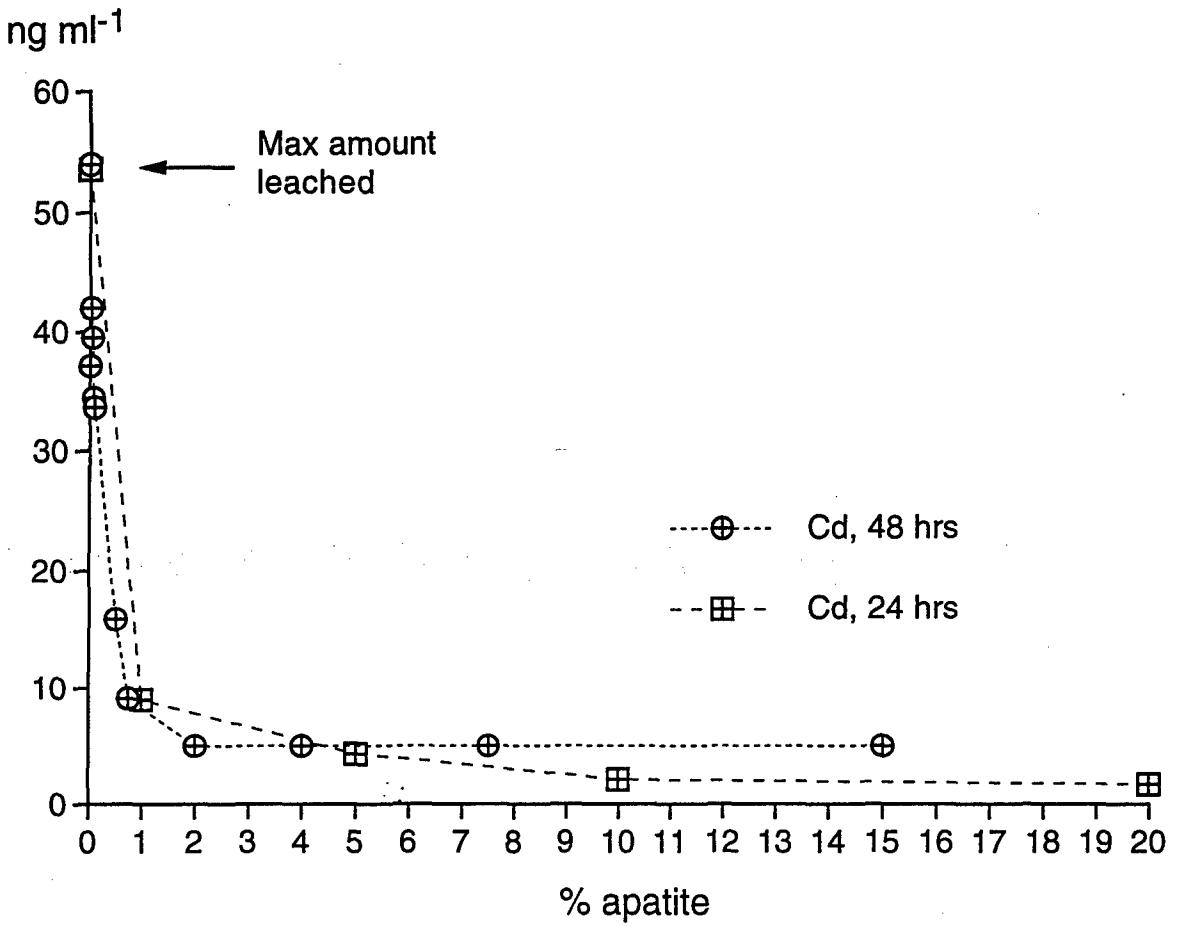

Figure 5. The Reduction of Desorbed Cd by NC Apatite Depicted by 24 and 48 hour Adsorption Isotherms.

2.3 NC APATITE ADSORPTION ISOTHERM - 48 HOURS REACTION TIME

To examine the effect of increasing the contact time between the desorbed metals and the NC apatite, a 48-hour adsorption isotherm was executed. The difference between the 48-hour and 24-hour adsorption isotherms is the amount of NC apatite added during each run.

2.3.1 EXPERIMENTAL

The same NC apatite adsorption isotherm tests were performed on the Bunker Hill 4000 soil as with the 24-hour isotherm tests. Three grams of the BH 4000, ground to pass through a 170 mesh screen and weighed to three decimal places, were combined with the percentages of NC apatite listed in Table 3. Thirty ml of deionized water were added to the mixtures in 40 ml polycarbonate centrifuge tubes. The polycarbonate tubes containing the 3.000 grams of BH 4000 soil, incremental percentages of NC apatite and 30 ml of DI H_2O were shaken continuously for 48 hours. At the end of 48 hours, the samples were taken from the shaker and centrifuged. The supernatant was filtered at 0.2μ, then analyzed for pH, metals, and anions as described in the elemental analysis section of this report. The data for this analysis is presented in Table 4.

2.3.2 RESULTS

2.3.2.1 Pb PRECIPITATION

Figure 2 represents the reduction of desorbed Pb with the addition of 0.005% through 15% NC apatite, with the precise increments listed in Table 2. At 0% NC apatite, the desorbed amount of Pb in the 48-hour period (control sample) is 1600 ng ml^{-1}. As with the 24-hour isotherm, the greatest reduction in Pb occurs at less than 1% addition of NC apatite, which is an 83% reduction of the desorbed Pb to 266 ng ml^{-1}. Increasing the NC apatite concentrations shows no significant decrease in the desorbed Pb. All additions less than 1% reduce the amount of desorbed Pb. The .005% addition of NC apatite reduces the desorbed Pb by 24%, corroborating the molar ratio amount of NC apatite needed to form a pyromorphyte. As also shown by the 24-hour adsorption isotherm, the major % of precipitation of Pb by the addition of NC apatite occurs at 1% or less.

Table 3. Percentages of NC Apatite Added to the BH4000 Soil for 48 Hour Adsorption Isotherm.

0
0.005
0.02
0.08
0.1
0.5
0.75
2
4
7.5
15

Table 4. Metal Analysis for the 48 Hour NC Apatite Adsorption Isotherm for the BH4000 Soil.

% NC apatite	pH	Zn	Pb	Ba	Cd	Mn	Al
15	7.5	44.2	36.5	159	5	402	23
7.5	7	100	92.9	163	5	467	88
4	6.5	201	115	148	5	551	112
2	6.4	401	192	146	5	376	216
0.75	5.1	824	266	154	9.1	776	253
0.5	6.3	1210	270	171	15.9	939	110
0.1	6.3	2400	635	204	33.6	1170	92.3
0.08	6.2	2970	641	345	34.4	1230	66.7
0.05	5.9	2640	798	346	39.5	1230	50.7
0.02	4.95	2805	846	370	42	1290	57
0.005	6.8	2720	1220	304	37.1	1540	55
0	5.5	2760	1600	486	54	1740	68

2.3.2.2 Zn PRECIPITATION

Figure 3 represents the reduction of desorbed Zn with the addition of 0.005% through 15% NC apatite, with the precise increments listed in Table 2. At 0% NC apatite, the desorbed amount of Zn in the 48-hour period (control sample) is 2760 ng ml^{-1}. As with the 24-hour isotherm, the greatest reduction in Zn occurs at less than 1% addition of NC apatite, which is a 70% reduction of the desorbed Zn to 824 ng ml^{-1}. As shown from the adsorption isotherm, increasing the NC apatite concentrations almost parallels the 24-hour adsorption isotherm, strongly suggesting that increasing the contact time to 48 hours does not increase precipitation. As also shown by the 24-hour adsorption isotherm, the major % of precipitation of Zn by the addition of NC apatite occurs at 1% or less.

2.3.2.3 Mn PRECIPITATION

Figure 4 represents the reduction of desorbed Mn with the addition of 0.005% through 15% NC apatite, with the precise increments listed in Table 2. At 0% NC apatite, the desorbed amount of Mn in the 48-hour period (control sample) is 1740 ng ml^{-1}. As with the 24-hour isotherm, the greatest reduction in Mn occurs at less than 1% addition of NC apatite, which is a 55% reduction of the desorbed Mn to 776 ng ml^{-1}. As in the 24-hour isotherm, the addition of NC apatite is not as great a reduction as Pb and Zn. Increasing the NC apatite concentration decreases the desorbed Mn amount more than in the 24-hour isotherm The precipitation of Mn by the addition of NC apatite appears to be greatest at less than 1% addition of NC apatite, with a further 12% decrease at 2% added apatite.

2.3.2.4 Cd PRECIPITATION

Figure 5 represents the reduction of desorbed Cd with the addition of 0.005% through 15% NC apatite, with the precise increments listed in Table 2. At 0% NC apatite, the desorbed amount of Cd in the 48-hour period (control sample) is 54 ng ml^{-1}. As with the 24-hour isotherm, the greatest reduction in Cd occurs at less than 1% addition of NC apatite, which is an 83% reduction of the desorbed Cd to 9.1 ng ml^{-1}. Increasing the NC apatite concentration to 2% decreases the desorbed Cd amount by 7.6%. Increasing the concentration of apatite past 2% does not reduce the concentration of desorbed Cd. As shown from the adsorption isotherm, the 48-hour isotherm parallels the 24-hour adsorption isotherm, strongly suggesting that increasing the contact time to 48 hours does not increase precipitation. It is suggested that the greatest precipitation of Cd by the addition of NC apatite occurs at 1% or less.

2.3.3 PRECIPITATION OF DESORBED METALS AS DEPICTED IN THE 24- AND 48-HOUR ADSORPTION ISOTHERMS

It can be seen from both the 24- and 48-hour NC apatite adsorption isotherms that very little NC apatite is required to reduce the desorbed concentrations of Pb, Zn, Mn and Cd from the BH 4000 soil to within or below regulatory limits. In all cases, the greatest reduction in the desorbed metals occurs at 1% or less added apatite. In all cases the % NC apatite increments less than 1% indicate strong and dramatic reductions of Pb, Zn, Mn and Cd, verifying that NC apatite is causing reduction of the desorbed metals at less than 1%.

Increasing the adsorption isotherm time to 48 hours does not increase the overall effectiveness of NC apatite, except for a slight decrease in the Mn 48-hour adsorption isotherm. Because the increase in contact time to 48 hours does not increase the precipitation for Pb, Zn, and Cd from the 24-hour experiment, it is suggested that the adsorption or formation kinetics of the apatite-metal system for these metals is less than 24 hours. This corroborates the work of other researchers in metal-PO_4 complexation (Ma, et al,1993, Ruby, et al, 1994, Xu and Schwartz, 1994).

2.4 VERIFICATION OF PRECIPITATED METALS USING MINTEQ-A2

In order to gain knowledge about the nature of metal-phosphate complexation and to determine how much PO_4 is needed to complex the desorbed metals of the BH 4000 soil, MINTEQ-A2, a geochemical thermodynamic speciation computer program, was used.

The natural soil system has both a solid phase and a solution phase. When chemical equilibrium is assumed to exist between the soil solution and the associated solid phases of the soil, one can elicit important information about solid phase formations by using thermodynamic calculations performed in geochemical thermodynamic speciation programs. Specifically, this computer program is used to examine the precipitation of selected metals, i.e., Pb, Zn, Mn, and Cd, induced by the application of a specific phosphate compound.

Saturation indices for the BH 4000 soil determined from MINTEQ-A2 indicate whether Pb, Zn, Mn, and Cd-phosphate minerals may be present. The saturation index is defined as

Ion Activity Product/Solubility Product

and is a thermodynamic indication of mineral dissolution or formation. Values < 0

indicate that the mineral is undersaturated with respect t the equilibrium concentration and should not precipitate, while values > 0 indicate saturation with respect to the equilibrium concentration, indicating that precipitation is likely to occur. The higher the number, the greater the probability of precipitation.

2.4.1 EXPERIMENTAL

Input data for the execution of the computer program was acquired from a complete metal and ligand analysis of saturation extracts (Page, et. al, 1982). The computer program used was MacMINTEQ-A2, acquired from Geochem Software, 1994. Metal concentrations on the extract were obtained by ICP analysis and anions by IC analysis (PNL-AL0-211.2 Rev. 0, and PNL-ALO-212 Rev. 1).

2.4.2 RESULTS

A great utility of the MINTEQ-A2 program is the versatility in configuring "what if" scenarios, based on thermodynamic principles. Data produced from the analysis of the BH 4000 saturation extract was input to the program. Included in the data input was the analysis of the metal and ligand concentration, pH, electrical conductivity, redox conditions and carbonate content. The input data exhibited a charge balance difference of 11%, which is within acceptable limits for program operation (Geochem Software, 1994).

The initial input data for the operation of MINTEQ-A2, derived from the analysis of the saturation extract, is presented in Table 5. The "what if" scenario to be analyzed using MINTEQ-A2, from a thermodynamic standpoint, is the effect of increasing amounts of NC apatite added to the BH 4000 soil. By varying the amount of NC apatite PO_4 on the solute composition, solubility products are calculated for possible precipitation reactions of PO_4 with those metals present in the analyzed saturation extract. Each incremental amount of PO_4 added requires a separate execution of the MINTEQ-A2 program. With each program run, the output lists the possible combinations of metal-PO_4 solid phases. The saturation index, described above, is listed in the output for each of the target metal-PO_4 minerals. As a result, each incremental amount of PO_4 added as NC apatite alters the solute composition favorably or unfavorably with respect to the formation of solid phases. The incremental amounts of PO_4 added as NC apatite and the resulting calculated saturation indexes are listed in Table 6.

Figure 6 shows the graphic representation of saturation indexes of Pb-PO_4 minerals relative to increasing amounts of PO_4 from NC apatite, and Figure 7 shows the graphic representation of saturation indexes of Zn, Mn, and Cd phosphate minerals relative to increasing amounts of PO_4 from NC apatite.

Table 5. Metal and Ligand Analysis of the BH 4000 Soil Saturation Extract.

Metal analysis, ng/ml

Na	Mg	Al	K	Ca	Mn	Fe	Ni	Cu	Zn	Sr	Cd	Ba	Pb
14,350	9530	79	19550	95250	6760	197	26	48	8390	556	162	302	581

Anion analysis, µg/ml

F	Cl	NO2	NO3	SO4	PO4
2.49	35.9	0.8	0.3	271	0

pH = 5.6

Electrical conductivity = .984 dS/M

CO3-2 = 3 µg/ml

Table 6. Saturation indexes relative to NC apatite concentrations for the formations of Pb, Cd, Zn and Mn-phosphate minerals.

% NC Apatite	PO_4, mg L^{-1}	Sat. Index $Pb(PO_4)_2$	Sat. Index $PbHPO_4$	Sat. Index $PbAl_3(PO_4)_2(OH)_5H_2O$
0	0	-6.206	-4.076	-10.505
0.02	9.4	1.74	-0.102	-2.559
0.05	23.5	4.065	0.661	1.762
0.07	32.9	4.727	0.893	2.925
0.1	47	5.754	1.209	4.953
0.5	235	7.154	1.91	6.349
1	470	7.759	2.213	6.949

% NC Apatite	PO_4, mg L^{-1}	Sat. Index $Pb_5(PO_4)_3Cl$	Sat. Index $Pb_5(PO_4)_3OH$	Sat. Index Mn HPO_4
0	0	2.347	-10.646	-0.807
0.02	9.4	14.267	1.273	3.166
0.05	23.5	17.751	5.158	3.933
0.07	32.9	18.744	6.251	4.166
0.1	47	20.283	7.989	4.487
0.5	235	22.382	10.089	5.189
1	470	23.288	10.994	5.492

% NC Apatite	PO_4, mg L^{-1}	Sat. Index $Zn_3(PO_4)\ 4H_2O$	Sat. Index $Cd_3(PO_4)_2$	Sat. Index $Mn_3(PO_4)_2$
0	0	-13.359	-18.771	-21.574
0.02	9.4	-5.412	-10.825	-13.628
0.05	23.5	-3.079	-8.492	-11.294
0.07	32.9	-2.413	-7.825	-10.627
0.1	47	-1.372	-6.784	-9.585
0.5	235	0.03	-5.382	-8.183
1	470	0.636	-4.776	-7.576

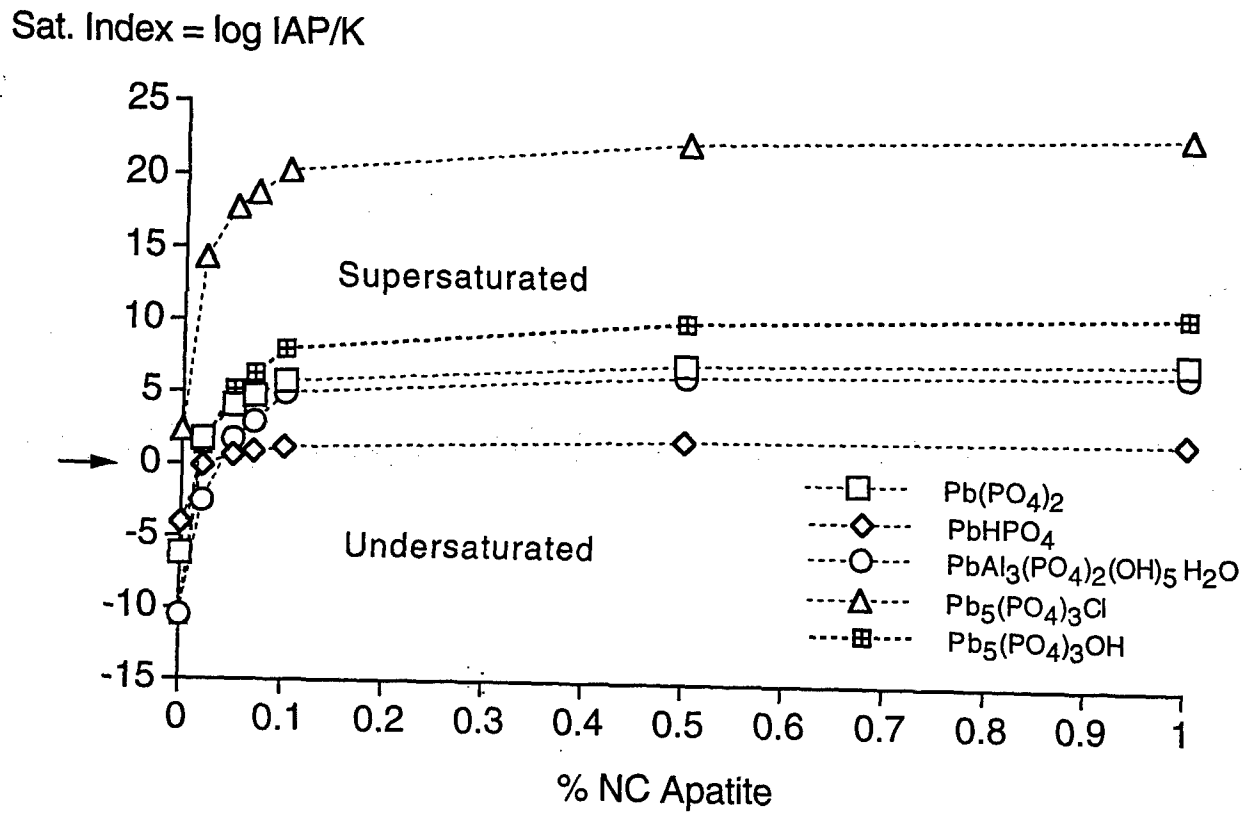

Figure 6. Saturation Indexes Relative to Increasing Amounts of NC Apatite for the Formation of Pb-Phosphate Minerals.

2.4.2.1 Pb-PHOSPHATE PREDICTIONS

The Pb-PO_4 minerals depicted in Figure 6 are all common minerals known to form under the given conditions. The chloro- and hydroxypyromorphytes, with the chemical formula $Pb_5(PO_4)_3(OH, Cl)$, are indicated as having the most positive saturation indexes, and are therefore most likely to form. This is substantiated by X-ray diffraction results on the Bunker Hill soils after treatment with apatite and by other researchers (Nriagu, 1974, Ma, et al, 1993, Ruby et al, 1994). Plumbogummite ($PbAl_3(PO_4)_2(OH)_5\ H_2O$) is also indicated as a possible precipitated mineral, as are two unnamed complexes, $Pb(PO_4)$ and $PbHPO_4$. For all of the Pb-PO_4 minerals presented in the MINTEQ-A2 output, the thermodynamic predictions occur at less than 0.1% addition of NC apatite. This thermodynamic prediction agrees with the previously calculated NC apatite amount from the Pb/PO_4 molar ratios of pyromorphytes and the adsorption isotherm data presented in Figure 2.

2.4.2.2 Mn-PHOSPHATE PREDICTIONS

Figure 7 shows the graphic representation of saturation indexes of Zn, Mn, and Cd phosphate minerals relative to increasing amounts of PO_4 from NC apatite. Rhodochrosite ($MnHPO_4$) shows the highest degree of supersaturation. Based on the solubility reported for $MnHPO_4$, this mineral is very stable in soils. The $MnHPO_4$ mineral is more stable than strengite ($FePO_4\ 2H_2O$), an important competing phase, at most pH and redox conditions of soils (Lindsay, 1979). The saturation index for strengite at .02% NC apatite is 2.910 and 3.166 for Rhodochrosite. The higher saturation index indicates a more likely formation for $MnHPO_4$ and suggests that the prediction is credible. As depicted in Figure 7, supersaturation with respect to $MnHPO_4$ formation exists at concentrations of less than 0.1% NC apatite. This thermodynamic prediction agrees with the NC apatite amounts shown to reduce desorbed Mn concentration in the adsorption isotherm data presented in Figure 4.

2.4.2.3 Zn-PHOSPHATE PREDICTIONS

The mineral hopeite ($Zn_3(PO_4)_2\ 4H_2O$) is reported to have a very low solubility, with a Log K° of -35.3 (Nriagu, 1973). This would indicate extreme stability in the soil environment. As can be noted from the thermodynamic prediction of MINTEQ-A2, the incremental additions of NC apatite raise the saturation index to 0 at 0.5% NC apatite. This condition is favorable for the formation of ($Zn_3(PO_4)_2\ 4H_2O$) but not as positive as Mn or Pb, discussed above. However, the adsorption isotherm presented in Figure 3 shows a drastic reduction of Zn at less than 1% addition of NC apatite, which would indicate a highly supersaturated condition with respect to the formation of ($Zn_3(PO_4)_2$

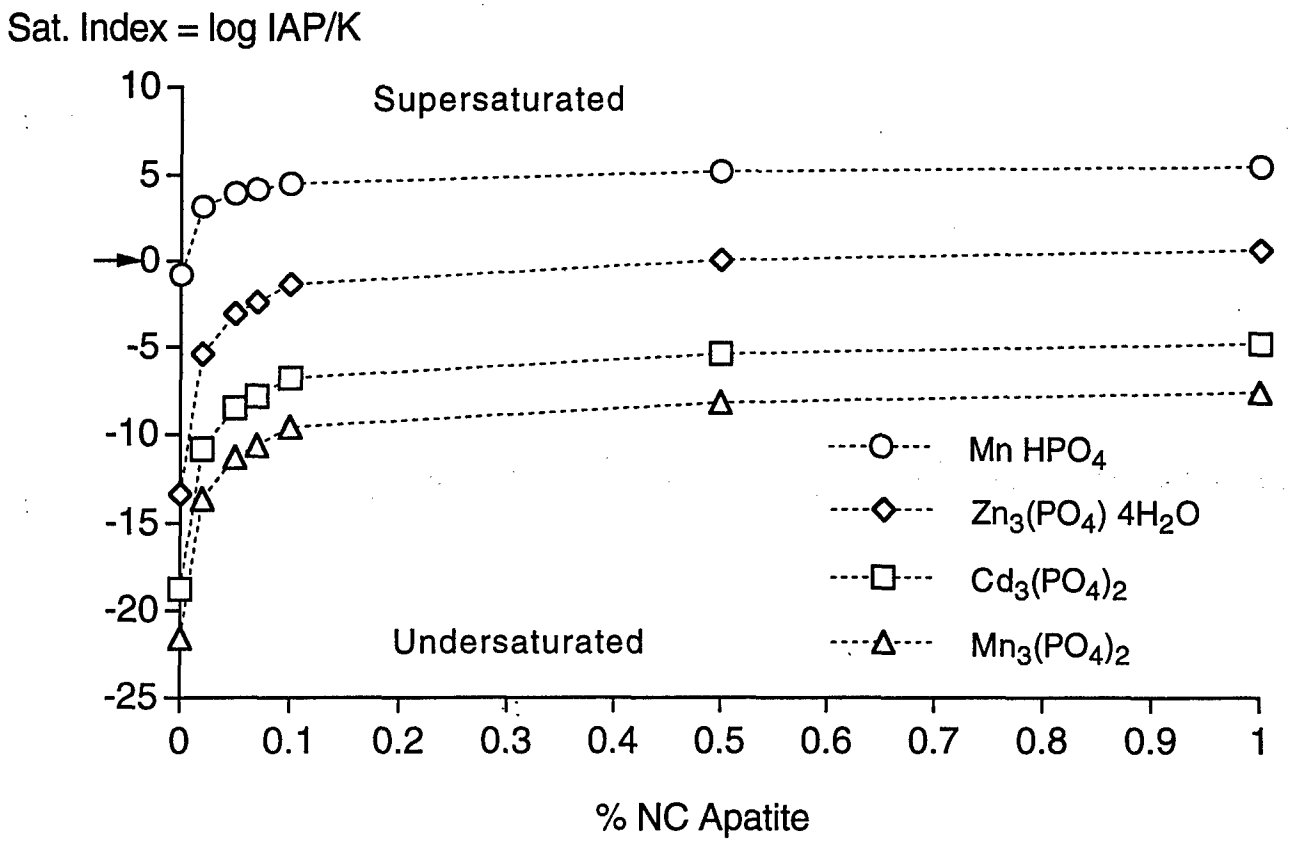

Figure 7. Saturation Indexes Relative to Increasing Amounts of NC Apatite for the Formation of Mn, Zn and Cd-Phosphate Minerals.

$4H_2O$). This discrepancy is best explained by the different solubilities for this mineral presented in the literature by various researchers. The values range from Log K° of -35.3 (Nriagu, 1973) to Log K° of 3.80 (Lindsay, 1979)

Observing the upward trend toward supersaturation at less than 0.1% NC apatite, the thermodynamic prediction partially agrees with the NC apatite amounts shown to reduce desorbed Zn concentration in the adsorption isotherm data presented in Figure 3.

2.4.2.4 Cd-PHOSPHATE PREDICTIONS

As indicated in Figure 7, the formation $Cd_3(PO_4)_2$ is not predicted to occur. The saturation indexes at all increments of less than 1% NC apatite are less than 0, indicating undersaturation with respect to the mineral. This is in contradiction to the adsorption isotherm presented in Figure 5. which depicts an 83% reduction of desorbed Cd at less than 1% addition of NC apatite. As with Zn, this discrepancy is best explained by the different solubilities for $Cd_3(PO_4)_2$ presented in the literature by various researchers. The values range from Log K° of -32.61 (NBS) to Log K° of 1.0 (Lindsay, 1979).

3.0 UNSATURATED FLOW-THROUGH STUDIES IN TREATMENT OF CONTAMINATED SOILS USING APATITE MINERALS

3.1 MATERIALS

The metal-contaminated soils used in this study are composite soils (BH2000 and BH4000) from the Bunker Hill Mining District, Idaho and were obtained from the University of Idaho. A natural apatite from North Carolina was used as a remedial additive to the contaminated soils. The apatites used were either un-ground (as-mined) or ground and sieved through a 170-mesh standard testing sieve (90 μm opening). A synthetic Hanford vadose zone water and deionized water were used in the flow-through experiments.

3.2 SOIL COLUMN AND UFA METHODOLOGY

Flow-through studies of untreated and apatite-treated contaminated soils were performed to replicate actual field conditions that batch studies cannot reproduce, e.g., natural flow rates, low water:soil ratios, channelized flow paths, etc. Two flow methods were used: traditional soil columns and the UFA method. Traditional soil

columns consist of a column of soil having solution dripping into the top at a fixed rate and effluent collected as it exits the bottom of the sample. Because the fluid driving force is only the unit gravitational acceleration, which is a very small whole body force, the degree of saturation in the sample is high, nearly saturated, for most soils if the experiment is to take less than a year. To achieve the low water contents that exist in most vadose zones, the flow rates would have to be so low that the experiment would take an unreasonable amount of time. The UFA method is used for unsaturated flow or flow in relatively impermeability materials. The UFA method is based upon open-flow centrifugation and achieves hydraulic steady-state in a matter of hours in most geologic materials even at very low water contents and permeabilities down to 10^{-10} cm/s (Wright et al., 1994). There are specific advantages to using a centripetal acceleration as a fluid driving force. It is a whole-body force similar to gravity, and so acts simultaneously over the entire system and independently of other driving forces, e.g., gravity or matric suction. The use of steady-state centrifugation to measure steady-state hydraulic conductivities has only recently been demonstrated (Nimmo et al., 1987; Conca and Wright, 1992). The UFA consists of an ultracentrifuge with a constant, ultralow flow-rate pump which provides any fluid to the sample surface through a rotating seal assembly and microdispersal system. Accelerations up to 20,000 g are attainable at temperatures from -20° to 150°C and flow rates as low as 0.001 ml/hr. The effluent is collected in a transparent, volumetrically-calibrated container at the bottom of the sample assembly which can be observed during centrifugation using a strobe light.

3.3 EXPERIMENTAL PROCEDURE

3.3.1 LEACHING OF UNTREATED CONTAMINATED SOILS

Two 3-cm diameter, 5-cm long core sample holders were each packed with 40 g of dry Bunker Hill 2000 soils. One of these two samples was for the UFA run, the other for the traditional soil column experiment. To reduce the possibility of preferential flow and fingering the samples were pre-wetted: 5 ml and 8 ml of synthetic vadose water were added to the UFA and column samples, respectively. Then, the column sample was placed on a sample rack with a pumping rate of 1 ml per hour, and the UFA sample was set up at 400 rpm and 1 ml per hour. Leachates were observed after variable amounts of water flow into the samples (5 ml for the UFA sample and 8 ml for the column). About four pore volumes of leachates were collected for each sample during the 47 hours of the experiment After the first 3 effluents were collected for each sample, the experiment was stopped and the samples were placed upright for 2 days in order to detect the effect of residence time on the leaching behavior. One half of each leachate was filtered through a 0.2 micron disposable filter, and the other half was analyzed unfiltered. Finally, selected filtered samples and

unfiltered portions of the samples were analyzed by ICP/MS. The results from these leaching studies will be used as baselines for the flow-through studies of apatite treatment as described below.

3.3.2 APATITE TREATMENT

The contaminated Bunker Hill soils were treated with North Carolina natural apatite in two different ways, either as a layer at the bottom of a UFA sample holder to reproduce the effect of field-emplaced permeable reactive barrier or mixed into the soils as an additive to reflect auguring or soil mixing as a field emplacement technology (Figure 8).

In the experiment of using an apatite layer at the bottom of a sample holder, 20 grams each of un-ground North Carolina (NC) natural apatite and Bunker Hill 2000 soil were packed into a UFA sample holder. To reduce the possibility of preferential flow and fingering, the sample was pre-wetted with 5 ml of synthetic vadose zone water. Then, the sample was run at 400 rpm and 1 ml per hour in a UFA. Leachate was observed after an additional 2 ml of water entered the sample. In total, about 7.5 pore volumes of leachate were collected from the sample during the 47 hours of the experiment. After the first three effluents were collected for each sample, the experiment was stopped and the samples were placed upright for two days in order to detect the effect of residence time on the metal leaching behavior after apatite treatment. One half of each leachate was filtered through a 0.2 micron disposable filter, and other half was analyzed unfiltered. Finally, selected filtered samples and unfiltered portions of the samples were analyzed by ICP/MS.

The Bunker Hill contaminated soils were also treated by mixing with ground and unground NC apatites. The unground apatite was mixed with Bunker Hill 2000 soil in the ratio of 10% apatite and 90% soil by weight, while the ground apatite was blended with Bunker Hill 4000 soil in the ratio of 1% apatite and 99% soil. Before each of the mixtures of soils and apatites were packed into UFA sample holder, a thin layer (~ 0.5 cm thick) of clean soil (McGee Ranch soil), which was also mixed with a corresponding amount of apatite, was packed into the bottom of the sample holder to serve as the lower contaminant boundary. All of the soil and apatite mixtures were packed pre-wetted into sample holders in a solid:water ratio of 5.5:1, in order to reduce the possibility of preferential flow and fingering. In the test of Bunker Hill 2000 soil mixed with unground apatite (10% by weight), two identical UFA samples were prepared, which were run with deionized water and with synthetic vadose zone water, respectively. The weights of the samples before and after running on a UFA at 1000 rpm and 0.6 ml per hour did not change much, indicating that the steady-state volumetric water content in the UFA run was approximately 30% and was reached

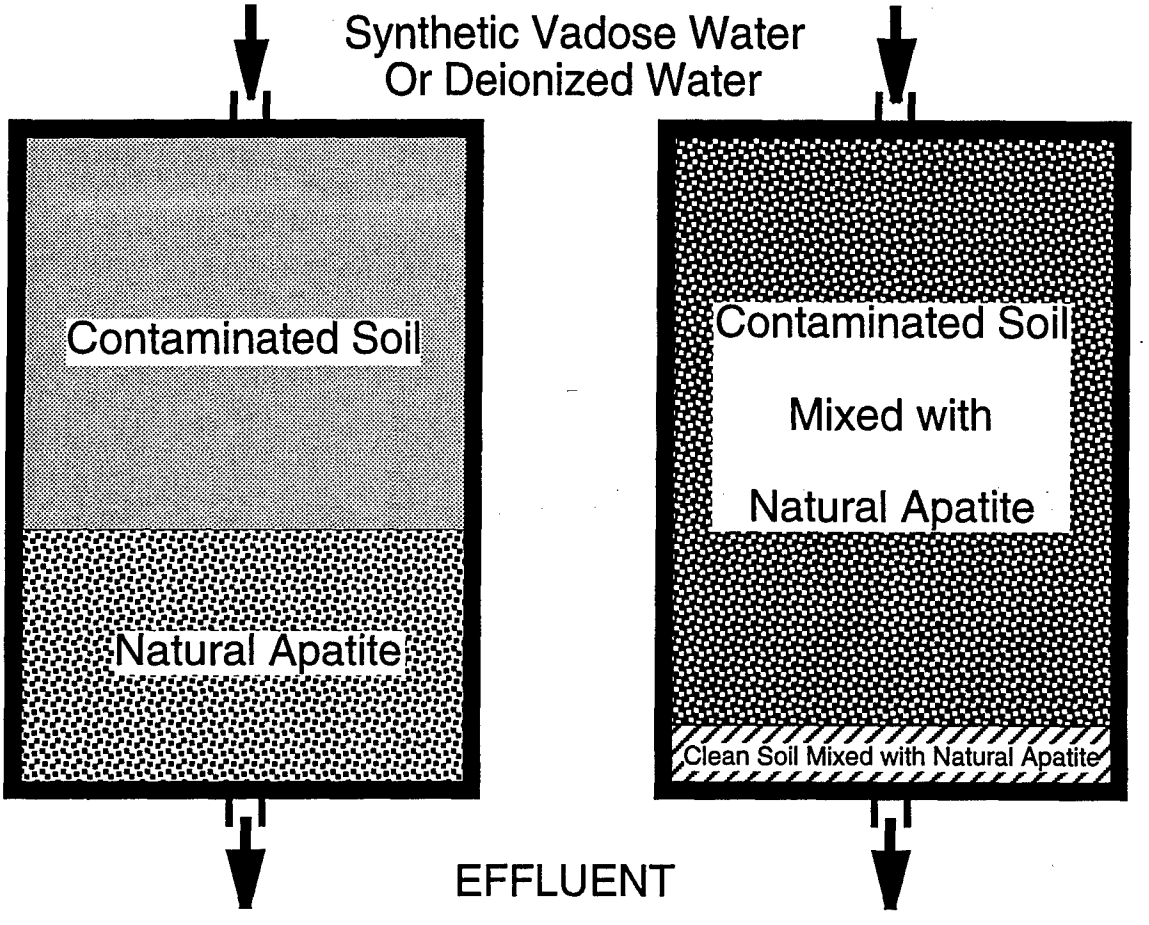

Figure 8. Apatite Treatment Experimental Designs for UFA Runs.

almost immediately. Leachates were collected every 24 hours in volumes equal to one effective pore volume. In total, thirty-two pore volumes were collected for the Bunker Hill 2000 soil with 10% un-ground apatite run with synthetic vadose water, eighteen for the Bunker Hill 2000 soil with 10% un-ground apatite run with deionized water, and fifty for the Bunker Hill 4000 soil with 1% ground apatite run with synthetic vadose water. Selected leachates were analyzed by ICP/MS and ion chromatography.

3.4 LEACHATE ANALYSIS

The leachate samples were analyzed for metal and anion concentrations on a VG PlasmaQuad II+ ICP/MS and an ion chromatograph. Two consecutive analytical runs were acquired for each sample. Results were then calculated using vendor-supplied software.

3.5 RESULTS

3.5.1 LEACHING OF UNTREATED CONTAMINATED SOILS

The elemental concentrations of the leachates from the UFA and column flow-through experiments are shown in Table 7 and Figures 9 and 10. In the UFA run, Pb concentrations constantly decrease from 586 $\mu g\ kg^{-1}$ in the first effluent of leachate to 296 $\mu g\ kg^{-1}$ in the fifth effluent, Zn from 17300 to 5400 $\mu g\ kg^{-1}$, and Cd from 256 to 49.5 $\mu g\ kg^{-1}$. In the soil column experiment, Pb concentrations range from 376 $\mu g\ kg^{-1}$ in the first leachate to 184 $\mu g\ kg^{-1}$ in the fifth leachate, Zn from 10700 to 3890 $\mu g\ kg^{-1}$, and Cd from 152 to 20.9 $\mu g\ kg^{-1}$. These suggest that the concentrations of the metals under progressive leaching decrease by several orders of magnitude. The metal leaching behaviors in the UFA and soil column runs are similar. The difference was observed in their response to the change in residence time. The fourth effluent of the leachates collected from the soil column after letting the sample sit for two days had higher Pb (but not Cd and Zn) concentrations than those of the third effluent, an effect not observed in the UFA run (Figures 9 and 10). However, the concentrations of Cd (but not Pb and Zn) in the fifth effluent of UFA run are slightly higher than those of the fourth effluent, which is different from the soil column data and may result from the variable response to the two-day sitting of the samples. Thus, it seems: 1) residence time has a significant effect on metal leaching, i.e., longer residence times may increase metal mobility; 2) UFA and soil column runs may respond to residence time differently, i.e., soil column run reacts faster than UFA runs; and 3) different metals may have variable responses to residence time even in the same run.

Table 7. Elemental Concentrations of untreated Bunker Hill Soil Leachates From UFA and Soil Column Experiments.

	Sample Type	Leaching Method	Filtered Leachate	Mg mg/L	Si mg/L	K mg/L	Ca mg/L	Mn mg/L	Zn mg/L	Al µg/L	Fe µg/L
1	BH2000	UFA-1	No	49.7	24.4	39.4	310	14	17.3	157	<100
2	BH2000	UFA-2	Yes	23.9	20.1	31.3	168	9.42	10.9	132	<100
3	BH2000	UFA-2	No	23.2	19.2	27.8	161	8.82	10.6	95.1	<100
4	BH2000	UFA-3	Yes	13.5	17.1	23.2	98.1	6.51	5.82	85.7	<100
5	BH2000	UFA-3	No	12.4	16.9	24.6	99.9	8.27	8.46	60.5	<100
6	BH2000	UFA-4	No	9.49	14.7	21	74	6.2	5.97	46.1	<100
7	BH2000	UFA-5	No	11.9	18.7	25.4	91.4	6.08	5.4	37	<100
8	BH2000	Column-1	Yes	31.1	19.7	32.4	198	9.36	10.7	156	<100
9	BH2000	Column-1	No	37.2	22.2	35.7	238	11.3	13.4	109	<100
10	BH2000	Column-2	Yes	19	18.1	26.6	128	8.25	8.56	102	<100
11	BH2000	Column-2	No	21.2	18.5	28	137	8.48	7.99	75.6	<100
12	BH2000	Column-3	Yes	11.9	14.8	23.3	94	7.08	6.48	82.2	<100
13	BH2000	Column-3	No	11.8	16	22.3	89.8	6.68	6.11	94.8	<100
14	BH2000	Column-4	No	13	19.4	22.4	81.4	7.89	5.34	737	800±100
15	BH2000	Column-5	No	11.3	16±2	20.1	75.2	16.3	3.89	255	490±50

	Sample Type	Leaching Method	Filtered Leachate	Ni µg/L	Cu µg/L	As µg/L	Sr µg/L	Cd µg/L	Ba µg/L	Hg µg/L	Pb µg/L
1	BH2000	UFA-1	No	51.577	42.36	<5	1080	255.5	274.73006	<5	586
2	BH2000	UFA-2	Yes	31.149	27±4	<5	675.08	125.7	165.82143	<5	449
3	BH2000	UFA-2	No	28.541	24±3	<5	640.49	121	156.32192	<5	442
4	BH2000	UFA-3	Yes	18.156	22.96	<5	418.25	59.31	131.48754	<5	353
5	BH2000	UFA-3	No	17.342	15.78	<5	430.06	72.19	146.56854	<5	339
6	BH2000	UFA-4	No	14±2	15.08	<5	331.76	43.37	129.84484	<5	327
7	BH2000	UFA-5	No	18±5	26±5	<5	429.26	49.52	155.91141	<5	296
8	BH2000	Column-1	Yes	73.614	34.45	<5	790.55	151.9	199.3599	<5	364
9	BH2000	Column-1	No	102.34	42±5	<5	885.47	175.2	219.40941	<5	376
10	BH2000	Column-2	Yes	28.656	23.12	<5	536.8	90.3	135.18587	<5	349
11	BH2000	Column-2	No	34±4	25±5	<5	581.52	98.04	143.40855	<5	367
12	BH2000	Column-3	Yes	22.206	15±2	<5	413.5	59.64	125.15782	<5	258
13	BH2000	Column-3	No	18.947	10.66	<5	392.73	53.97	116.19437	<5	264
14	BH2000	Column-4	No	30.163	19±4	<5	348.59	37.36	141.45405	<5	353
15	BH2000	Column-5	No	20.682	11.6	<5	364.7	20.94	125.46775	<5	184

Note --- Cs, La, Ce, Pr, Nd, Eu, Sm, Gd, Tb, Dy, Ho, Er, Tm, Yb, Lu, Th, and U were all detected at < 5 ppb.

Table 8. Soil Column and UFA Leaching Results for Pb, Zn, and Cd in Bunker Hill 2000 Soil.

Soil Column

Effluent Number	Filtered Leachate	Leachate Volume (ml)	Cumulative Pore Vol.	Zn (mg/kg) wt.%	Cd (mg/kg) wt.%	Pb (mg/kg) wt.%
1	Yes	6	1.75	0.0014	0.1519	0.0027
1	No	6	1.75	0.0017	0.1752	0.0028
2	Yes	6	2.50	0.0011	0.0903	0.0026
2	No	6	2.50	0.0010	0.0980	0.0028
3	Yes	5	3.13	0.0007	0.0497	0.0016
3	No	5	3.13	0.0007	0.0450	0.0017
4	No	6	3.50	0.0007	0.0374	0.0026
5	No	7	3.94	0.0006	0.0244	0.0016
Total		47	3.94	0.0078	0.6720	0.0184
ppm Concentration in Soil >>>>>>				1171	15	2000

UFA

Effluent Number	Filtered Leachate	Leachate Volume (ml)	Cumulative Pore Vol.	Zn (mg/kg) wt.%	Cd (mg/kg) wt.%	Pb (mg/kg) wt.%
1	No	6	1.50	0.0022	0.2555	0.0044
2	Yes	6	2.50	0.0014	0.1257	0.0034
2	No	6	2.50	0.0014	0.1210	0.0033
3	Yes	5	3.33	0.0006	0.0494	0.0022
3	No	5	3.33	0.0009	0.0602	0.0021
4	No	6	3.83	0.0008	0.0434	0.0025
5	No	7	4.42	0.0008	0.0578	0.0026
Total		41	4.42	0.0081	0.7129	0.0204
ppm Concentration in Soil >>>>>>				1171	15	2000

Table 8 shows the leaching behaviors of Cd, Pb, and Zn in the UFA and soil column experiments. After approximately four pore volumes of synthetic vadose water had flowed through the samples, less than 1 percent of each metal in the soil was leached out from the UFA and soil columns. This indicates that water leachable metals account for only a small amount of the total metals bound to the Bunker Hill samples. This is similar to other leaching studies on various metal-contaminated soils (e.g. Silviera and Sommers, 1977; Förstner and Kersten, 1988; Howard and Sova, 1993). In addition, the mobilities of the metals shown in Table 8 are in the order: Cd > Pb > Zn.

The above concentrations of metals in the leachates are from tens to tens of thousands of $\mu g\ kg^{-1}$(ppb) and establish the general ranges of metal concentrations in leachates to be expected during subsequent leaching tests. These are the concentrations that must be addressed by the apatite treatments.

3.5.2 APATITE TREATMENT

The elemental and anion concentrations of selected leachates from the UFA flow-through experiments are shown in Tables 9 and 10. The concentrations of selected metals (Pb, Cd, and Zn) are plotted along with untreated soil leachate metal concentrations, demonstrating the efficacy of the North Carolina apatite in the remediation of metal-contaminated soils (Figures 11 to 14). With the treatment by apatite either as a layer at the bottom of a UFA sample holder (Figure 11) or as a mixing additive (10% by weight) to the contaminated soils (Figures 12 and 13), the metal concentrations of the leachates are substantially decreased, most of them below ICP/MS detection limits. Even with only 1% ground apatite mixed with BH4000, the leachates have Pb, Cd, and Zn concentrations below ICP/MS detection limits (Figure 14). The use of synthetic vadose zone water or deionized water on the UFA runs does not show a major effect on the leaching behavior of apatite-treated soils (Figures 12 and 13). Although longer residence times increase metal mobility and different metals have variable responses to residence time in the leaching experiments of the untreated soils (Figures 9 and 10), the leaching behavior of the metals are not affected by the change of residence time after apatite treatment (Figure 11 to 14).

Table 9. Elemental Concentrations of Bunker Hill Soil Leachates From UFA Experiments After Apatite Treatment (Part 1).

Sample Type	Apatite (wt%)	Ground Apatite	Apatite Treatment	Water Used	Pore Volumes	Filtered Leachate	Mg (25) ng/ml	Al (27) ng/ml	Si (29) ng/ml	K (39) ng/ml	Ca (44) ng/ml	Mn (55) ng/ml
BH2		No	Layer	SVW	2.57	Yes	29200	33.9	14100	24300	174000	1720
BH2		No	Layer	SVW	2.57	No	27300	25.1	14600	24900	173000	1610
BH2		No	Layer	SVW	4.29	No	24300	27.5	12500	21400	138000	739
BH2		No	Layer	SVW	5.71	Yes	18000±2000	<5	9500±1200	16400	117000	420
BH2		No	Layer	SVW	5.71	No	22200	<5	12000	20600	138000	465
BH2		No	Layer	SVW	6.57	No	24000±3000	25.0	12000	21100	148000	416
BH2		No	Layer	SVW	7.43	No	36600	<5	8160	19500	215000	198
BH2	10	No	Mixed	DI	1	No	54100	73.3	25300	18500	295000	610
BH2	10	No	Mixed	DI	2	No	39000	21±5	20200	17800	232000	1410
BH2	10	No	Mixed	DI	3	No	28500	13±4	20100	17400	188000	1730
BH2	10	No	Mixed	DI	10	No	8310	15.1	12600	9890	96200	2330
BH2	10	No	Mixed	DI	18	No	4970	44±10	10900	6800	67400	2310
BH2	10	No	Mixed	SVW	1	No	58600	31±4	25800	18100	306000	123
BH2	10	No	Mixed	SVW	2	No	43500	19±3	21600	19200	247000	1420
BH2	10	No	Mixed	SVW	3	No	31800	15.2	20100	18900	182000	941
BH2	10	No	Mixed	SVW	10	No	9510	65±27	12200	11400	100000	2390
BH2	10	No	Mixed	SVW	20	No	6260	11±3	11000	8360	76700	2840
BH2	10	No	Mixed	SVW	30	No	5180	<5	13800	8270	70300	5420
BH2	10	No	Mixed	SVW	40	No	4740	<5	12700	6410	60300	5610
BH4	1	Yes	Mixed	SVW	1	No	42700	17±2	25700	15900	245000	17.3
BH4	1	Yes	Mixed	SVW	2	No	31000	18±5	20400	13600	195000	342
BH4	1	Yes	Mixed	SVW	3	No	22700	24±15	23900	16900	185000	969
BH4	1	Yes	Mixed	SVW	10	No	8740	<5	18800	12600	108000	4650
BH4	1	Yes	Mixed	SVW	20	No	4080	<5	13300	7320	72700	5510

Note: DI = Deionized water; SVW = Synthetic vadose water.

Table 9. Elemental Concentrations of Bunker Hill Soil Leachates From UFA Experiments After Apatite Treatment (Part 2).

Sample Type	Apatite (wt%)	Ground Apatite	Apatite Treatment	Water Used	Pore Volumes	Filtered Leachate	Fe (56) ng/ml	Ni (60) ng/ml	Cu (65) ng/ml	Zn (68) ng/ml	As (75) ng/ml
BH2		No	Layer	SVW	2.57	Yes	<100	31.0	8.6±3.2	198	<5
BH2		No	Layer	SVW	2.57	No	<100	34±6	7.1±2.8	200±30	<5
BH2		No	Layer	SVW	4.29	No	<100	31.1	<5	74.7	<5
BH2		No	Layer	SVW	5.71	Yes	<100	21.6	<5	22.2	<5
BH2		No	Layer	SVW	5.71	No	<100	29.2	<5	20±10	<5
BH2		No	Layer	SVW	6.57	No	<100	42.6	<5	51.4	<5
BH2		No	Layer	SVW	7.43	No	<100	60±7	<5	19±3	<5
BH2	10	No	Mixed	DI	1	No	(<50)	20±4	79.4	<1	54±6
BH2	10	No	Mixed	DI	2	No	(<50)	12±2	33.7	<1	21.8
BH2	10	No	Mixed	DI	3	No	(<50)	11.0	11.2	<1	17.1
BH2	10	No	Mixed	DI	10	No	(82±20)	10.6	7.5±2.0	<1	30.2
BH2	10	No	Mixed	DI	18	No	(682)	3.1±0.5	6.87	<1	42.0
BH2	10	No	Mixed	SVW	1	No	(<50)	14.2	62.6	<1	43.1
BH2	10	No	Mixed	SVW	2	No	(<50)	8.8±1.1	32.4	<1	29.3
BH2	10	No	Mixed	SVW	3	No	(<50)	10.3	25.7	<1	24±3
BH2	10	No	Mixed	SVW	10	No	(<50)	10.3	8.52	<1	36.3
BH2	10	No	Mixed	SVW	20	No	(641)	5.73	6.5±3.2	<1	46.5
BH2	10	No	Mixed	SVW	30	No	1850	7.26	<5	<5	44.0
BH2	10	No	Mixed	SVW	40	No	1670	<5	<5	<5	37.1
BH4	1	Yes	Mixed	SVW	1	No	(<50)	11.4	45.0	<1	57.2
BH4	1	Yes	Mixed	SVW	2	No	(<50)	6.8±2.2	21±7	<1	37.0
BH4	1	Yes	Mixed	SVW	3	No	<100	9.31	9.05	<5	24±6
BH4	1	Yes	Mixed	SVW	10	No	<100	8.35	<5	<5	15.1
BH4	1	Yes	Mixed	SVW	20	No	543	<5	10.5	<5	27.7

Note: DI = Deionized water; SVW = Synthetic vadose water.

Table 9. Elemental Concentrations of Bunker Hill Soil Leachates From UFA Experiments After Apatite Treatment (Part 3).

Sample Type	Apatite (wt%)	Ground Apatite	Apatite Treatment	Water Used	Pore Volumes	Filtered Leachate	Sr (88) ng/ml	Cd (114) ng/ml	Ba (138) ng/ml	Hg (200) ng/ml	Pb (208) ng/ml
BH2		No	Layer	SVW	2.57	Yes	1710	<5	10.3	<5	1.7±1.5
BH2		No	Layer	SVW	2.57	No	1600	<5	9.59	6.26	<1
BH2		No	Layer	SVW	4.29	No	1510	<5	<5	<5	<1
BH2		No	Layer	SVW	5.71	Yes	1340	<5	<5	<5	<1
BH2		No	Layer	SVW	5.71	No	1560	<5	<5	<5	<1
BH2		No	Layer	SVW	6.57	No	1670	<5	<5	<5	<1
BH2		No	Layer	SVW	7.43	No	2570	<5	<5	<5	<1
BH2	10	No	Mixed	DI	1	No	1700	<5	795	<5	<1
BH2	10	No	Mixed	DI	2	No	1310	<5	695	<5	<1
BH2	10	No	Mixed	DI	3	No	979	<5	541	5.5±1.4	<1
BH2	10	No	Mixed	DI	10	No	501	<5	247	<5	<1
BH2	10	No	Mixed	DI	18	No	371	<5	148	<5	<1
BH2	10	No	Mixed	SVW	1	No	1670	<5	867	<5	<1
BH2	10	No	Mixed	SVW	2	No	1350	<5	706	<5	<1
BH2	10	No	Mixed	SVW	3	No	1110	<5	501	<5	<1
BH2	10	No	Mixed	SVW	10	No	594	<5	274	<5	<1
BH2	10	No	Mixed	SVW	20	No	449	<5	173	<5	<1
BH2	10	No	Mixed	SVW	30	No	432	<5	133	<5	<5
BH2	10	No	Mixed	SVW	40	No	388	<5	110	<5	<5
BH4	1	Yes	Mixed	SVW	1	No	1120	<5	575	<5	<1
BH4	1	Yes	Mixed	SVW	2	No	1020	<5	563	<5	<1
BH4	1	Yes	Mixed	SVW	3	No	979	<5	560	<5	<5
BH4	1	Yes	Mixed	SVW	10	No	520	<5	352	<5	<5
BH4	1	Yes	Mixed	SVW	20	No	376	<5	222	<5	<5

Note: DI = Deionized water; SVW = Synthetic vadose water.

Table 10. Anion Concentrations of Bunker Hill Soil Leachates From UFA Experiments After Apatite Treatment.

Sample Type	Apatite (wt%)	Ground Apatite	Apatite Treatment	Water Used	Pore Volumes	pH	Phosphate µg/ml	Fluoride µg/ml	Chloride µg/ml	Nitrite µg/ml	Nitrate µg/ml	Sulfate µg/ml
BH2	10	No	Mixed in	DI	1	NA	0.19	NA	NA	NA	NA	NA
BH2	10	No	Mixed in	DI	2	NA	<0.10	NA	NA	NA	NA	NA
BH2	10	No	Mixed in	DI	3	NA	<0.10	NA	NA	NA	NA	NA
BH2	10	No	Mixed in	DI	6	8.0	<0.10	0.90	1.90	<0.90	1.62	133.00
BH2	10	No	Mixed in	DI	10	NA	<0.10	NA	NA	NA	NA	NA
BH2	10	No	Mixed in	DI	16	4.2	<0.10	0.75	2.02	<0.90	1.55	22.20
BH2	10	No	Mixed in	SVW	1	NA	<0.10	NA	NA	NA	NA	NA
BH2	10	No	Mixed in	SVW	2	NA	<0.10	NA	NA	NA	NA	NA
BH2	10	No	Mixed in	SVW	6	8.1	<0.10	1.04	21.50	<0.90	1.66	175.00
BH2	10	No	Mixed in	SVW	10	NA	<0.10	NA	NA	NA	NA	NA
BH2	10	No	Mixed in	SVW	16	8.4	<0.10	0.96	22.00	<0.90	1.60	56.90
BH2	10	No	Mixed in	SVW	20	NA	<0.10	NA	NA	NA	NA	NA
BH4	1	Yes	Mixed in	SVW	1	NA	0.22	NA	NA	NA	NA	NA
BH4	1	Yes	Mixed in	SVW	2	NA	0.13	NA	NA	NA	NA	NA

Note: DI = Deionized water; SVW = Synthetic vadose water; NA = Not analyzed.

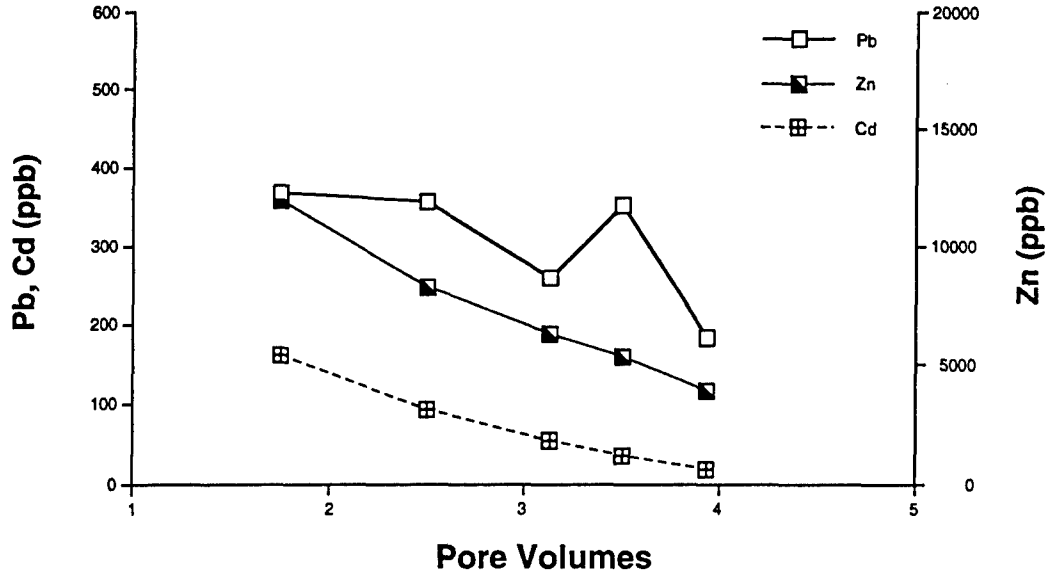

Figure 9. Concentrations of Metals in Effluents From the Soil Column Gravity Drain Experiment on Untreated BH2000 Soil.

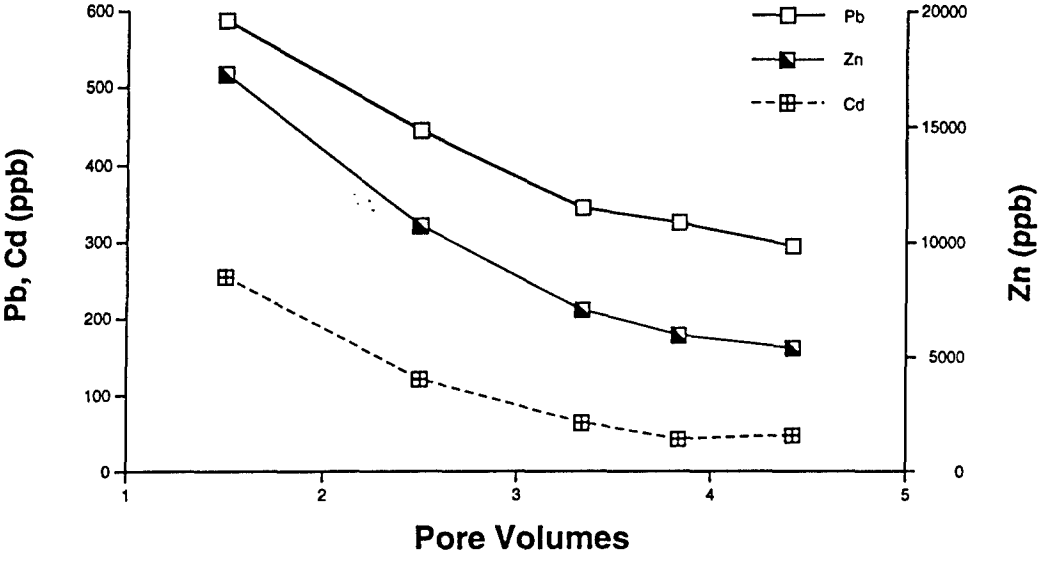

Figure 10. Concentrations of Metals in Effluents From UFA Flow Through Experiments on Untreated BH2000 Soil.

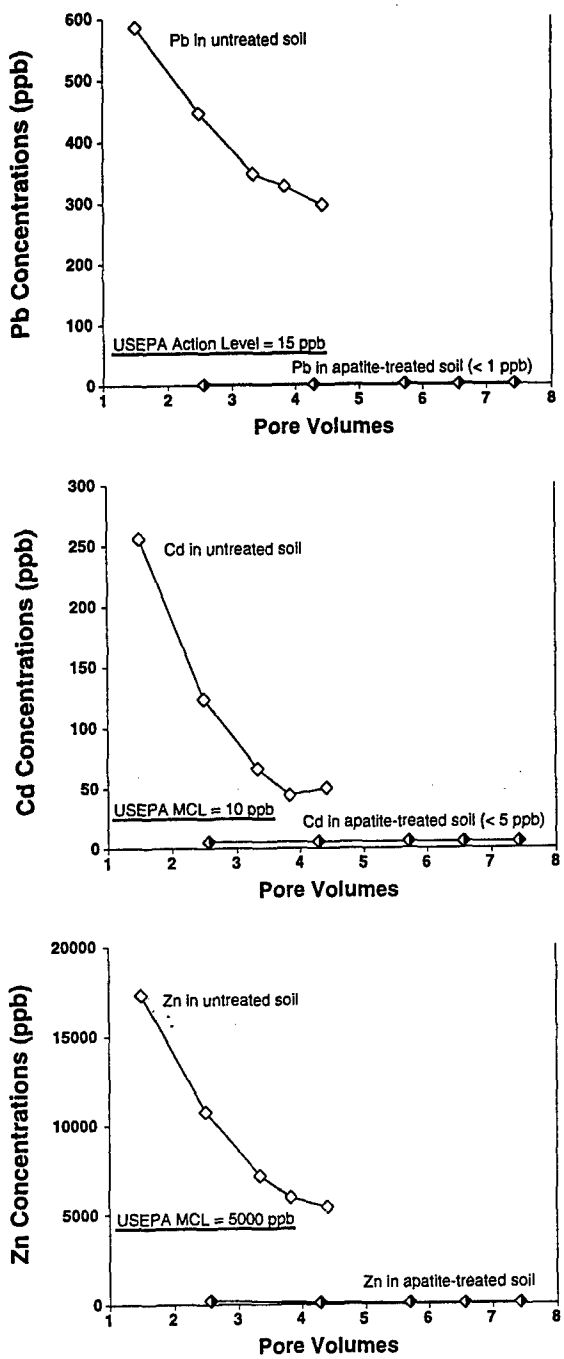

Figure 11. UFA Desorption/Sorption run on BH2000 Soil With a Layer of Un-Ground NC Apatite at the Bottom of the Sample Holder using Synthetic Vadose Zone Water, Recharge = 2×10^{-7}cm/s.

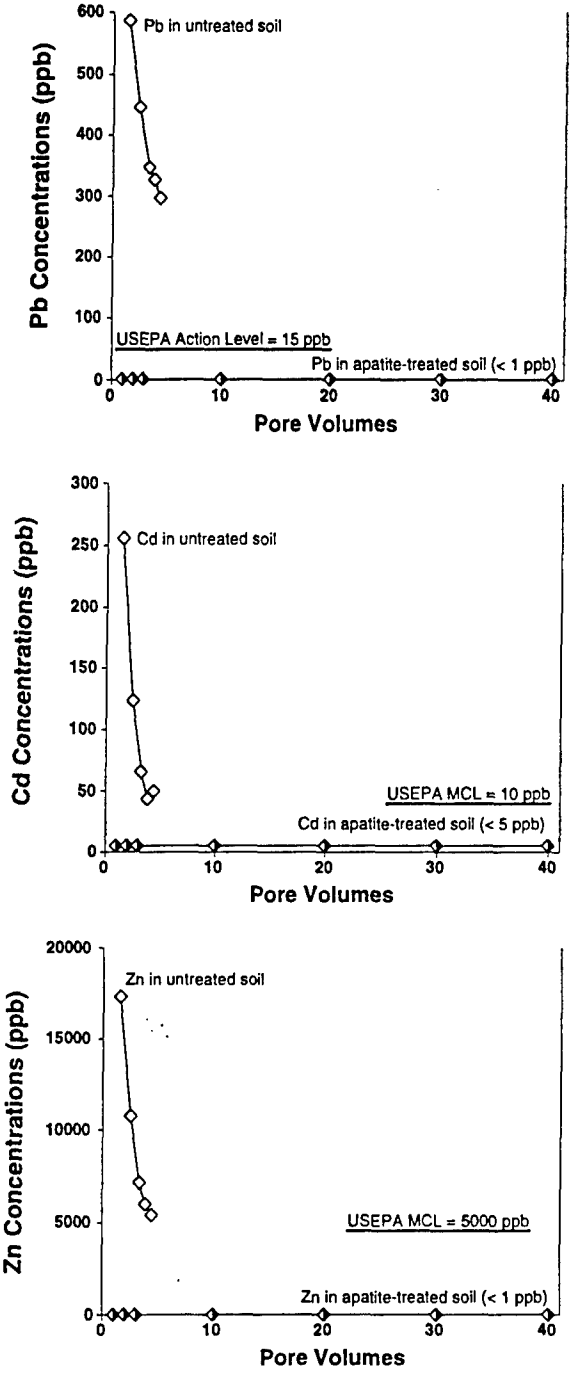

Figure 12. UFA Desorption/Sorption run on BH2000 Soil Mixed With 10% Un-Ground NC Apatite using Synthetic Vadose Zone Water, Recharge = 2 x 10^{-7}cm/s.

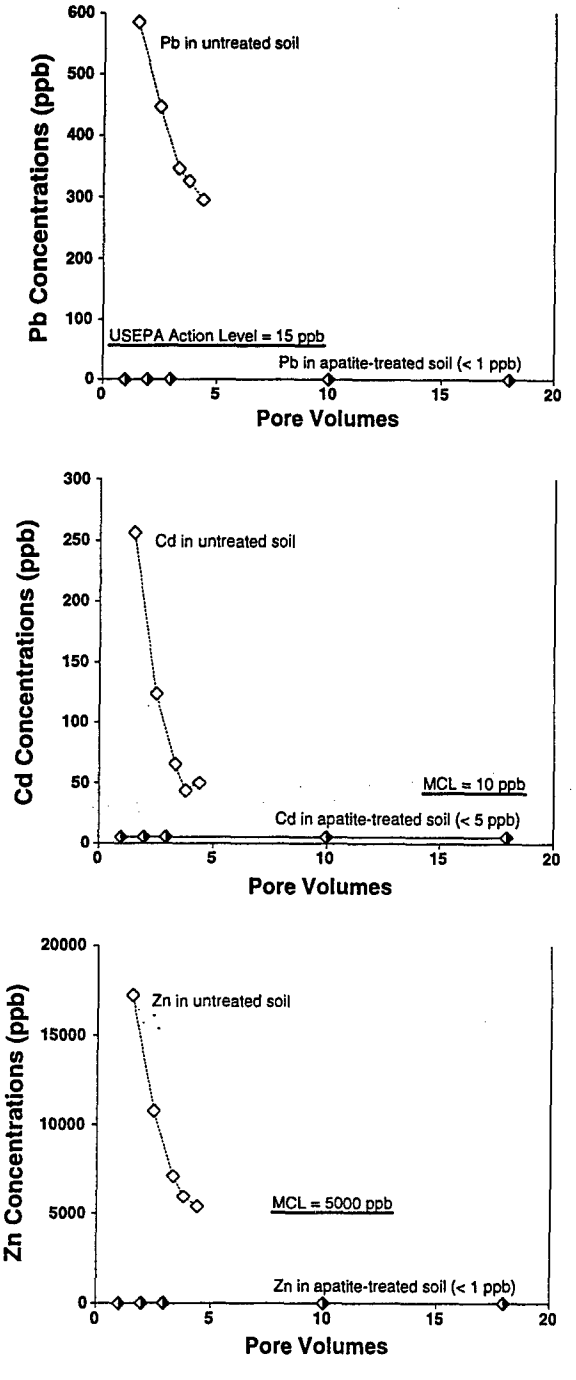

Figure 13. UFA Desorption/Sorption run on BH2000 Soil Mixed With 10% Un-Ground NC Apatite using Deionized Water, Recharge = 2 x 10^{-7}cm/s.

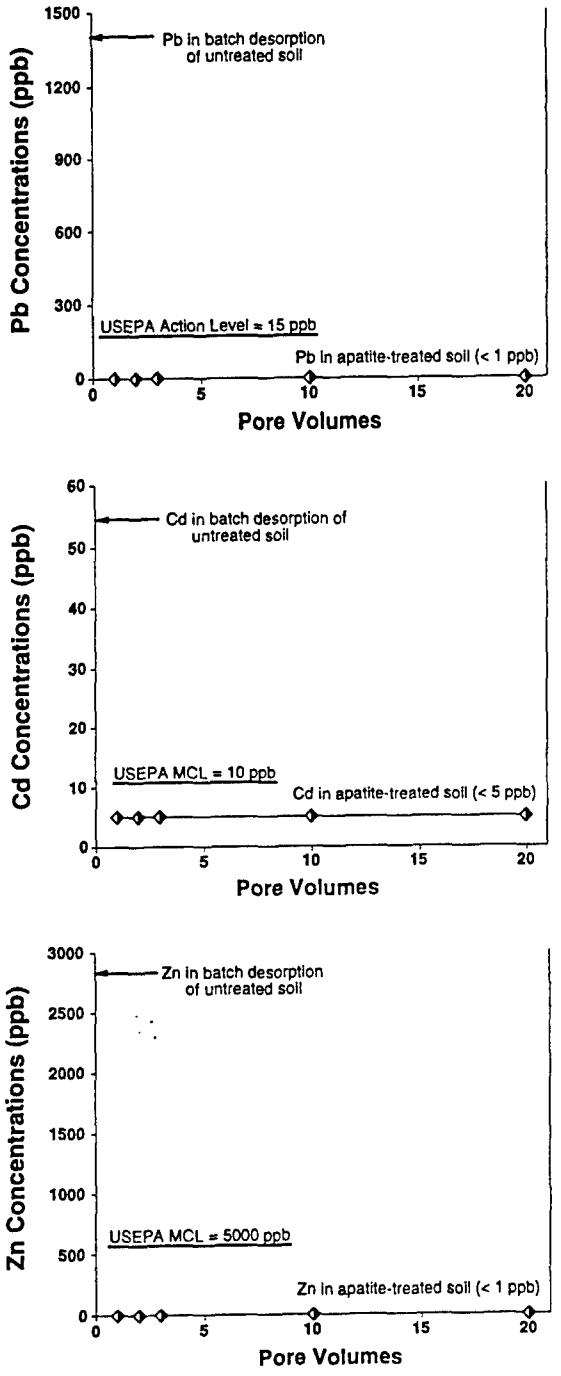

Figure 14. UFA Desorption/Sorption run on BH4000 Soil Mixed With 1% Ground NC Apatite using Synthetic Vadose Zone Water, Recharge = 2 x 10^{-7}cm/s.

3.6 CONCLUSIONS OF THE BATCH AND FLOW-THROUGH STUDY

In summary, the results of the batch and flow-through experiments of both untreated and apatite-treated contaminated soils result in the following conclusions.

- The concentrations of Zn, Pb, and Cd in the leachate effluents of the UFA and soil column flow through experiments for the untreated Bunker Hill contaminated soils differ by several orders of magnitude, varying from tens to tens of thousands of µg/kg (ppb).

- The metal leaching behaviors in the UFA and soil column runs for the untreated soils are similar. A difference was observed in their response to the change of residence time. Soil column runs react faster than UFA runs, and different metals may behave differently within each of the flow through experiments.

- Longer residence times increase metal mobility in the untreated soils.

- Water leachable metals account for only a small amount of the total metals in the untreated soils. The mobility of the primary metals of concern are in this order: Cd > Pb > Zn.

- All of the concentrations of Pb, Cd, and Zn in the leachate effluents of the UFA flow-through experiments of apatite-treated Bunker Hill soils are below USEPA regulatory limits and most of them are below the detection limits of ICP/MS.

- The change of residence time has no apparent effect on the leaching behaviors of the metals after apatite treatment.

- During the 24-hour adsorption isotherm, the greatest reduction of desorbed Pb, Zn, Mn, and Cd by the addition of NC apatite is at 1% or less.

- During the 48-hour adsorption isotherm, the greatest reduction of desorbed Pb, Zn, Mn and Cd by the addition of NC apatite is at 1% or less and is actually depicted by the NC apatite concentrations of .005, .002, and .08%.

- The greatest reduction of desorbed Pb at less than 1% added NC apatite confirms the molar ratio calculation scenario of Pb:PO_4 for pyromorphytes.

- The kinetics of formation for Pb, Zn, and Cd phosphate complexes are 24 hours or less.

- Thermodynamic predictions for the formations of pyromorphytes at less than 1%

addition of NC apatite confirm the molar ratio calculation scenario of Pb:PO_4 for pyromorphytes and also confirm the precipitation of Pb at less than 1% NC apatite in the adsorption isotherms.

- Thermodynamic predictions for the formation of rhodochrosite ($MnHPO_4$) at less than 1% addition of NC apatite confirm the precipitation of Mn at less than 1% NC apatite in the 24- and 48-hour adsorption isotherms.

- Thermodynamic predictions for the formation of Hopeite ($Zn_3(PO_4)_2\ 4H_2O$) at less than 1% addition of NC apatite confirm the precipitation of Zn at less than 1% NC apatite in the 24- and 48-hour adsorption isotherms.

- The thermodynamic prediction for the formation of $Cd_3(PO_4)_2$ is not substantiated by MINTEQ-A2. However, the adsorption isotherm shows an 83% reduction of desorbed Cd at less than 1% addition of NC apatite.

4.0 APATITE FORMULATIONS AND EMPLACEMENT STRATEGIES

The results of the experiments described above establish that apatite can be an effective chemical stabilization agent for lead, cadmium, manganese, and zinc. The purpose of this section is to discuss potential apatite formulations, both chemical and physical, that could be used for remediating contaminated soils or other solids. The chemical properties of apatite vary depending on its source. It may be chemically synthesized, biogenic, or mined, and the particular source of the mined deposit or biogenic material will affect its chemical constituents and its reactivity. Grinding the material has also been seen to improve its reactivity, perhaps by creating a larger and "fresher" surface for reaction with ions in solution. Several types of apatite have been tested as part of this project, and the results are presented in section 5.1 below.

In addition to the chemical makeup, the physical formulation of the apatite can be varied. In our experiments to date, apatite material was simply added as a granulated solid to the samples being treated. However, we recognize that remediation of soils or other solids in the field may require delivery of the apatite into the ground in the form of a slurry or solution. Section 5.2 discusses several potential emplacement strategies, technical issues associated with those strategies, characteristics of sites for which those strategies are appropriate, and their relative advantages and disadvantages. An emplacement contractor will require certain data on the physical properties of the apatite in order to ensure that the equipment can deliver it. Section 5.3 provides such data, including measurements of the flow properties of apatite slurries as a function of solids content and particle size. Finally, costs of apatite treatment per unit of treated soil are estimated in section 5.4.

4.1 CHEMICAL FORMULATION

Apatite is available commercially from a variety of sources, each having slightly different chemical compositions. These materials vary in their effectiveness in immobilizing metals depending on their carbonate and trace metal concentrations. Carbonate substitution into apatite increases the solubility of its the phosphate (Chien and Hammond,1978), which can then react with metal contaminants. However, trace metal impurities reduce phosphorus solubility and hence effectiveness.

We compared the effectiveness of four different apatites using batch adsorption tests of the type described above in section 3. The four apatites tested were:

- A synthetic hydroxyapatite (HAP), tribasic calcium phosphate, from Aldrich Chemical Company. This material is a reagent grade, laboratory precipitated powder with few impurities. Its chemical composition is given in Table 11.

Table 11. Reported Analysis for Reagent Grade Synthetic Apatite.

CALCIUM PHOSPHATE TRIBASIC **CERTIFIED**
Precipitated powder

Hydroxylapatite
Approx. $Ca_{10}(OH)_2(PO_4)_6$

Product Specifications
Actual Lot Analysis is reported on label.

Insolube in dilute HCl	≤0.010%
Dibasic or Free CaO	To pass test
Chloride	≤0.010%
Sulfate	≤0.02%
Ammonia	≤0.02%
Arsenic	≤1ppm
Barium	≤0.01%
Heavy Metals (as Pb)	≤0.002%
Iron	≤0.005%
Magnesium	≤0.20%
Soluble Salts	≤1.5%

- SRM 120b Florida phosphate rock, a naturally occuring apatite mineral mined in Florida. This material serves as a NIST chemical standard, for which it has been ground into a fine powder and is well mixed to provide homogeneous aliquots. The composition of Florida apatite is given in Table 12.

- North Carolina apatite, an unprocessed (not acidified or ground), natural ore commercially available from Texasgulf, Inc, for use as a fertilizer. Its composition is given in Table 13.

- A biogenic apatite from fish cannery wastes. This material is primarily fish bones, cleaned and dried to remove most of the organic material and ground to pass a 170-mesh (0.090 mm) sieve. Such wastes are a potential low-cost source of apatite, but they also contain organics, the effect of which have not been investigated, although they appear to have little influence on the stabilization of metals.

Both the Florida and North Carolina apatites are carbonate fluorapatites from naturally occurring marine deposits. Therefore, they contain some impurities that will affect the amount of phosphate available for dissolution.

As received from the supplier, the North Carolina apatite is a fairly coarse material, with more than 50% retained on a 65-mesh (0.210 mm) screen. The other apatite samples are fine powders, which have larger specific surface areas and can also dissolve quickly. To control for and study the effect of particle size, we also tested a sample of the North Carolina apatite ground to pass a 170-mesh sieve.

In each experiment, three grams of the BH4000 soil was mixed with apatite at apatite-to-soil ratios of 1:100, 1:20, 1:10, and 1:5 by weight. Thirty grams of deionized water were added to the solids in polycarbonate tubes. The tubes containing the slurries were shaken continuously for either 24 or 48 hours. Supernatants were obtained by centrifuging and filtering the samples and were analyzed by ICP-MS.

The results for several metals are shown in Figures 15-18. Similar tests without apatite, described in the Milestone Two Report, established the baseline concentrations of leached metals. These values are included in the figures as the results for 0% apatite. The treated values are reported as 1%, 5%, 10%, and 20% apatite as a fraction of total solids. Figure A shows lead concentration versus per cent apatite addition for the different types of apatite. The cannery material is the most effective at pulling lead out of solution, with 1% apatite sufficient to bring the lead concentration nearly below the ICP-MS detection limit of 1 ng ml^{-1} (ppb). The synthetic, powdered hydroxyapatite is nearly as effective, and the ground NC apatite also performs well. The unground NC apatite and the Florida apatite are less effective.

Table 12. Reported Analysis for Florida Phosphate Rock

U. S. Department of Commerce
Peter G. Peterson
Secretary

National Bureau of Standards

Certificate of Analysis

Standard Reference Material 120b

Phosphate Rock

(Florida)

This standard is a finely powdered material intended for use in checking chemical methods of analysis and in calibration with optical emission and x-ray spectrometric methods of analysis.

Percent by Weight

ANALYST[a]	P_2O_5	CaO	SiO_2	F	Soluble Fe_2O_3	Soluble Al_2O_3	MgO	Na_2O	MnO	K_2O		TiO_2	CO_2	CdO
1	34.51[a]	49.42[h]	4.70[c]	3.82[d]	1.10[e]	1.09[f,g]	0.29[h]	0.33[f]	0.032[i]	0.12[f,j]	--	0.15[k]	--	0.002[l]
2	34.51[m]	49.35[m]	4.73[n]	3.79[m]	1.10[h]	1.07[h]	.28[h]	.36[h]	.031[h]	.12[j]	0.09[o]	--	2.76[p]	.002[h]
3	34.66[n]	49.38[m]	4.67[q]	3.83	1.09[h]	1.07[h]	.30	.36[h]	.032[h]	.12[j]	.098[o]	.15	2.79	.002[h]
4	34.67[r]	49.47[m]	4.69[q]	3.81[s]	1.13[h]	1.04[h]	.28[h]	.35[h]	.032[h]	--	.087[o]	.15[k]	2.78[p]	.003[h]
5	34.57	49.32[m]	4.63[q]	3.86	1.06[h]	1.05[h]	.25[h]	.34[h]	--	--	.085[o]	--	2.83	--
6	34.48[m]	49.45[m]	--	3.92[s]	1.14[m]	1.07[t]	--	--	--	--	--	--	--	--
Average	34.57	49.40	4.68	3.84	1.10	1.06	0.28	0.35	0.032	0.12	0.090	0.15	2.79	0.002

[a] Phosphorus precipitated with magnesia mixture, ignited and weighed as $Mg_2P_2O_7$.

[b] Calcium precipitated as oxalate, ignited and weighed as CaO.

[c] Sample fused with Na_2CO_3, silica precipitated with ZnO and dehydrated with HCl. Traces of SiO_2 recovered by H_2SO_4 dehydration.

[d] Fluorine distilled into NaOH solution and precipitated as lead chlorofluoride. Chloride is precipitated with excess $AgNO_3$ and excess $AgNO_3$ is titrated with standard KCNS solution.

[e] $SnCl_2$ reduction – $K_2Cr_2O_7$ titration.

[f] Flame emission spectrometry with repetitive optical scanning.

[g] A value of 1.13 percent was obtained for total Al_2O_3 by gravimetry.

[h] Atomic absorption spectrometry.

[i] KIO_4 spectrophotometric method.

[j] Sample digested with mixed acids for 1 hour. Determination completed by atomic absorption spectrometry.

[k] H_2O_2 spectrophotometric method.

[l] Polarographic method.

[m] Volumetric method.

[n] Gravimetric method.

[o] Sample digested with dilute HCl or aqua regia for 15 minutes. Determination completed by atomic absorption spectrometry.

[p] CO_2 absorbed and weighed.

[q] Dehydration with $HClO_4$ in presence of boric acid.

[r] Molybdovanadophosphate spectrophotometric method.

[s] Distillation – titration with standard thorium nitrate solution.

[t] Aluminum precipitated with 8 hydroxyquinoline and weighed.

Washington, D.C. 20234
July 31, 1972

J. Paul Cali, Chief
Office of Standard Reference Materials

Table 13. Reported Analysis for North Carolina Natural Phosphate

Texasgulf

North Carolina Natural Phosphate (NCNP)

30% P_2O_5 - For Use As A Fertilizer In Acid Soil

NCNP is a natural source of Phosphorus and Calcium derived from marine sediments. NCNP has not been subjected to acidulation or grinding.

Typical Analysis - (dry basis)

Component	Typical Percent
Total Phosphorus, as P	13.2
Total Phosphorus, as P_2O_5	30.3
Calcium, as CaO	48.8
Magnesium, as MgO	0.6
Total Sulphur, as S	1.3
Total Carbon, as C	3.1
Zinc, as Zn	313 ppm
Boron, as B	95 ppm
Molybdenum, as Mo	45 ppm
Copper, as Cu	13 ppm

Soluble Phosphorus	% of total P
–in Water	0
–in Neutral Ammonium Citrate	13
–in 2% Citric Acid	37
–in 2% Formic Acid	72
–in HNO_3/HCl	100

Physical Characteristics

Screen Analysis (Tyler)	Sieve Opening	%
Passing 14 mesh	1.190 mm	100
Passing 35 mesh	0.420 mm	97
Passing 65 mesh	0.210 mm	49
Passing 100 mesh	0.149 mm	19
Passing 200 mesh	0.074 mm	1
Surface Area (B.E.T.)	22 m^2/mg	

Bulk Density	
Loose	1.44 g/cm^3 (90 lbs/ft^3)
Tamped	1.60 g/cm^3 (100 lbs/ft^3)

Color	Brownish Black

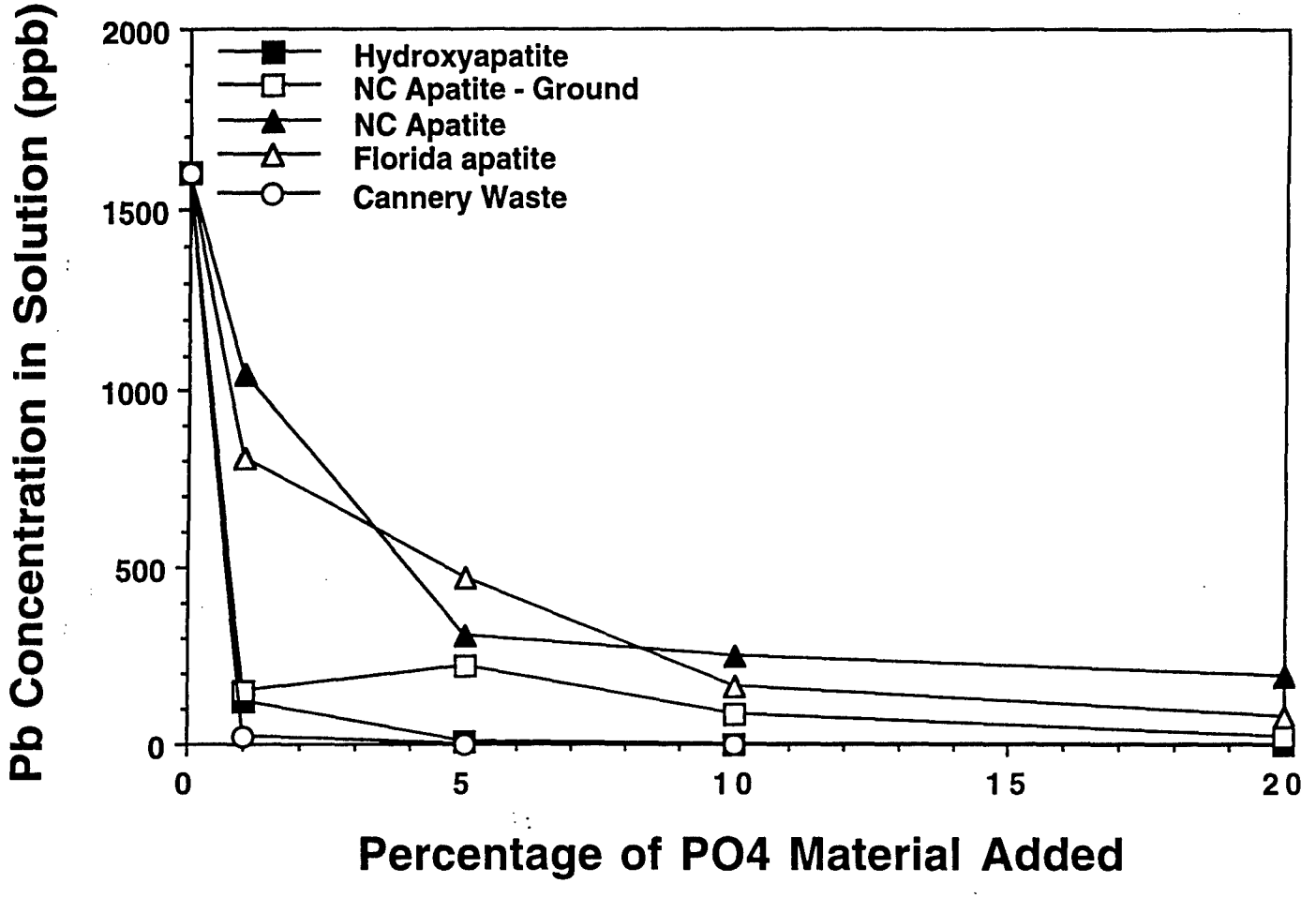

Figure 15. Lead Desorption/Sorption Results From Batch Tests Using Bunker Hill 4000 Soil and Deionized Water in a Water:Soil Ratio of 10:1. Lead Concentrations are Plotted as a Function of Phosphate Material Added as a Weight Percent of Total Sample.

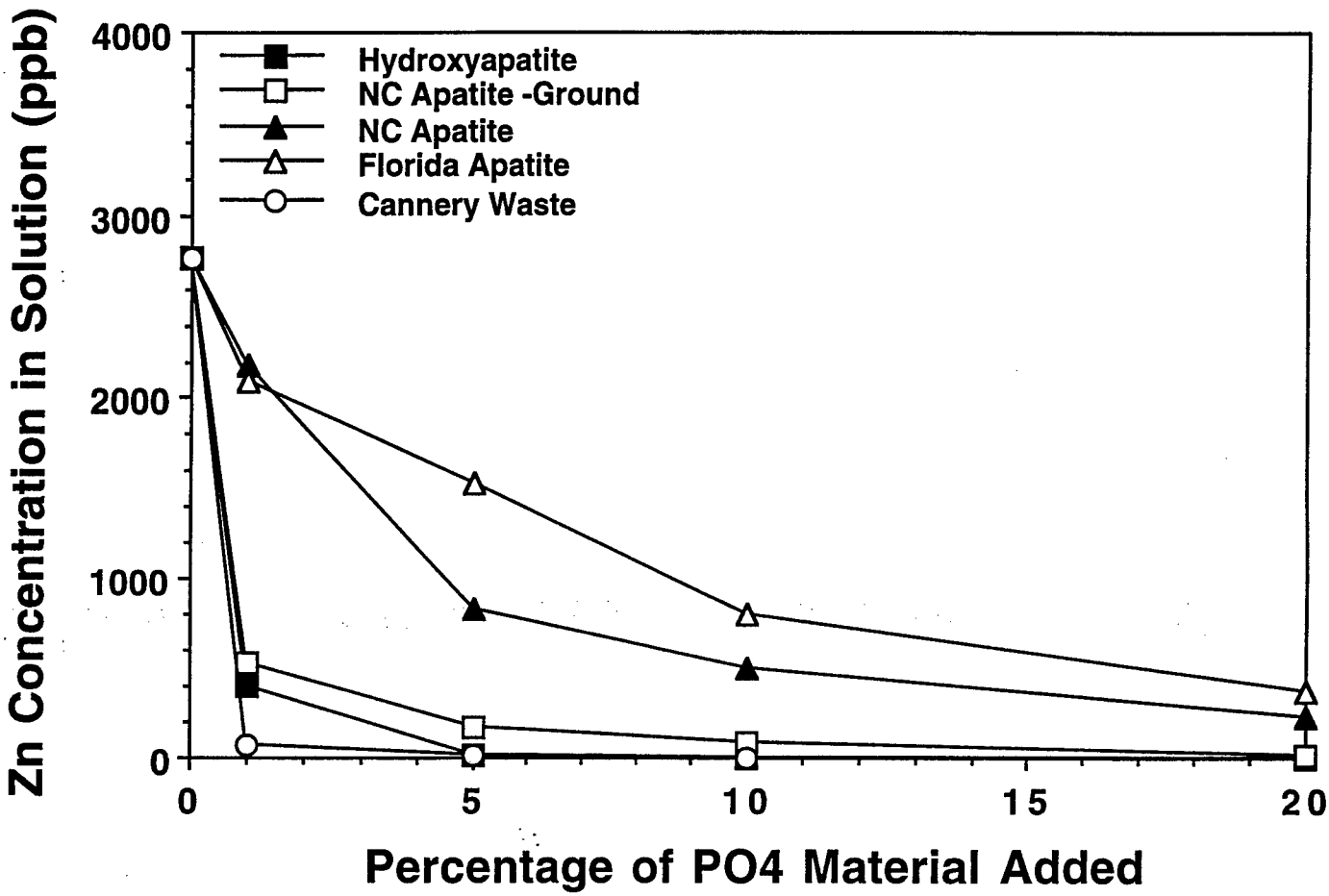

Figure 16. Zinc Desorption/Sorption Results From Batch Tests Using Bunker Hill 4000 Soil and Deionized Water in a Water:Soil Ratio of 10:1. Zinc Concentrations are Plotted as a Function of Phosphate Material Added as a Weight Percent of Total Sample.

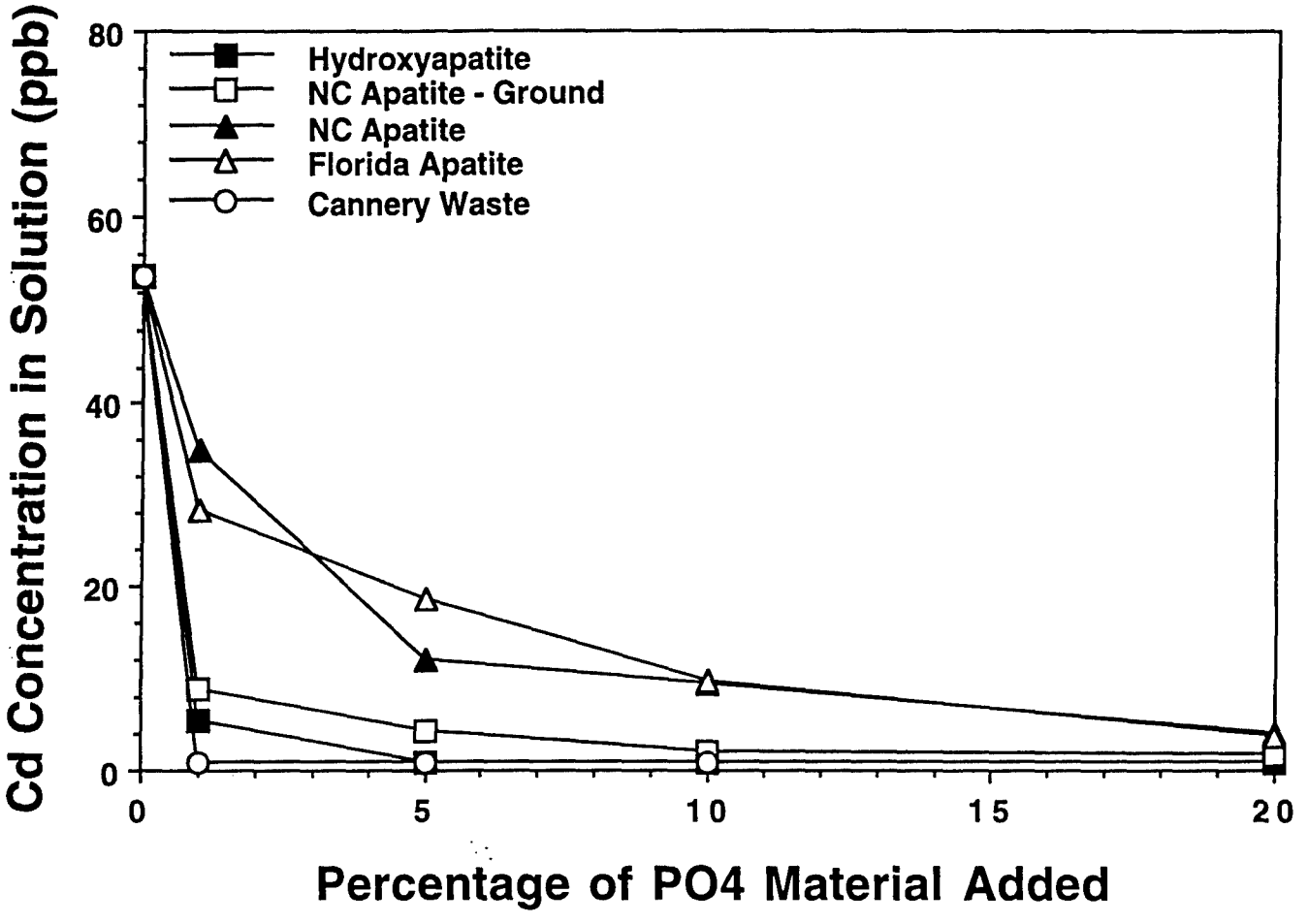

Figure 17. Cadmium Desorption/Sorption Results From Batch Tests Using Bunker Hill 4000 Soil and Deionized Water in a Water:Soil Ratio of 10:1. Cadmium Concentrations are Plotted as a Function of Phosphate Material Added as a Weight Percent of Total Sample.

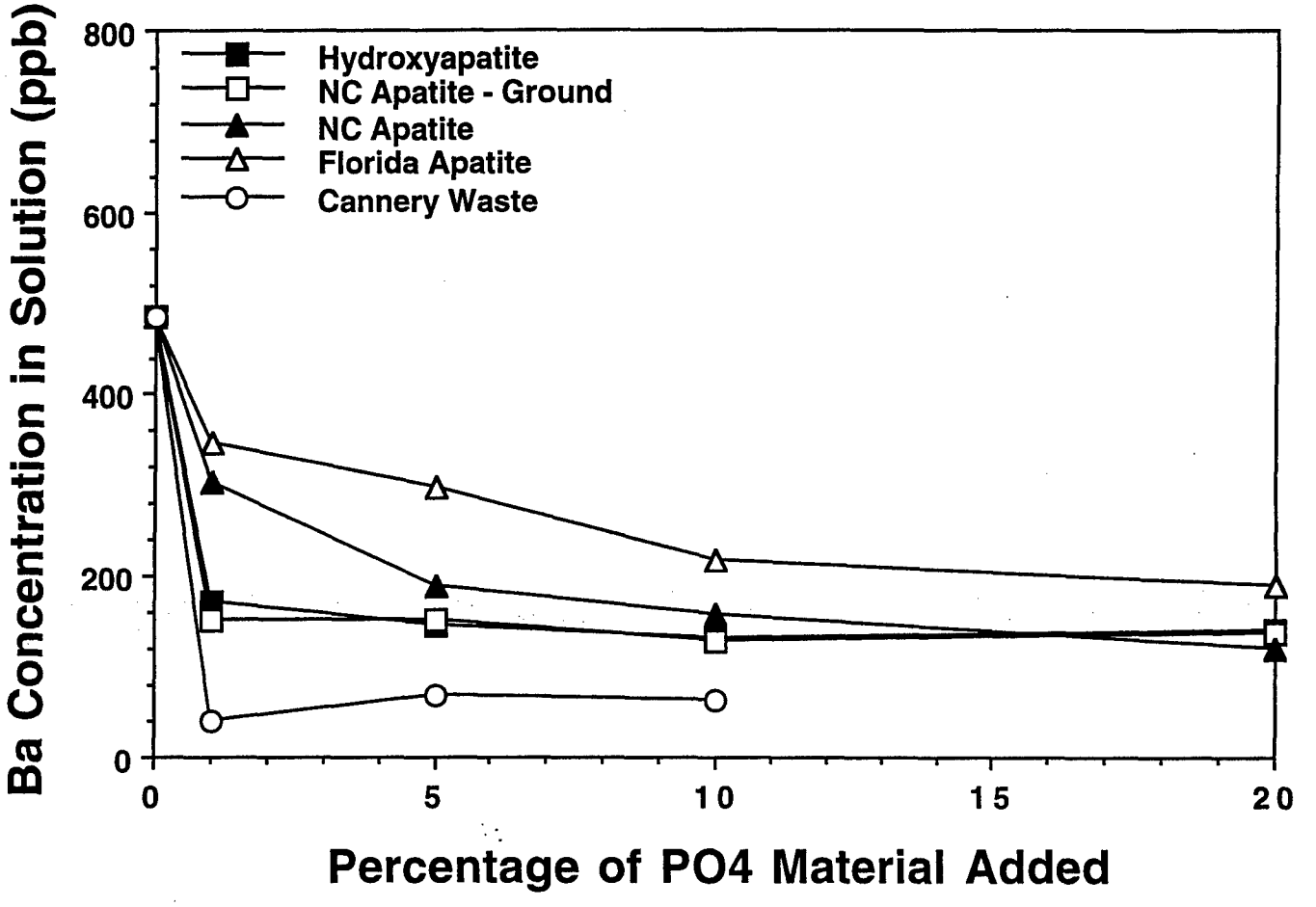

Figure 18. Barium Desorption/Sorption Results From Batch Tests Using Bunker Hill 4000 Soil and Deionized Water in a Water:Soil Ratio of 10:1. Barium Concentrations are Plotted as a Function of Phosphate Material Added as a Weight Percent of Total Sample.

(Note that the flow-through tests discussed in section 4 showed that even the unground NC apatite would bring lead leachate concentrations below detection limits under more soil-like conditions.) The results for ground and unground NC apatite show that particle size does affect the amount of lead immobilized.

Figure 16 shows results for zinc. Again, even though the Florida apatite was finely-ground, it is not as effective as even the unground NC apatite. The cannery material, the ground NC apatite, and the synthetic HAP have the best performance. Less than 5% of the biogenic apatite or the HAP drops the zinc concentration below the detection limit of 1 ng ml^{-1}, while small amounts of zinc remain in solution for the other materials. Figure 17 shows results for cadmium, with similar results. The detection limit for cadmium is 5 ng ml^{-1}. Finally, the results for barium in solution are shown in Figure 18. In this case, biogenic apatite is able to reduce the leachate concentration by a factor of ten or so, but none of the five materials tested can bring the level below a threshold of about 50 ng ml^{-1}.

In all of these results, the cannery material (ground fish bones and teeth) is the most effective at reducing dissolved metal concentrations. When available locally, cannery wastes may be an inexpensive raw material for soil remediation. If, however, processing is required to clean and grind the material before it can be used, its cost effectiveness may decline. Its properties may also vary from source to source. The highly pure, high-surface area synthetic material is also very effective. Synthetic hydroxyapatite has not been exposed to metals and other ions in a natural environment, which tends to reduce apatite's reactivity. The Florida deposits, being geologically older than those in North Carolina, produce a less reactive material. Surface area is also clearly a factor, as the ground and unground NC apatite results show. Higher surface areas make dissolution kinetics faster. However, increasing the reaction time from 24 to 48 hours was shown in section 4 to not substantially affect metal immobilization. Grinding the material may simply be exposing more reactive material to the metal-containing solutions. Precipitation onto apatite surfaces may also be effectively "extinguishing" them, preventing further dissolution of phosphate or direct reaction between the solid apatite and dissolved metals.

While synthetic hydroxyapatite is highly effective, it may not be the material of choice for soil remediation due to its higher cost. A kilogram purchased from Aldrich Chemical Company costs $155. Limited quantities (200-1000 kg) at bulk rates are available for about $20/kg from Sigma Chemical. There may be other sources of bulk hydroxyapatite as well at somewhat lower purity. Alternatively, Texasgulf charges only $85/ton for its NC apatite, $185/ton delivered from the East Coast to the West Coast.

4.2 POTENTIAL EMPLACEMENT STRATEGIES AND METHODS

This section discusses several methods that could be used to introduce apatite into a soil for in situ treatment. The treatment strategy can be broken down into two general categories: direct treatment and barrier placement. In many cases, the geotechnical methods for emplacing the apatite can be used for either strategy.

In direct treatment, apatite is delivered into the contaminated soil region. The contaminant and the apatite are therefore mixed and in intimate contact. Heavy metals in solution in the soil pore waters are rapidly immobilized, and metal ions that go into solution at a later time are similarly precipitated in place. Leaching of metals into groundwater from the contaminated region is thereby prevented. Note that apatite acts on leached metals in solution. There is some evidence that if dissolved metals precipitate out of solution as insoluble phosphates and rind, or coat, individual metal-bearing particles, those particles have reduced metal bioavailability (Davis et al, 1992; PTI Environmental Services, 1994). However, apatite treatment cannot convert entire metal-containing solid particles into a harmless form. Neither does it form a solid monolith of physically stabilized material. As such, it is not an appropriate remediation technology for cases such as blowing dust or particulates swept into surface waters.

Apatite can also be emplaced as a permeable, reactive barrier downgradient of a contaminated region. All groundwater seeping through the metal-containing soil would pass through the barrier. The apatite would react with the dissolved metals, stripping them out of solution and purifying the water. In this strategy, apatite acts much like a chemical filter.

The factors that determine which treatment strategy to apply include physical characteristics of the site, cost, client preference, and regulatory issues. Direct treatment is just that -- direct, and simple. One application mixes all of the contaminant with the treatment agent, and the problem is over. However, there are cases in which a barrier approach may be preferable. For very large sites, delivery of apatite into the whole soil volume may be prohibitively expensive. If the contaminants are highly toxic (such as radionuclides), worker exposure and contamination of equipment may be a concern. Drilling, mixing, and excavation operations may be more safely undertaken in relatively clean soil downgradient from the plume. If the metals have economic value, a barrier may be a way to concentrate and recover some of the material. The barrier could be periodically "mined" and replaced with fresh apatite.

Reactive barriers would be somewhat more complicated to engineer than direct treatment. The permeability of the barrier should be greater than or equal to that of the surrounding soil or aquifer, or else contaminated water may go around the barrier instead of through it. The barrier should be reasonably contiguous, with no large

gaps. A barrier may need to be placed under a plume as well as to the sides. For both remediation strategies, the apatite particle size cannot be too much smaller than the soil particle size in order to keep the apatite from being washed out. In some cases where groundwater flow rates are very high, a barrier may need to be lined with a geofabric or other material to hold the apatite in place.

4.2.1 INJECTION

Figure 19 illustrates emplacement of apatite by injection. Here we envision injection of a slurry of apatite particles in water rather than a solution. Hydroxyapatite is only sparingly soluble in water: with a pKs of 116.4, its solubility at a pH of 7.15 is 5.73 µmol/liter (Christoffersen and Christoffersen, 1982). Only with the addition of strong acids does the phosphorus dissolve out of the mineral, as shown in Table 13. Very little material could be injected as a solution, and the dissolved apatite would probably be washed out of the soil readily. Slurries can be injected by direct pumping into wells, but frequently the particles are unable to penetrate far due to the filtering action of the soil. The borehole clogs as the sides are coated in particles. Slurry injection therefore has a limited range. However, new techniques have been developed which overcome this problem, such as jet injection. Jet injection uses high pressures to fluidize the soil in the region around the injection nozzle. A two-inch diameter borewell can produce a well-mixed region three to six feet in diameter, depending on the soil type and fluids used (Malone and Lundquist, 1994; Phillips, 1995). Solids can be injected into the fluidized region with air, water, or both. Treatment of a large area is accomplished by injecting in a pattern of overlapping circles. Treatment depths of up to 150 feet are possible, with 90 feet more typical.

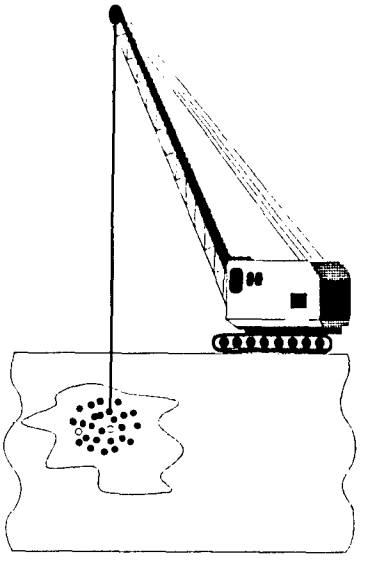

Figure 19. Slurry Injection

We are currently developing a proposal to deliver apatite by jet injection using the Casa Grande system developed by Westinghouse Hanford Company. This demonstration, to be submitted to the Department of Energy, would be for protection against radionuclide migration in soils at the Idaho National Engineering Laboratory.

4.2.2 SOIL MIXING

For very shallow contaminant plumes, apatite can be mixed into the soil by simply spreading it on the surface and using a rotary tiller, as was done in a demonstration at an orchard in Wisconsin involving lead arsenate pesticides (Stanforth and Chaudhuri, 1994). For deeper applications, equipment is available that can mix soil and a treatment agent in place. The arrangement is shown in figure 20. "Shallow" soil mixing uses a twelve-foot diameter auger on a crawler crane to mix material to a depth of ten to twenty feet. The treatment material is introduced coaxially through the drill string. Processing rates of 500-1,000 yd^3/day are typical (Malone and Lundquist, 1994). "Deep" soil mixing is a unique capability of the geotechnical firm GeoCon, Inc. Their deep soil mixing equipment consists of four three-foot diameter augers operated in parallel from a crane. Treatment depths of up to 150 feet are claimed, and processing rates are 150-400 yd^3/day. As part of the EPA SITE program, GeoCon demonstrated deep soil mixing using a proprietary pozzolonic grout material at a PCB-contaminated site in Florida (U.S. EPA, 1989).

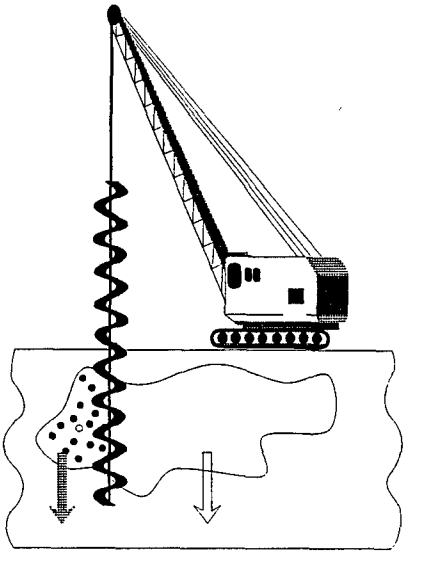

Figure 20. Soil Mixing/Auguring

As with jet injection, large areas can be treated by auguring in a pattern of overlapping circles. We have contacted GeoCon and secured their interest in using deep soil mixing in an apatite demonstration.

Injection and soil mixing can both be used for introducing apatite directly into a contaminated soil region. They can also be used to emplace a downgradient permeable barrier.

5.2.3 EXCAVATION AND BACKFILL

Creation of a barrier by excavation and backfill is shown in Figure 21. A backhoe can dig a fairly shallow trench without the need for sheetpile or other confining walls. A dragline or clamshell crane can dig a deeper trench if confining walls are driven or vibrated into place. Material may also be sluiced out with jets of water. After excavation, the trench is filled with granular material. Apatite could be added as is or mixed with some of the excavated soil.

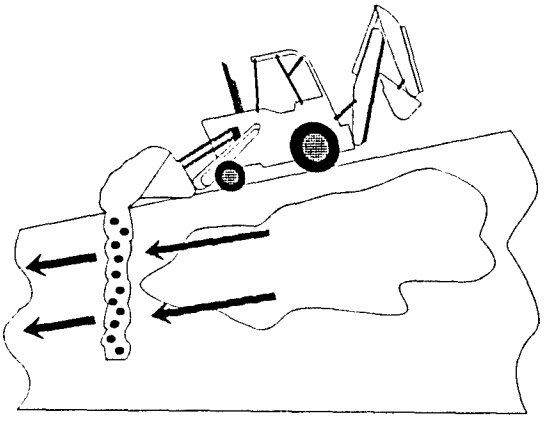

Figure 21. Excavation and Backfill

4.2.4 HORIZONTAL OR OFF-VERTICAL DRILLING

To emplace a barrier underneath a plume, somewhat more innovative (and less mature) methods are necessary. Figure 22 illustrates one approach, horizontal/off-vertical well drilling. Another technology, still in a developmental stage with support from the Department of Energy, is to jet inject horizontally through a rectangular manifold buried beneath the plume. This approach is being investigated for emplacing concrete barriers and slurry walls beneath existing waste tanks, etc. Overlapping "panels", each twelve feet long, 1.5 feet wide, and two feet thick, would be jet grouted beneath a plume.

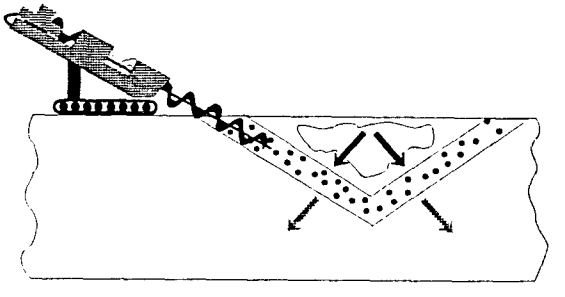

Figure 22. Horizontal Drilling

4.3 PHYSICAL PROPERTIES

Geotechnical contractors will require some information about the physical properties of apatite in order to ensure that it can be handled properly in the field. In discussions with potential emplacement collaborators, particularly the jet injection experts at Westinghouse Hanford Company, several key properties were identified. These include solubility in water, specific gravity, particle size distribution, and slurry viscosity.

4.3.1 SOLUBILITY

As discussed earlier, apatite is only sparingly soluble in natural water. Table 13 shows the percentage of total soluble phosphate from the rock in a media of increasing acidity. (Christoffersen and Christoffersen, 1982) report hydroxyapatite solubility as a function of pH, shown in Table 14.

Table 14. Solubility of Hydroxyapatite, $Ca_{10}(PO_4)_6(OH)_2$, at Various pH Values.

pH	Solubility, µmol/liter
5.03	442.
5.51	146.
6.31	26.9
6.76	11.3
7.15	5.73

4.3.2 SPECIFIC GRAVITY

The material safety data sheet provided by Texasgulf gives the specific gravity of the North Carolina apatite as between 2.9 and 3.1 g/cm^3. Other sources (Weast, 1983) list a range of 3.1 to 3.35 g/cm^3. As a granular solid or powder, a bulk density of 90-100 lbs per cubic foot (1.4-1.6 g/cm^3) is typical.

4.3.3 PARTICLE SIZE DISTRIBUTION

Particle size distribution is determined by processing history. Table 13 gives the screen analysis for the Texasgulf material. As received from the supplier, nearly all of the material is less than 0.5 mm in diameter, and very little is smaller than 0.074 mm. We ground the synthetic hydroxyapatite until it would pass a 170 mesh sieve.

4.3.4 SLURRY VISCOSITY

Several of the emplacement methods deliver the treatment agent in the form of a slurry, i.e. solids suspended in water. In order to ensure that such slurries can be pumped through equipment and to predict what pressures will be required to do so,

we have investigated the flow properties of slurries of the NC apatite.

Slurry viscosity should be affected by particle size and rock to water ratio. At very low solid fractions (less than 10%), the fluid should have the properties of water -- a Newtonian fluid with a viscosity of 1 cP. The tests below were limited to samples that were 43 vol% apatite, 57 vol% water. Unfortunately, we were not able to test intermediate solids fractions because the particles would quickly settle. In commercial practice, suspension agents are available that would help keep the apatite homogeneously mixed with water.

Samples with three particle sizes, 35, 75, and 212 microns, were generated by grinding the NC apatite and sifting out the different size fractions using sieves. These particles were weighed out and mixed with a known mass of water to make samples with a weight fraction of 65-70 wt% apatite. The resulting slurry density was approximately 2.4 g/ml. Specific values for each run are listed in Table 15. Water content was measured before and during experiments using a Denver moisture analyzer.

Table 15. NC apatite slurry samples. For each particle size listed, a concentrated slurry of the given weight and volume fraction was tested by capillary rheometry.

Particle diameter, μm	Solids fraction, weight %	Solids fraction, volume %
38	65	38
75	69	43
212	69	43

Flow properties were determined using a capillary rheometer. In capillary rheometry, one measures the pressure drop resulting from flow at a known rate through a round tube of known diameter and length. This raw data can be converted to shear stress as a function of shear rate. For a Newtonian fluid, shear stress is proportional to shear rate, with a proportionality constant equal to the viscosity.

The pump flow rate vs. revolutions per minute (rpm) was calibrated for each slurry sample. Differences in pump calibration were observed between samples. To demonstrate the validity of the data, the 400 rpm flow rate was reproduced between each flow rate. Differences in pressure drop at 400 rpm generally indicate particle settling and thus changes in slurry composition. During the course of the tests, insignificant changes in the 400-rpm pressure drop were noted for each sample.

The 38- and 75-micron particles were run in a 4 ft long, 1/8" diameter tube which resulted in pressure drops between 2-16 psig. The 212-micron slurry was run through a 22" long, 0.25" diameter tube to minimize settling effects (caused by excessive pressure drop) which were observed in the 1/8" tube. Since pressure drops were much lower for the 212-micron slurry, reliable shear rate data between 10 and 30 sec^{-1} could not be obtained.

Figure 23 plots viscosity versus shear rate. Slurry viscosities were in the 1-40 Poise range. All three slurries exhibited shear thinning characteristics, or decreasing viscosity at higher shear rates. The 212-micron slurries, however, seemed to stabilize and become less shear-rate dependent above 30 sec^{-1}. As expected, the 38-micron sample had the highest viscosity and greatest viscosity/shear rate dependence. The 212-micron slurry viscosity seemed to flatten out above 30 sec^{-1} and exhibited less of a shear rate dependence.

For ease of handling, a slurry should have a viscosity less than about 10 Poise, should not settle into a hard-packed material during standing, and should be easily redispersed after standing (TVA, 1976). Suspending agents and viscosity-reducing agents are available that are EPA-approved for soil applications. Spray application of apatite slurries as fertilizers was once investigated by the Tennessee Valley Authority (1976). They ground samples of a North Carolina apatite to a fine powder, with 67 or 87% of the material passing a #325 sieve (45 μm). Slurries were made with 65-70% rock by weight along with 0.5% suspending clay, up to 1% tetrasodium pyrophosphate (TSPP) dispersant, and 1% ammonium nitrate electrolyte. The viscosity was found to vary substantially with the amount of TSPP, decreasing from 25 Poise with no added TSPP to 2 Poise with 1% TSPP for 70% rock loading and the finer grind. The more coarsely ground material had a lower viscosity by a factor of three, and reducing the rock loading to 65% also reduced the viscosity by about a factor of four. With no TSPP, 65% loading of the 45-μm apatite particles gave a viscosity of 6 Poise. These results are consistent with our own. (The shear rate for these measurements was not specified in the article except to say that they were done in a Brookfield viscometer at a high shear rate.)

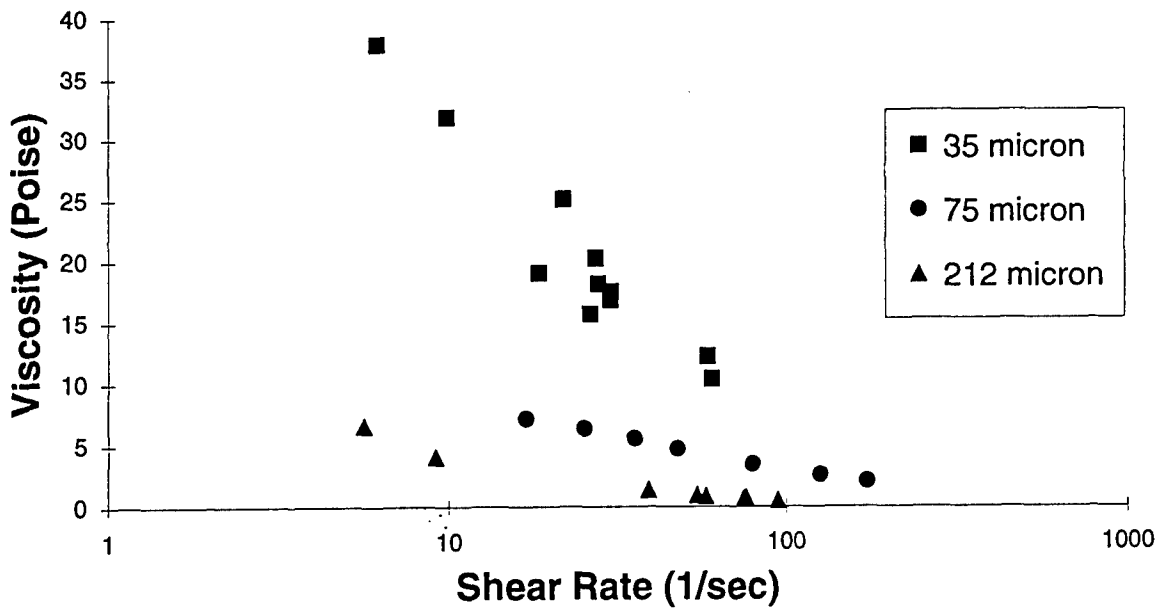

Figure 23. Viscosity as a Function of Shear Rate for Apatite Slurries of Various Particle Sizes.

4.4 TREATMENT COST

The cost of treatment will depend significantly on the emplacement method required and the amount of apatite added. For this kind of work, raw materials (including delivery to the site) and equipment operator expenses dominate the economics (Malone and Lundquist, 1994). One literature citation quotes $12/treated ton of soil for the apatite used in their demonstration (Stanforth and Chowdhury, 1994). For in situ grout treatment, a similar technology, costs run about $50/yd^3 for shallow contaminants and $150/yd^3 for deep ones (Malone and Lundquist, 1994). The deep soil mixing demonstration with grout by IWT and GeoCon (EPA, 1989) quoted a cost of $111/treated ton or $194/treated ton for a one- or four-auger system, respectively.

We expect that treatment with apatite will be less than that for grouting because much less additive is required. For shallow soil mixing or jet injection applications, we would estimate treatment costs at $35-$50/treated ton of soil. Deep soil mixing would probably be substantially more but less than for the grout demonstration. Vertical barriers could be substantially less expensive per treated ton, since a single barrier could filter contaminated waters from a very large area.

5.0 EVALUATION OF HEAVY METAL REMEDIATION USING MINERAL APATITE

EPA Land Disposal Restrictions (LDR) Program (40 CFR 268) sets treatment standards for the wastes banned from land disposal. The treatment standards (US EPA, 1990) are often based on the constituent concentrations in the Toxicity Characteristic Leaching Procedure (TCLP) extract from the wastes. Thus, TCLP, which replaced the Extraction Procedure (EP), is commonly used either to determine whether a waste is hazardous or determine whether a treated waste meets the treatment standards for land disposal. The procedure is designed to study the mobility of both organic and inorganic analytes present in liquid, solid, and multiphasic wastes, and, thus, must be considered in the development of treatment technologies.

Ma et al. (1995) studied the interaction of mineral apatites with Pb from aqueous solutions and contaminated soils. However, the leachabilities of reaction products under variable pH conditions were not investigated, and no attempt was reported to characterize the reaction products in the interaction of mineral apatites with Pb from contaminated soils. Therefore, the objectives of this milestone report are to (1) characterize the reaction products of a mineral apatite with Pb, Cd, and Zn from both aqueous solutions and a contaminated soil; (2) evaluate the leachabilities of the reaction products under acidic and basic conditions; and (3) investigate the effectiveness of apatite minerals in the sorption of heavy metals from contaminated soil under variable conditions, in particular, TCLP extraction fluids. The term sorption is

used loosely as a general term to describe attachment of species from a solution to its coexisting solid surfaces (Sposito, 1986). The results of this study indicate that due to their ready availability and low cost, mineral apatites may be the most economical and effective choice to use in the remediation of contaminated soils, wastes, and water.

5.1 MATERIALS

The mineral apatite used in this study came from a sedimentary phosphate rock deposit situated in North Carolina (NC) and was supplied by Texasgulf as raw mining ore without physical and chemical treatment. Two types of apatite samples were prepared. First, an apatite powder for X-ray diffraction (XRD) analysis was prepared by grinding the raw apatite to a fine powder to pass through a 400-mesh (38 μm) standard sieve using an 8000 Spex Mixer/Mill equipped with a tungsten carbide sample holder. XRD analysis of the apatite powder indicates that it is mainly carbonate fluorapatite and can be described by the empirical formula $Ca_{9.53}Na_{0.34}Mg_{0.13}(PO_4)_{4.77}(CO_3)_{1.23}F_{2.49}$ (Chien et al., 1980).

Second, apatite slides (~ 1 x 1 cm^2) were prepared to obtain clean, smooth, fresh, and flat apatite surfaces for scanning electron microscopy (SEM) analysis. The raw apatite sample was first sieved to obtain grains with diameters between 0.300 and 0.425 mm. The sieved apatite grains were then impregnated onto thin-section glass slides using Norland optical adhesive (ultraviolet curing) to avoid high temperature heating process. In order to avoid hydration or dissolution during grinding, a mixture of polishing oil and Mineral Spirits® at a volume ratio of 1:1 was used as paste solvents instead of water. After grinding on 9T grits, the fresh apatite surfaces on the slides were polished to 0.25 μ diamond paste. The diamond paste on the polished slides were wiped off with alcohol using Kimwipes®, and then cleaned with alcohol in an ultrasonic bath for 5 minutes.

Deionized distilled water (DD-H_2O) was used throughout this study. Three heavy metal solutions used in this study were prepared separately and applied to the apatite powder and slides in the sorption tests described below. Individual aqueous solutions of Pb, Cd, and Zn were prepared in the concentration of 2.50 x 10^{-2} M (5180 mg/L), 4.50 x 10^{-2} M (5058 mg/L), and 7.50 x 10^{-2} M (4904 mg/L), respectively, from their nitrate salts [$Pb(NO_3)_2$, $Cd(NO_3)_2 \cdot 4H_2O$, and $Zn(NO_3)_2 \cdot 6H_2O$].

Four solutions of varying pH were prepared for this study. Two acidic solutions were made from glacial acetic acid at a pH of approximately 3 and 5 following the preparation of the extraction fluids used in the TCLP test. Two basic solutions were prepared by diluting purified and concentrated sodium hydroxide to pH values of approximately 10 and 12. In addition to the acidic and basic solutions, DD-H_2O was also used in the leaching of a contaminated soil.

The metal-contaminated soil used in this study was a composite soil from the Bunker Hill Superfund site in Idaho obtained from the University of Idaho. Selected properties of the contaminated soil are shown in Table 16. The Bunker Hill site is contaminated by heavy metals, especially Pb, Zn and Cd, from mine tailings and smelter emissions. The heavy metal-bearing components in the soil are primarily sulfides and oxides, including PbS, $PbSO_4$, and PbO.

Table 16. Selected properties of the contaminated soil from the Bunker Hill Superfund site, Idaho (Data from Bero, 1994).

Particle Size Distribution (%)

Clay (< 2 μm)	Silt (2-50 μm)	Sand (<50-200 μm)
12	45	43

Other Properties

pH	Organic Matter (%)	Organic Carbon (%)	[1]EC (mmhos)	[2]CEC (mol/kg)
5.2	2.06	1.20	0.72	9.3

Metal Content (mg/kg)

Total Pb	Pb in Sand	Pb in Silt and Clay	Total Zn	Total Cd
4123	2668	4225	1226	15

5.2 METHODOLOGY

5.2.1 AQUEOUS HEAVY METALS SORPTION/DESORPTION

1.20 g of apatite powder was equilibrated with an aliquot of 35 ml of the heavy metal solutions in acid-washed 50-ml Nalgene polycarbonate centrifuge tubes. This resulted in an amount of heavy metal applied to apatite powder equal to 151.1 mg of Pb, 147.5 mg of Cd, and 143 mg of Zn per gram of apatite powder. A group of five tubes of these solid/solution slurries were prepared for each of the heavy metal solutions. The slurries were then shaken continuously at ambient temperature for 24 hours. After the 24-hour reaction period, the apatite suspensions were centrifuged for 15 minutes and the supernatants were filtered through 0.2-μm Nalgene Syringe filters with cellulose acetate membranes. An aliquot of 30 ml of the supernatant from each group of the slurries was acidified to pH 2 with concentrated nitric acid for metal

determination by inductively coupled plasma-mass spectroscopy (ICP-MS). A 5-ml subsample of the supernatant was used for pH measurement immediately using a Beckman Φ12 pH/ISE meter after filtration. After the sorption experiments described above, one tube of the solid residue from each group was air-dried and stored for at least 30 days for XRD analysis. The solid residue in the remaining tubes were thoroughly washed three times with DD-H_2O, and the supernatants were discarded immediately after 15-minute centrifugation. Then, one of the washed solid residues from each group were treated with 25 ml of each of the leaching solutions, and the slurries were shaken at ambient temperature for 24 hours before the suspensions were centrifuged, and their supernatants were filtered, acidified and analyzed as described above. After such sorption and desorption experiments, the final solid residues were saved as described above for XRD analysis.

To prepare apatite slide samples for SEM analysis, 10 ml of each of the heavy metal solutions was added to 40-ml beakers containing one apatite slide and 0.3429 g apatite powder at ambient temperature for 24 hours. Compared to the powder, the surface area of the apatite on the slide was negligible, thus the apatite powder was added in the same apatite:solution ratio as described above in the apatite powder experiments, to obtain similar solution conditions for the interaction between the apatite on the slide and metal ions in solution. A group (5 tubes) of the apatite slurries with an apatite slide were prepared for each of the metal solutions. The beakers were covered with Parafilm® to reduce evaporation and shaken 3 times during the 24-hour reactions before the supernatants were discarded. One of the reacted slides from each group of beakers were cleaned with deionized water and stored in a clean box for 30 days for later analysis by SEM to characterize the reaction products. Then, approximately 10 ml of each of the acidic and basic leaching solutions was added to the remaining beakers of each group. The beakers were shaken 3 times during a 24-hour treatment at ambient temperature. Then, the final slides were retained as described above for SEM examination.

5.2.2 SORPTION OF HEAVY METALS FROM A CONTAMINATED SOIL

In this sorption experiment, leachates of the Bunker Hill soil were used to react with the apatite powder and slides to obtain samples for XRD and SEM examinations. To prepare the leachates, 30 g of the contaminated soil was combined with 300 ml of the leaching solutions or DD-H_2O in a solid:liquid ratio of 1:10 in 500-ml Nalgene bottles. The soil slurries were continuously shaken at ambient temperature for 24 hours before they were centrifuged, and the supernatants were filtered, subsampled for pH and metal determinations, as previously described. An aliquot of 10 ml of each of the supernatants was then acidified to pH 2 for metal determination. Then, 0.48 g of the apatite powder was combined with 240 ml of each of the leachates in 250-ml Nalgene bottles. This made the amount of the apatite powder applied equal to 2 g of

apatite per 100 g of contaminated soil. The apatite slurries were shaken for 24 hours at ambient temperature, centrifuged, and the supernatants were filtered and measured for pH immediately. An aliquot of 10 ml of each of the supernatants was then acidified to pH 2 for metal determination while the solid residues were retained as described above for XRD examination.

Reacted apatite slide samples were also prepared for SEM analysis. The procedure was similar to that described above. A 30 ml subsample of each leachate was transferred into 80-ml beakers containing an apatite slide and 0.06 g apatite powder. The apatite slurries with apatite slides were allowed to react at ambient temperature for 24 hours. For these slides, no steps were taken to desorb the metals and the reacted apatite slides were retained for SEM analysis.

5.2.3 ANALYTICAL METHODS

The solid residues obtained in the sorption and desorption experiments were examined with a X-ray diffractometer (Siemens D-5000) operated at 35 kV and 30 mA using CuKα radiation. Measurements were made using a step scanning mode with a fixed 0.02° 2θ step and a count time of 2 s/step. All XRD analyses were performed with back-filled, randomly oriented cavity mounts prepared using a powder-press technique modified from Gibbs (1971). Apatite slides were investigated under a Hitachi S570 SEM equipped with a X-ray energy dispersive spectroscopy (SEM-EDX). The samples were mounted on stainless steel stubs using double-stick tape and coated with either Au or C. The surfaces of apatite pellets on the slides were observed through secondary and back-scattered electron (SE and BSE) imaging and X-ray dispersion analysis. The SEM was operated at 25 kV for electron imaging and 15 kV for EDX analysis.

5.3 RESULTS AND DISCUSSION

5.3.1 AQUEOUS HEAVY METALS SORPTION/DESORPTION

5.3.1.1 LEAD

Figures 24A and 24B show the XRD patterns of the mineral apatite powder and the solid residue from the reaction of the mineral apatite powder with Pb from aqueous solution. These XRD data indicate the formation of hydroxyl fluoropyromorphite after the sorption experiment. The species of pyromorphite formed in the interaction were highly pH-dependent and have been discussed in previous chapter. In recent studies of interactions of synthetic hydroxyapatites with aqueous Pb, Ma et al. (1993) and Xu

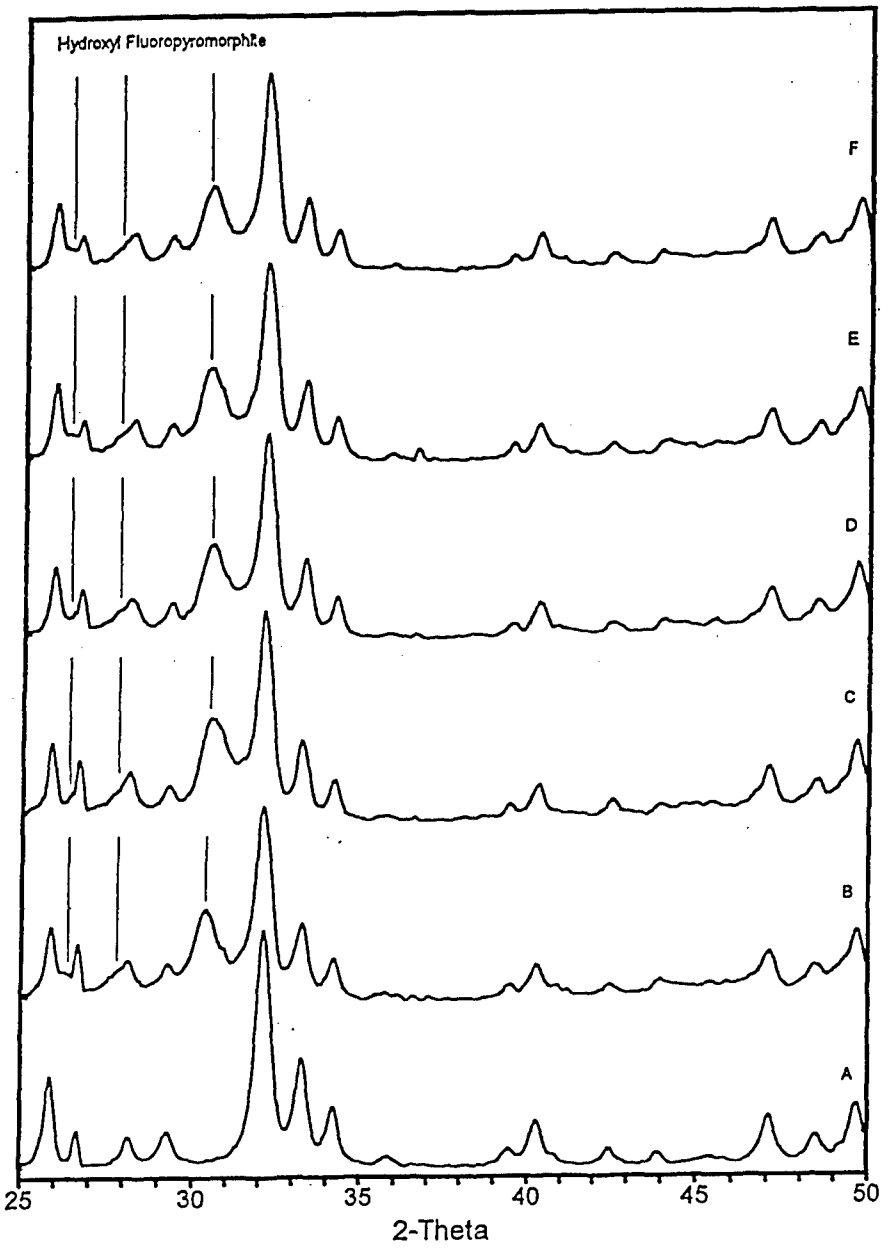

Figure 24. XRD Patterns of North Carolina Apatite Before (A), After Interaction With Aqueous Pb Solution (B) and After Leaching of Solid Residues From Interaction With TCLP Solutions of pH 3 (C), pH 5 (D), pH 10 (E), and pH 12 (F).

and Schwartz (1994) proposed that dissolved Pb was removed from solution mainly through hydroxyapatite dissolution and pyromorphite precipitation. Ma et al. (1995) further suggested that such a dissolution-precipitation process was the primary mechanism in the immobilization of Pb in the presence of apatite minerals and resulted in the formation of carbonate fluoropyromorphite-type phases [$Pb_{10}(PO_4)_3(CO_3)_3FOH$]. However, in their earlier work, Ma et al. (1994a) concluded that the incorporation of carbonate ions into the structure of pyromorphite was very limited. In the current study, the XRD maximum of the pyromorphite-type compound suggests that carbonate ions did not occur in its crystal structure (previous chapter). Thus, the general reactions involved in the formation of hydroxyl fluoropyromorphite [$Pb_{10}(PO_4)_6(F,OH)_2$] can be summarized as follows:

$$Ca_{10}(PO_4)_{6-x}(CO_3)_xF_{2-y}(OH)_y + (12 - x + y)H^+ \rightarrow 10Ca^{2+} + (6 - x)H_2PO_4^- + xHCO_3^- + (2 - y)F^- + yH_2O \quad (1)$$

$$10Pb^{2+} + 6H_2PO_4^- + 2(F^-,OH^-) \rightarrow Pb_{10}(PO_4)_6(F,OH)_2 + 12H^+ \quad (2)$$

Previous studies have demonstrated that the members of the pyromorphite family are the most stable environmental Pb compounds under a wide variety of conditions, and the solubility products of pyromorphites are extremely low, i.e., $10^{-71.6}$, $10^{-76.8}$, $10^{-78.1}$, and $10^{-84.4}$ for fluoro-, hydroxy-, bromo-, and chlorpyromorphite, respectively (Nriagu, 1972, 1973a and b, 1974). Thus, the reaction product, hydroxyl fluoropyromorphite, formed in this study should be able to resist the leaching of variable pH solutions. In the desorption experiments, the solid residues containing the hydroxyl fluoropyromorphite were extracted with leaching solutions of variable pH ranging from 3.0 to 12.0. After desorption treatment, the hydroxyl fluoropyromorphite formed in the sorption experiment stayed intact as indicated by their respective XRD patterns (Figure 24C-F). The intensities of the XRD peaks before and after desorption treatment remained the same, suggesting that the hydroxyl fluoropyromorphite is stable under a wide range of pH. The fact that the treatments by the TCLP extraction fluids did not destroy the pyromorphite-type compound suggests that the mineral apatite would decrease aqueous Pb concentration to below regulatory requirements and could be used to remediate Pb contamination.

The apatite slides obtained from the sorption and desorption experiments were also examined with SEM-EDS. Two methods were used to search for hydroxyl fluoropyromorphite crystals formed on the apatite surfaces. SE and BSE imaging were conducted by comparing with the SEM micrographs of apatite slides treated with DD-H_2O. BSE imaging was more effective because of the high contrast between the hydroxyl fluoropyromorphite grains and the background of the slides (Figure 25). These mineral grains were also observed on the apatite surfaces after the desorption experiments with variable pH leaching solutions, further supporting the stability of the

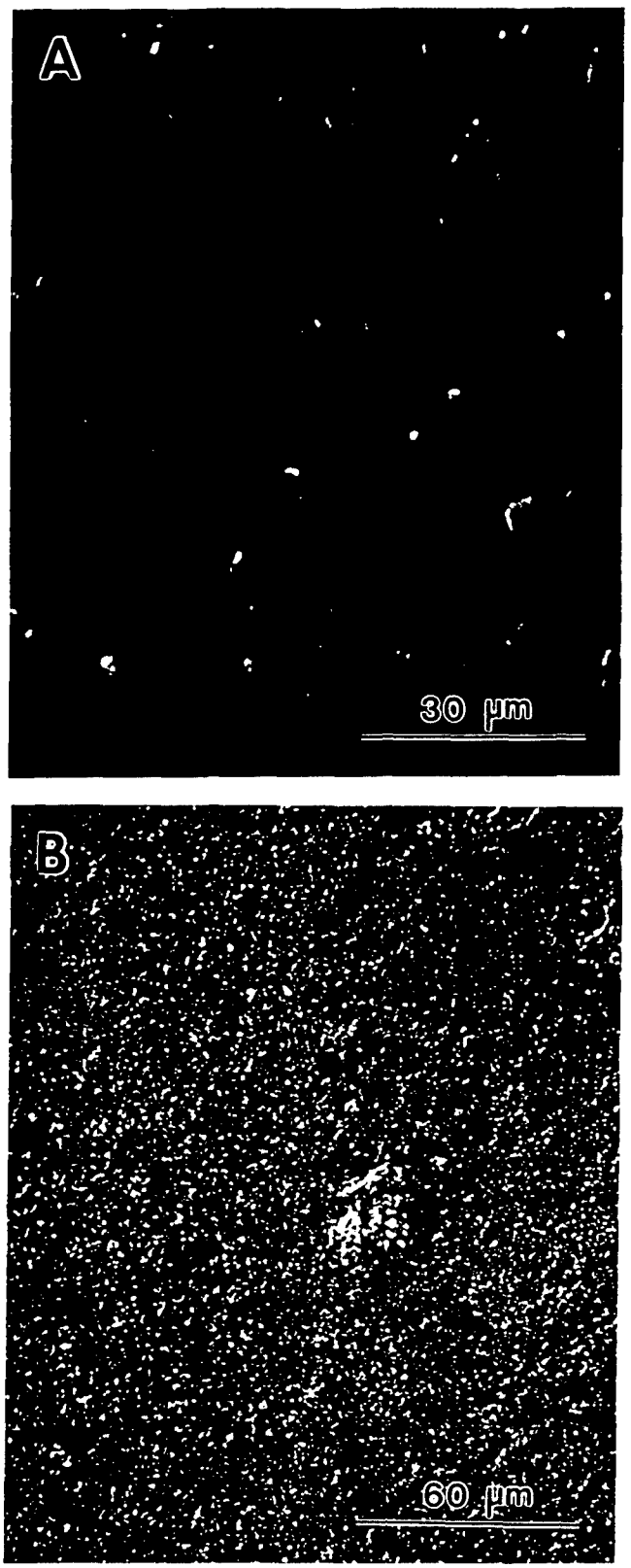

Figure 25. BSE Imagery of North Carolina Apatite Before (A), and After (B) Interaction With Aqueous Pb Solution.

newly formed hydroxyl fluoropyromorphite under a wide range of pH. The shape of the mineral grains was anhedral which is dramatically different from those reported by Ma et al. (1995), whose SEM micrographs indicated that needle-shaped crystals were present in some of their samples. This indicates poor crystallinity of the pyromorphite-type phase in our samples. Previous chapter has indicated that the degree of pyromorphite crystallization in the reaction of the mineral apatite with Pb solutions were highly pH dependent, in addition to other factors.

In this study, the mineral apatite was very effective in lowering aqueous Pb concentrations from 5180 to 1 mg/l, representing removal of 99.9% of the Pb applied (Table 17). The capacity of the mineral apatite in removing Pb was 151 mg of Pb/g of apatite, which is higher than the removal capacities of synthetic hydroxyapatite (125 mg/g) and phosphate rocks (20 mg/g) reported by Ma et al. (1993, 1995), but lower than that of a synthetic hydroxyapatite (400 mg/g) reported by Suzuki et al. (1985). The reason for the difference is unclear, but probably reflects differences in the surface areas and reactivities of different types of apatite powders prepared for different studies, as well as the difference in the initial Pb concentrations applied. The mineral apatite was also effective in neutralizing the acidic pH of the Pb solution (Table 17).

Table 17. Concentrations of aqueous heavy metal solutions after 24-hour reaction with North Carolina apatite powder (1) and further after desorption with variable pH solutions (2).

	(1) Sorption					
	Initial		After 24-hour Reaction with Apatite			
Metal	conc (mg/l)	pH	conc (mg/l)	capacity[1]	%sorbed	pH
Pb	5180	4.38	1	151	99.98	6.66
Cd	5058	4.85	2563	73	49	5.83
Zn	4904	5.11	3485	41	29	5.79

	(2) Desorption with Varible pH Solutions							
	pH3[2]		pH5[2]		pH10		pH12	
Metal	conc (mg/l)	% desorbed	conc (mg/l)	% desorbed	conc (mg/l)	% desorbed	conc (mg/l)	% desorbed
Pb	2	0.03	2	0.03	2	0.03	2	0.03
Cd	839	23	525	14	9	0.3	2	0.1
Zn	333	14	165	7	5	0.2	2	0.1

In addition to the great effectiveness in lowering Pb concentrations, the Pb sorbed was strongly retained (approximately 0.03% leached) in the desorption experiments with the TCLP extraction fluids and basic leaching solutions (Table 17). These results of the sorption and desorption experiments support our observations in XRD and SEM analyses that hydroxyl fluoropyromorphite was formed in the interaction of the mineral apatite with aqueous Pb, and was very stable over a wide range of pH. Table 17 also shows that the concentrations of Pb in all the extracts were below the maximum concentration of Pb allowed in TCLP (5 mg/l, US EPA, 1990). Thus, the mineral apatite should be employed in the remediation of Pb in soils, wastes, and water, if the sorption mechanism described here will also function in its reaction with contaminated soil leachates. The results of desorption experiments also suggest that other sorption processes, e.g., ion exchange and surface complexation, are not important mechanisms in the removal of Pb from solution.

5.3.1.2 CADMIUM AND ZINC

The XRD patterns for the solid residues generated in the reactions of the mineral apatite powder with aqueous Cd and Zn solutions were compared with the original apatite powder. In the reaction of the mineral apatite with aqueous Cd, otavite ($CdCO_3$) was formed (Figures 26A and 26B):

$$Cd^{2+} + HCO_3^- \text{---> } CdCO_3 + H^+ \qquad (3)$$

The HCO_3^- involved in the reaction was mainly derived from the dissolution of the carbonate-bearing mineral apatite because gas-free DD-H_2O was used in this study and the centrifuge tubes in which the reaction proceeded were air-tight. Also, the reaction of synthetic hydroxyapatite with Cd reported by Xu et al. (1994) did not produce otavite. In the XRD pattern, only one peak of otavite can be identified, and the intensity of the peak is very small, suggesting a very limited amount of otavite precipitated. SEM analysis supported these findings, in which nearly no new solid phases were observed on the apatite grain surfaces of the reacted apatite slides. After the desorption experiments of the reacted solid residues, the otavite peak disappeared if the leaching solutions were acidic TCLP extraction fluids (Figures 26C and 26D) but remained intact if basic leaching solutions were used (Figures 26E and 26F). This further indicates that the new XRD peak belongs to otavite because otavite is soluble under acidic conditions but is stable in basic solutions (Lindsay, 1979).

In the sorption of aqueous Zn with mineral apatite, the XRD patterns were identical for the original mineral apatite and the solid residues generated (data not shown), suggesting that new crystalline solid phases were either not formed or not detectable by XRD. SEM examinations of apatite slides through SE and BSE imaging techniques were unable to detect new solid phases on the polished surfaces of

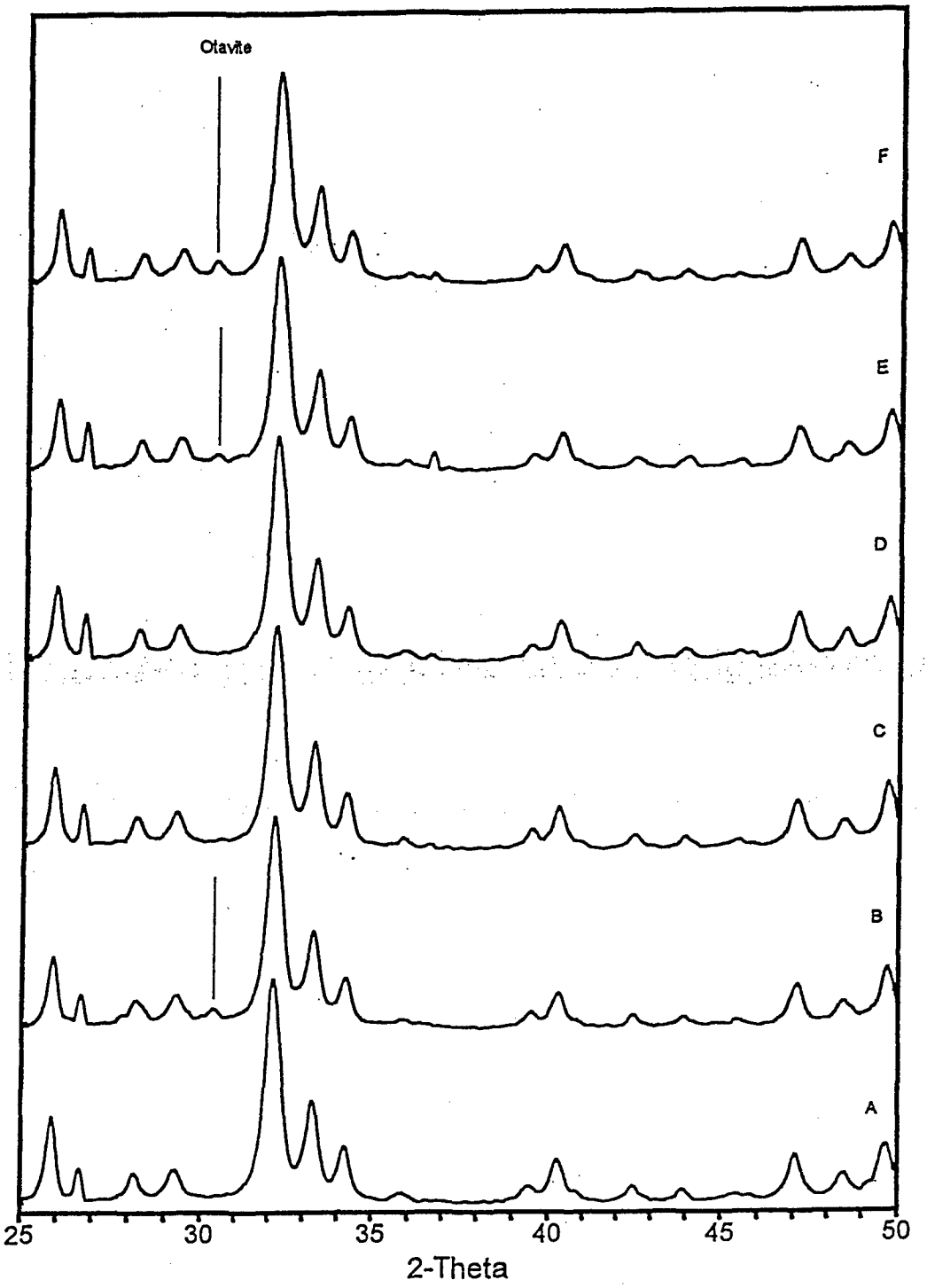

Figure 26. XRD Patterns of North Carolina Apatite Before (A), After Interaction With Aqueous Cd Solution (B) and After Leaching of Solid Residues From Interaction With TCLP Solutions of pH 3 (C), pH 5 (D), pH 10 (E), and pH 12 (F).

apatite grains. EDS scanning analysis was also conducted on the apatite slides reacted with Cd and Zn solutions, which indicated uniform coverage of Zn and Cd.

Therefore, otavite was the only new solid phase identified through XRD and SEM-EDS analysis in the solid residues that were produced in the reactions of mineral apatite with Cd and Zn solutions. Whether any other new amorphous and/or crystalline solid phases, e.g. Cd and Zn phosphates, were formed is uncertain, based on the information available. In the studies of the interactions of synthetic hydroxyapatite with aqueous Cd and Zn, Ma et al. (1994) inferred that amorphous to poorly crystalline Cd and Zn phosphates were precipitated while Xu et al. (1994) suggested that Cd and Zn cations were coprecipitated with calcium to form solid solutions of apatite. In these studies, however, no direct evidence was obtained to prove the existence of new solid phases.

The Cd and Zn concentrations from the sorption and desorption experiments are presented in Table 17. The amounts of Cd and Zn sorbed were calculated from the changes of metal concentrations in solutions before and after the reactions with the apatite powder. The percentages of Cd and Zn sorbed were 49% and 29%, respectively. The sorption capacities were 73 mg of Cd and 41 mg of Zn per gram of the mineral apatite powder. These results indicate that the amounts of Cd and Zn sorbed by the apatite powder were much less than that of Pb discussed above. The sorption capacities of apatite powder for Cd and Zn were approximately a half and one third of that for Pb. Similar to the Pb sorption discussed above, the reactions of the apatite powder with the solutions can neutralize the solution pH. The magnitudes of pH change were in proportion to the amounts of individual metal sorbed (Table 17), which were in the order of Pb >> Cd > Zn.

In the desorption experiments, the amounts of Cd and Zn desorbed by the acidic solutions were much more than that of Pb while the sorbed Cd and Zn were significantly less re-mobilized in the presence of the basic solutions compared to those in acidic solutions (Table 17). Table 17 also indicates that, with the pH increase of the acidic leaching solutions from 3 to 5, the percentages of desorption changed from 14 to 23% for Cd and 7 to 14% for Zn. This suggests that the sorbed Cd is less strongly retained than that of Zn with variable pH solutions. This type of desorption behavior was also observed by Xu et al. (1994), in which 0.5 M $CaCl_2$ and $MgCl_2$ solutions were used. They offered two possibilities to interpret such desorption patterns: first, when Cd and Zn were sorbed, more Cd was removed through coprecipitation with Ca, thus more Cd was desorbed due to the apatitic coprecipitate dissolution in the presence of $CaCl_2$; second, Zn diffused faster and further into the apatite hydration shell and/or crystal structure than Cd did due to the smaller ionic radius of Zn. We believe the mechanism of such desorption pattern need to be studied further. For example, the results of our current study imply that the percentages of Cd and Zn desorbed were in a ratio of approximately 1.64-2:1depending on the pH of leaching solution, while the

ratio of percentages of Cd and Zn sorbed was 1.69:1. This suggests that the amounts desorbed were highly related to the amounts of metals originally sorbed, the sorption mechanisms, and the solid phase relations. As an example, the dissolution of carbonate phases released Cd into solution from the otavite in the desorption experiments, but no Zn carbonate exists to release Zn.

Comparing the data obtained in the sorption and desorption experiments, it is apparent that the sorption mechanisms in the interactions of the mineral apatite with aqueous Cd and Zn were different from that of aqueous Pb. The formation of pyromorphite-type or other phosphate compounds was not the principal process responsible for the removal of aqueous Cd and Zn from solution. Instead, other sorption mechanism (e.g., surface complexation, ion exchange, solid diffusion, and precipitation of metal carbonate) may act individually or together in the attenuation of Cd and Zn in the presence of the mineral apatite. The significant difference between sorbed Pb and sorbed Cd and Zn in the desorption experiments also suggests different sorption mechanisms. The low solubility of metal phosphates, such as hydroxyl fluoropyromorphite, would minimize the metal desorbed while metals sorbed through other mechanisms, such as adsorption, would become readily re-mobilized in the acidic desorption tests. Therefore, in the reaction of the apatite with Cd and Zn, their sorption capacities were primarily limited by the sorption sites available in the apatite instead of by the amount of dissolved phosphate ions, which controls the Pb removal in the interaction of the apatite with Pb.

5.3.2 SORPTION OF HEAVY METALS FROM A CONTAMINATED SOIL

Figure 27 shows the concentrations of dissolved Pb, Cd, and Zn in the leachates of the Bunker Hill contaminated soil before and after reaction with the mineral apatite powder. As expected, the amounts of heavy metals leached generally decreased with increasing pH, except for Pb at pH 12. The higher concentration of dissolved Pb at pH 12 may be associated with large amounts of dissolved organic materials leached from the soil. The tan coloration of the leachate at pH 12 was different from other clear leachates under leaching solution pH below 10. The dissolved organic materials may act as complexing agents, which compete with the soil surfaces for Pb cations, and thus increased the concentration of Pb in the leachate. This phenomena has been observed in other studies (McBride and Blasiak, 1979; Kuo and Baker, 1980). It has also been reported that the presence of organic ligand might inhibit the adsorption of heavy metals onto solid surfaces (e.g., Baham and Sposito, 1986; Peters and Shem, 1992).

After the reaction of all the leachates with the apatite powder in the amounts equivalent to an apatite:soil ratio of 1:50 (2%), the heavy metal concentrations of the

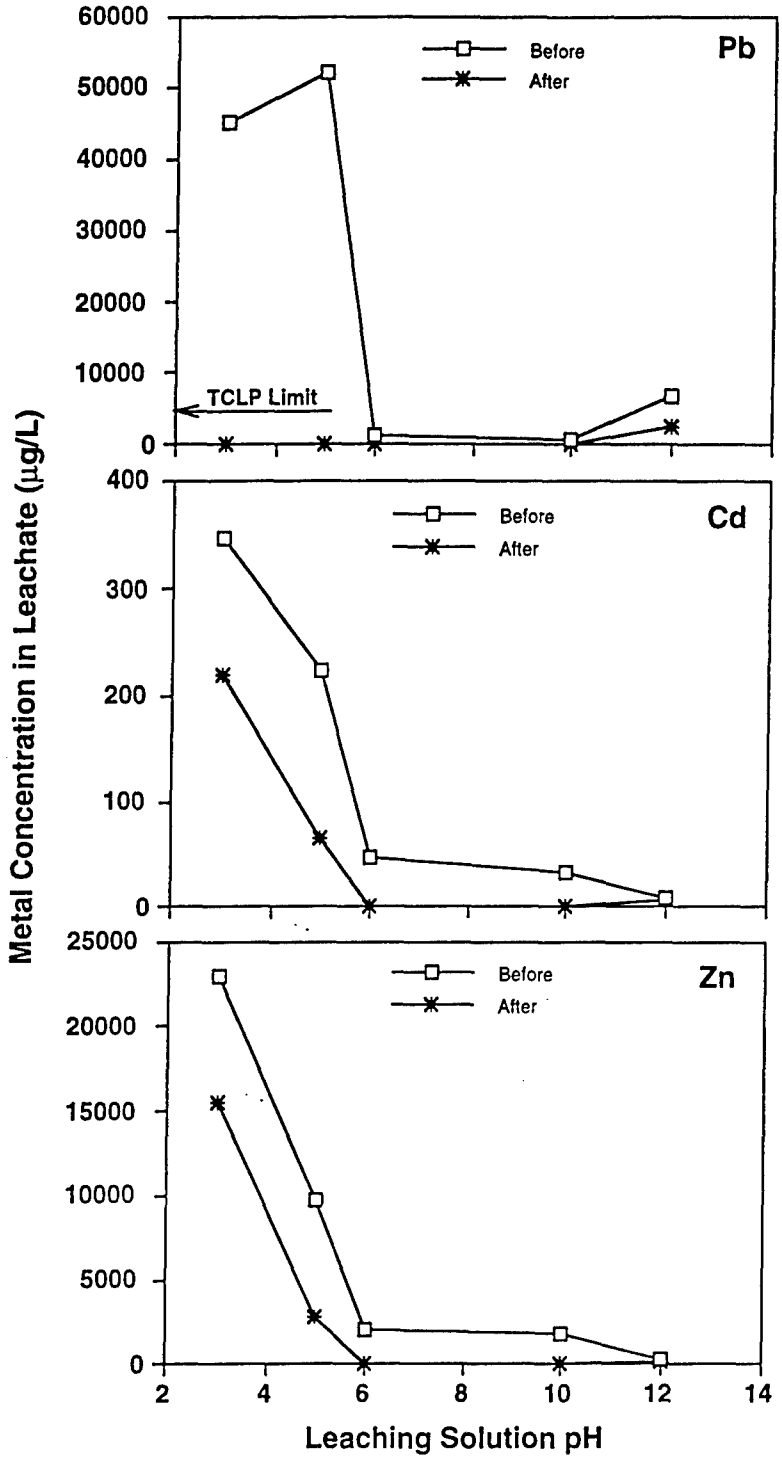

Figure 27. Concentrations of Dissolved Pb, Cd, and Zn in Leachates From the Bunker Hill Contaminated Soil Before and After Reaction With North Carolina Apatite.

leachates were substantially decreased in most cases. The percentages of the dissolved heavy metals removed ranged from 62.3 to 99.9 for Pb, 20 to 97.9 for Cd, and 28.6 to 98.7 for Zn (Table 18). The most efficient conditions for all three metals to be removed were the pH of leaching solutions ranging from 6 to 10, which resulted in over 97% removal for all three metals and reduced the concentrations of dissolved Pb, Cd, and Zn to levels below the EPA drinking water limits (US EPA, 1976). This is the pH range to which apatite strongly buffers natural solutions.

Table 18. Percentages of Pb, Cd, and Zn removed from leachates of Bunker Hill soil after reaction with North Carolina apatite powder.

	After Reaction with Apatite (%)			
Leaching Solution	pH	Pb	Cd	Zn
pH3 (TCLP1)	3.90	99.7	36.3	32.6
pH5 (TCLP2)	5.08	99.5	70.7	71.4
pH6 (DD H_2O)	7.45	99.8	97.9	98.7
pH10	7.80	99.9	97.0	98.4
pH12	10.63	62.3	20.0	28.6

The results of leaching of the un-treated contaminated soil using TCLP solutions suggest that it was a hazardous waste because the Pb concentrations exceeded EPA maximum allowable level of 5 mg/L. After the soil leachates were reacted with apatite powder, the concentrations of Pb in the leachates were reduced to below the EPA regulatory limit. Thus, the results of this study suggest that Pb-contaminated soils, such as the Bunker Hill soil, may be remediated to EPA requirements using apatite.

As observed previously in the reaction of the apatite with aqueous heavy metals, the pH of the leaching solutions were also neutralized after the reaction with the apatite powder. Thus it might be an advantage to apply mineral apatite to treat acid mine drainage from mine tailings, in particular, those containing high concentrations of dissolved heavy metals. In addition, when the leaching solutions were decreased in pH from 10 to 3, the removal efficiencies for Pb were still maintained at over 99.5 percent while those for Cd and Zn decreased gradually (Table

18), indicating that the removal patterns of Cd and Zn were very similar, but different from that of Pb. The sorption mechanisms responsible for the removal of Pb, Cd, and Zn in the reactions of the mineral apatite with the soil leachates are probably the same as those described above for the aqueous Pb, Cd, and Zn.

The solid residues resulting from the reaction of the soil leachates with the apatite powder were examined using XRD. If all the Pb sorbed in the reaction of apatite with the soil leachates obtained using the TCLP extraction fluids of pH 3 and 5 was converted into fluoropyromorphite, then the amounts of fluoropyromorphite in the solid residues would be 2.90 and 3.35 wt%, respectively, which exceed the general XRD detection limit of 1 wt%. However, in all the XRD patterns obtained, no peaks indicated the formation of new solid phases in the residues. However, the reacted apatite slides from soil leachates viewed under BSE imaging of SEM show that scattered bright particles occurred on the surfaces of apatite grains. These scattered particles were most likely to be a fluoropyromorphite-type compound because under variable pH conditions Pb concentrations were low after reaction with apatite and the sorption behavior of the contaminated soil Pb was similar to that of aqueous Pb, where fluoropyromorphite-type compounds formed (previous chapter). SEM imaging also showed that the number of such particles decreased with increasing pH. This may have resulted from the decrease in the amount of dissolved Pb and/or P in solutions due to the increase of pH, thus fewer particles were precipitated. These data also support the possibility that the scattered particles are newly-formed fluoropyromorphite-type compounds with poor crystallinity. Previous studies also claimed the formation of pyromorphite-type compounds in the interaction of phosphate materials with contaminated soils (Stanforth and Chowdhury, 1994; Ma et al., 1995).

Similar to the sorption of aqueous Cd and Zn with the apatite powder, the removal mechanisms of the dissolved Cd and Zn from the leachates of the contaminated soil were probably surface adsorption, while the primary mechanism for Pb removal was a process of dissolution of the mineral apatite and precipitation of an amorphous hydroxyl fluropyromorphite compound.

5.4 CONCLUSIONS

North Carolina mineral apatite was extremely effective in removing Pb, and was moderately effective in sorbing Cd and Zn, from solutions. Approximately 100% Pb was removed from solutions, representing a capacity of at least 151 mg of Pb/g of apatite, while 49% Cd and 29% Zn added were attenuated, with removal capacities of 73 and 41 mg/g, respectively. The immobilized Pb stayed intact under a wide variety of pH conditions ranging from 3 to 12, while the sorbed Cd and Zn, which were also nearly intact under alkaline conditions, were only re-mobilized by 14-23% and 7-14%, respectively, under TCLP acidic conditions.

The mineral apatite was also effective in reducing dissolved Pb, Cd, and Zn

leached from Bunker Hill contaminated soil using pH3-12 solutions by 62.3-99.9, 20-97.9, and 28.6-98.7%, respectively. In particular, the mineral apatite was able to reduce the metal concentrations in the TCLP-extracted soil leachates to below EPA maximum allowable levels. These results imply that mineral apatites could be a cost-effective option in the remediation of metal-contaminated soils, wastes, and water.

Two types of new solid precipitates were identified in this study. Hydroxyl fluoropyromorphite was formed in the reactions of the apatite with aqueous Pb solution and contaminated soil leachates. The formation of this compound was through the dissolution of the fluoride-bearing apatite followed by its precipitation from solutions, and was the primary mechanism for removing Pb from aqueous solution and the soil leachates. Minor amounts of otavite were formed in the reaction of the apatite with aqueous Cd solution.

Indirect evidence suggests that the principal sorption mechanisms responsible for the decrease of Cd and Zn concentrations in aqueous metal solutions and soil leachates were surface adsorption and/or the formation of amorphous solids. If enough apatite is used in the remediation in the field, then the neutralization capacity of the apatite could buffer the system enough to optimize the stabilization of Cd, Zn and other metals in pH-sensitive phases.

6.0 pH EFFECTS ON SORPTION AND SELECTIVITY OF HEAVY METALS ON APATITE

Many studies have been conducted on the crystal structure and chemistry of synthetic and mineral apatites (McConnell, 1973; Wright, 1990). Apatites, the tenth most abundant mineral, occur commonly in soils and sediments, and are the primary inorganic constituent of bones, teeth and some biological calculi. Industrially, apatites serve as the basic structural framework for certain phosphors and laser crystals, but more importantly, apatites are the principal mineral component of phosphate rock. Phosphate rock serves as the raw material in all phosphate fertilizers and can also be directly applied to the field. Geochemical studies have demonstrated that a variety of trace elements are enriched in phosphate rocks (Altschuler, 1980; Wright etal., 1987). Thus, the presence of apatites or phosphate rocks could regulate the concentrations of calcium, phosphate, lead, cadmium, zinc, and other heavy metals (Lindsay, 1979) in natural environments, and may provide a cost-effective technology for the remediation of metal-contaminated soils and water.

Sedimentary phosphorite is one of the primary sources of phosphate rock, which contributes more than 80 percent of the world's production, and can be readily obtained at low cost. The principal phosphate mineral in sedimentary phosphorites is

carbonate fluorapatite (McClellan, 1980), which is microcrystalline and differs in composition from pure synthetic fluor- and hydroxyapatites because of extensive substitution of carbonate for phosphate and of other metals for calcium (McClellan and Lehr, 1969). Summaries of ion substitutions in apatite structures can be found in McConnell (1973), LeGeros (1981), LeGeros and LeGeros (1984), and Wright (1990), among others. The substitutions result in a tremendous variation in the chemical reactivity and stability of carbonate fluorapatites. In general, their solubility increases with the increase in carbonate substitution (e.g., Chien and Black, 1976; LeGeros, 1981).

The interaction of apatites with heavy metals may lead to the formation of relatively insoluble heavy metal phosphate compounds and/or the adsorption of aqueous heavy metals on apatites, and thus can significantly reduce the concentrations of heavy metals in the aqueous phase. For instance, studies have suggested that the reaction of synthetic hydroxyapatite with aqueous Pb can result in the formation of pyromorphites (or lead apatites), whose species could be hydroxypyromorphite [$Pb_{10}(PO_4)_6(OH)_2$], chloropyromorphite [$Pb_{10}(PO_4)_6Cl_2$], or fluoropyromorphite [$Pb_{10}(PO_4)_6F_2$], depending on the presence or absence of Cl and F in solution (Suzuki et al., 1984; Ma et al., 1993; Xu and Schwartz, 1994). However, the mechanisms of these interactions are not agreed upon in the literature. Earlier work proposed an ion exchange reaction responsible for the formation of these solid compounds (Suzuki et al., 1984; Miyake et al., 1986; Takeuchi et al., 1988; Takeuchi and Arai, 1990), while recent studies concluded that the dissolution of hydroxyapatite and the precipitation of pyromorphites were the operational mechanism responsible for reduction of Pb concentration to below regulatory limits (Ma et al., 1993, 1994a; Xu and Schwartz, 1994). Previous work (Nriagu, 1972, 1973a and b, 1974, 1984) indicated that the solubilities of these compounds are extremely low. In addition, the interactions of apatites with other heavy metals have also been investigated, including Cd (Middelburg and Comans, 1991; Xu et al., 1994) and Zn (Misra and Bowen, 1981; Xu et al., 1994). In these studies, the interaction processes were also not well understood, and proposed mechanisms included adsorption, absorption, complexation, and precipitation or coprecipitation. Because the mechanisms of removal of heavy metals from solution in the presence of apatite are still controversial, the term sorption, as suggested by Sposito (1986), is herein used loosely as a general term to describe attachment of heavy metals from a solution to its coexisting apatite surfaces.

The previous studies discussed above were mainly concerned with the interaction of synthetic hydroxyapatite with heavy metals. The competition and interference of cations and anions on the sorption processes were only studied occasionally (Suzuki et al., 1984, 1985; Takeuchi and Arai, 1990; Ma et al.,1994a and b). Furthermore, the reaction of natural phosphate rock with heavy metals has rarely been studied and is more complicated because of the coexistence of PO_4^{3-}, CO_3^{2-}, F^-,

OH^-, and other cations in the structure of mineral apatite, and thus of their possible presence in aqueous solution. Recently, the reaction of phosphate rocks with aqueous Pb were reported (Ma et al., 1995). However, the effect of pH on the interaction and its products was not considered. The influence of pH on the sorption of heavy metal ions on calcite, oxides, clay minerals and soils has been extensively studied (e.g., Harter, 1983; Elliott et al., 1986; Davis et al., 1987; Zachara et al., 1991; Yong and Phadungchewit, 1992). Therefore, the objectives of this milestone are to: (1) investigate the effects of pH on the sorption behaviors and selectivity of Pb, Cd, and Zn in the presence of mineral apatite, and (2) examine the solid residues from the interactions of mineral apatite with aqueous heavy metals and the mechanisms possibly involved in the interaction under variable pH.

6.1 METHODOLOGY

The mineral apatite used in this investigation was from a sedimentary phosphate rock deposit situated in North Carolina (NC) and was supplied by Texasgulf as raw mining product without any physical or chemical treatment. The pelletal grains of the raw apatite were ground to a fine powder to pass through a 400-mesh (38 μm) standard sieve using an 8000 Spex Mixer/Mill equipped with a tungsten carbide sample holder. X-ray diffraction (XRD) analysis of the powder indicates that it is a carbonate fluorapatite. Its chemical composition has been reported by Chien et al. (1980) and is described by the empirical formula

$$Ca_{9.53}Na_{0.34}Mg_{0.13}(PO_4)_{4.77}(CO_3)_{1.23}F_{2.49}.$$

Deionized distilled water (DD-H_2O) was used to prepare all solutions and suspensions. Three heavy metal solutions were used in this study, which were prepared separately and applied to the apatite powder at different pH. Individual heavy metal solutions of Pb, Cd, and Zn were prepared in the concentration of 2.50 x 10^{-2} M (5180 mg/L), 4.50 x 10^{-2} M (5058 mg/L), and 7.50 x 10^{-2} M (4903.5 mg/L), respectively, from their nitrate salts [$Pb(NO_3)_2$, $Cd(NO_3)_2 \cdot 4H_2O$, and $Zn(NO_3)_2 \cdot 6H_2O$]. For each heavy metal solution, a set of 11 solutions with pH ranging from 1 to 12 were prepared. The pH was adjusted with concentrated nitric acid or sodium hydroxide to the desired values. The heavy metal solutions were equilibrated in one replicate with the apatite powder separately or in combination as described below.

6.1.1 SINGLE-SPECIES SORPTION TESTS (SSST)

1.20 g of the apatite powder was equilibrated with each of the pH-adjusted metal solutions (35 ml) in acid-washed 50-ml Nalgene polycarbonate centrifuge tubes.

The amount of each heavy metal applied to the apatite powder was approximately equal to 0.15 g/g apatite. The apatite suspensions were then shaken at ambient temperature for 24 hours. Additionally, a series of "blank" solutions with no metal added were also prepared as control tests.

6.1.2 MULTIPLE-SPECIES SORPTION TESTS (MSST)

The individually prepared heavy metal solutions of Pb, Cd, and Zn were mixed in equal volumes to form a multiple-species mixture. The mixed solutions were then adjusted to the desired pH accordingly. The experiments of the interaction of the apatite powder with the heavy metals in the mixed solution were set up the same way as the SSST.

6.1.3 ANALYTICAL METHODS

After a 24-h equilibration period, the apatite suspensions from all of the tests were centrifuged for 15 minutes and supernatants were filtered through 0.2-μm Nalgene Syringe filters with cellulose acetate membranes. Solution pH was measured with a Beckman Φ12 pH/ISE meter. The amount of heavy metal remaining in the supernatants was analyzed with inductively coupled plasma-mass spectroscopy (ICP-MS). The solid residues were examined with X-ray diffractometer. XRD was performed on a Siemens D-5000 X-ray diffractometer operated at 35 kV and 30 mA using CuKα radiation. Measurements were made using a step scanning mode with a fixed 0.02° 2θ step and a count time of 2 s/step. All XRD analyses were performed with back-filled, randomly oriented cavity mounts, which were prepared using a powder-press technique modified from Gibbs (1971). Selected samples of the solid residues were also observed under a Hitachi S570 scanning electron microscope equipped with X-ray energy dispersive spectroscopy (SEM-EDX). The samples were mounted on stainless steel stubs utilizing double-stick tape and were then coated with either Au or C. The SEM was operated at 25 kV for secondary electron (SE) imaging and 15 kV for EDX analysis.

6.2 RESULTS AND DISCUSSION

6.2.1 SSST OF HEAVY METALS WITH APATITE

The amount (mg of M^{2+}/g apatite) of heavy metal removed was calculated from the difference between initial metal concentration and final metal concentration remaining in the supernatant. The sorption of Pb, Cd, and Zn in the presence of the apatite powder in relation to initial aqueous metal solution pH for individual application

of the heavy metals are shown in Figure 28. Overall, the sorption curves of Cd and Zn are similar to each other, with differences in the amounts sorbed. They both are, however, dramatically different from the Pb sorption curve. The effects of the initial pH of the aqueous metal solutions on the final pH of apatite suspensions are summarized in Figure 29. The sorption behaviors of Pb, Cd, and Zn in the presence of apatites vary for each individual metal and thus will be discussed separately.

6.2.1.1 LEAD

The influence of pH on the sorption of aqueous Pb onto the mineral apatite is substantially different than onto clay minerals and soils. In general, the amount of Pb sorbed by clays increases with pH (e.g., Farrah and Pickering, 1979; Elliott et al., 1986; Yong and Phadungchewit, 1992). As seen from Figure 28, however, the effects of pH on the sorption of aqueous Pb in the presence of the apatite powder is not significant, with a 99.9% reduction for pH 1-11 and 95.5% reduction at pH 12.1. The removal capacities of the mineral apatite powder for aqueous Pb under most of the initial pH conditions were about 151 mg of Pb/g of apatite, which is significantly higher than previously reported (Ma et al., 1995).

Recent investigations on the interactions of aqueous Pb^{2+} with synthetic hydroxyapatite revealed that the removal of dissolved Pb from solutions was mainly through the dissolution of hydroxyapatite and the precipitation of pyromorphites (Ma et al., 1993, 1994a, b; Xu and Schwartz, 1994). Ma et al. (1995) studied the attenuation of aqueous Pb by mineral apatite samples from different localities and concluded that the primary mechanism of Pb removal was also through the dissolution of mineral apatites and the precipitation of carbonate fluoropyromorphite [$Pb_{10}(PO_4)_3(CO_3)_3FOH$] and/or hydrocerussite [$Pb_3(CO_3)_2(OH)_2$ or $Pb(OH)_2 \bullet 2PbCO_3$].

In this study, the XRD patterns of the solid residues from the reactions of aqueous Pb with the apatite powder are shown in Figure 30, which indicate the formations of new solid phases depending on solution pH. Fluoropyromorphite was formed at initial solution pH 1 - 2; hydroxyl fluoropyromorphite [$Pb_{10}(PO_4)_6(F, OH)_2$] was precipitated at initial pH 2.5 - 5.5; carbonate hydroxyl fluoropyromorphite was identified at initial pH6 - 8; hydrocerussite was formed at the initial pH of 6 - 12; and hydroxypyromorphite may have precipitated at initial pH 10 - 12, with possible formation of lead oxide fluoride (Pb_2OF_2). The peaks of the pyromorphite-type compounds became weaker and broader as the initial solution pH increased, suggesting that the quantity and crystallinity of the pyromorphite-type compounds decreased with increasing pH; whereas those of hydrocerussite became stronger with increasing pH, with the strongest peaks at initial pH 7 - 8.

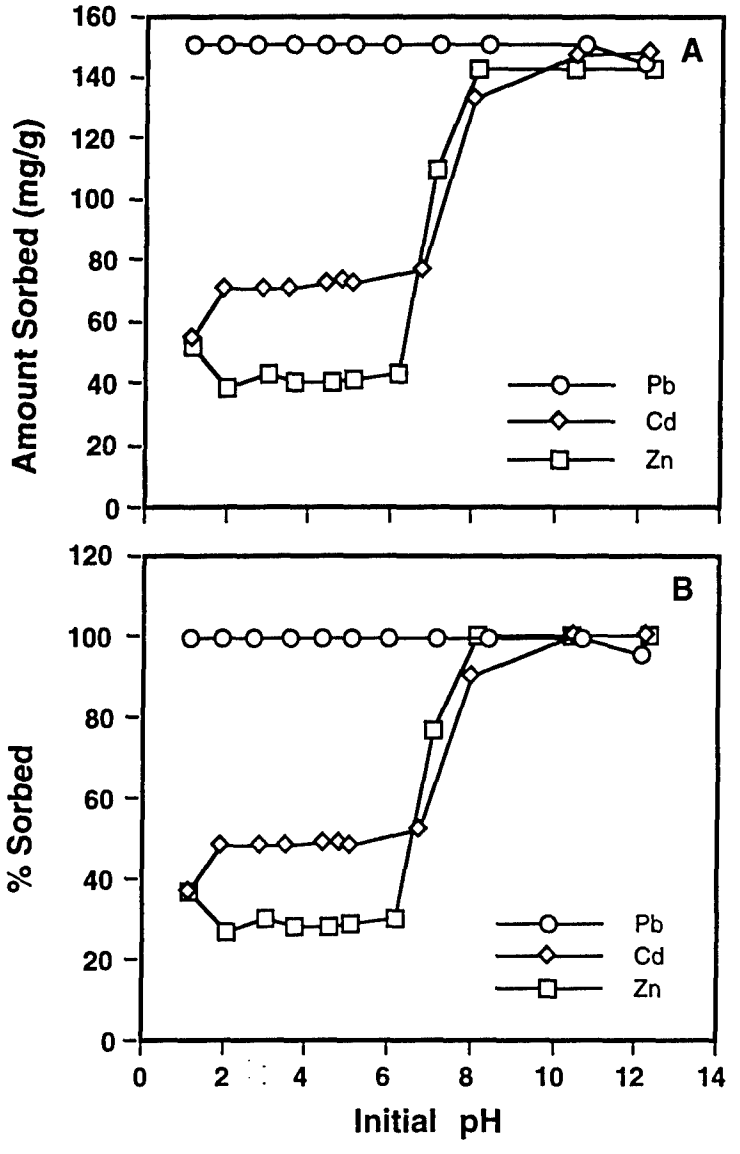

Figure 28. Sorption of Heavy Metals in North Carolina Apatite With Respect to pH in SSST.

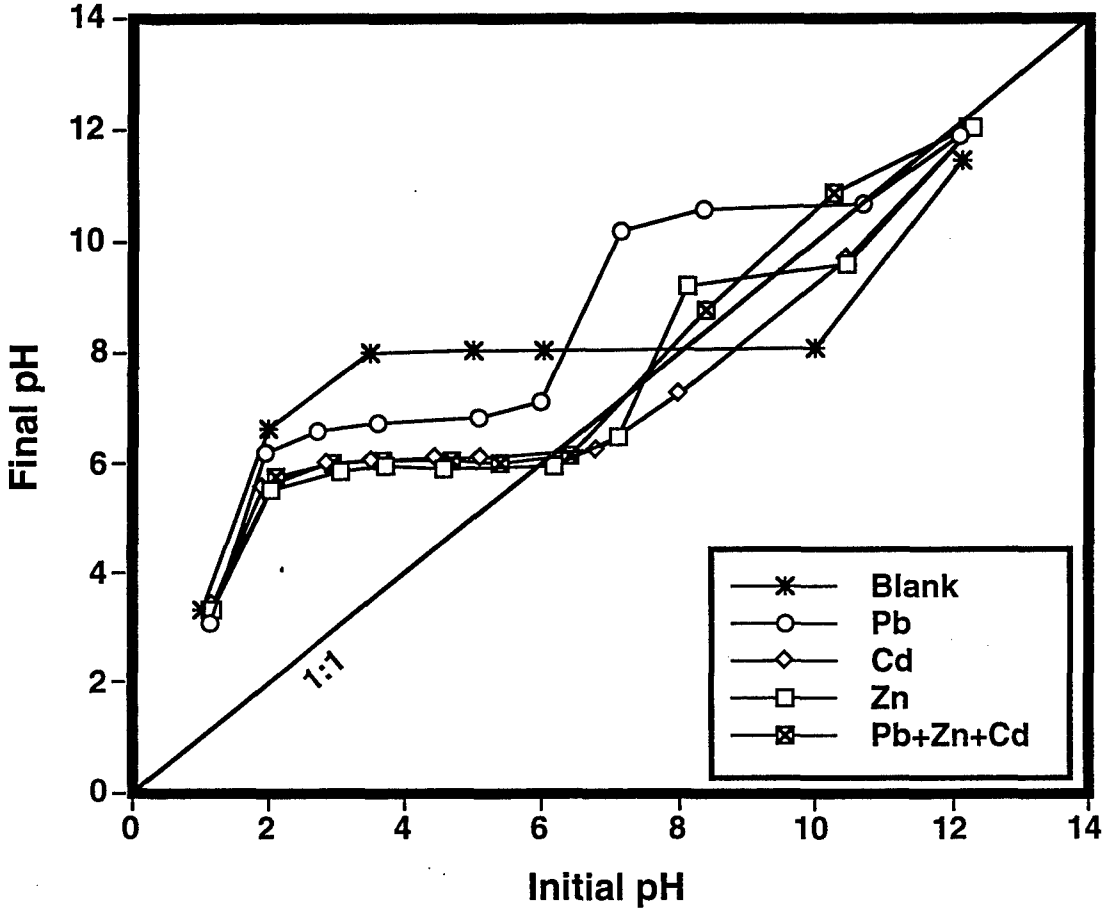

Figure 29. Relationship of Initial and Final pH After Solutions Reacted With North Carolina Apatite.

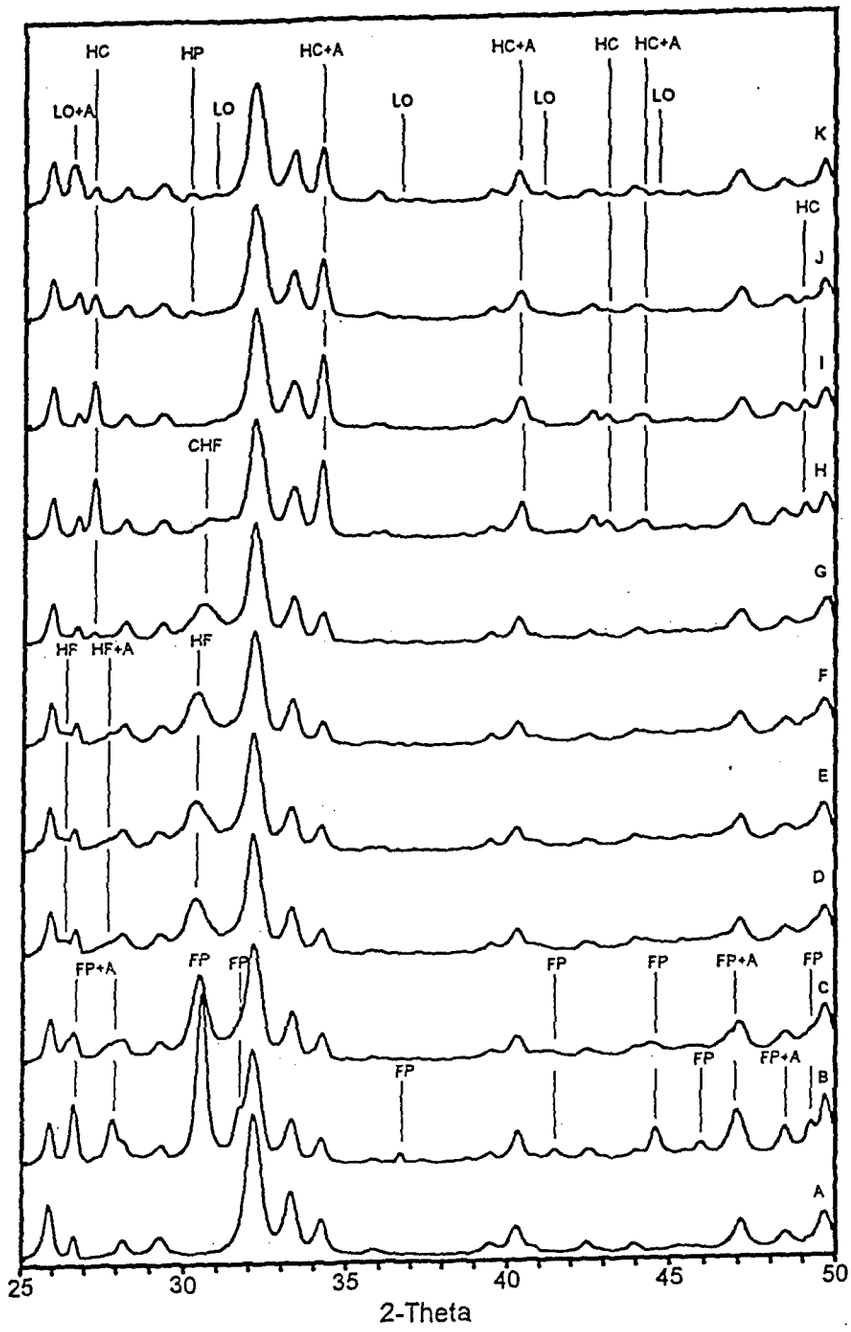

Figure 30. XRD Patterns of North Carolina Apatite Before (A) and After Interaction With Aqueous Pb Solutions of pH 1.14 (B), 1.94 (C), 2.71 (D), 3.62 (E), 5.11 (F), 6.01 (G), 7.17 (H), 8.38 (I), 10.69 (J), and 12.10 (K). Peak Labels: A=Apatite; FP=Fluoropyromorphite; HF=Hydroxyl Fluoropyromorphite; CHF=Carbonate Hydroxyl Fluoropyromorphite; HP=Hydroxypyromorphite; HC=Hydrocerussite; LO=Lead Oxide Fluoride.

The identification of different pyromorphite-type compounds was based on a comparison of the shifting of their XRD maxima with the standard XRD patterns of pyromorphites given by the Joint Committee on Powder Diffraction Standards (JCPDS). Such comparison is summarized in Table 19. The XRD maxima of synthetic fluoropyromorphite and hydroxypyromorphite are 2.92 Å and 2.97 Å, respectively. Thus, the incorporation of OH^- into the crystal structure of fluoropyromorphite will cause the shifting of its XRD maximum to larger d-spacing. The pyromorphite-type compounds formed at an initial solution pH of 1 - 2 have a XRD maximum equal to 2.93 Å, which was identified as fluoropyromorphite without incorporation of OH^-. However, at initial pH 2.71 - 5.11, the newly precipitated solid phases have XRD maxima of 2.95 Å, indicating a certain amount of OH^- incorporated into the structure of pyromorphite. In addition, the XRD data suggest that carbonate ions did not exist in the crystal structure of the compound because the incorporation of carbonate into the structure of apatites would have caused their XRD maxima to shift to smaller d-spacings (Table 19). Thus, the pyromorphite-type compound was classified as hydroxyl fluoropyromorphite. At initial pH 6.01 and 7.17, the compounds formed had relatively smaller d-spacing (Table 19) and were identified as carbonate hydroxyl fluoropyromorphite. The phosphate compound formed at very alkaline conditions in this study was recognized as hydroxypyromorphite because of the XRD maximum of about 2.97 Å.

The formation of the new solid phases described above involved apatite dissolution followed by the precipitation of solids. The type of reaction product precipitated was pH-dependent. In the following discussion, the species of dissolved phosphate and carbonate are determined on the basis of the final pH of the reaction systems, while the dominant species of dissolved lead are present according to the initial pH of the metal solutions. When the initial pH of aqueous metal solutions was very low, ranging from 1 to 2, the final pH was from 3 to 6.2 after 24-h equilibration (Figure 29). At such acidic pH range, the carbonate resulting from the dissolution of mineral apatite exists mainly as $H_2CO_3^0$, and thus, the activities of carbonate ions as well as OH^- are extremely low (Stumm and Morgan, 1981; Drever, 1988), resulting in the difficulty of incorporating carbonate and OH^- into the pyromorphite structure. Assuming $Ca_{10}(PO_4)_{6-x}(CO_3)_xF_{2-y}(OH)_y$ as the general formula for this mineral apatite, the chemical reactions involved can be summarized as:

$$Ca_{10}(PO_4)_{6-x}(CO_3)_xF_{2-y}(OH)_y(c) + (12 + y)\ H^+ \rightarrow 10Ca^{2+} + (6 - x)H_2PO_4^- + xH_2CO_3^0 + (2 - y)F^- + yH_2O \quad (1)$$

$$10Pb^{2+} + 6H_2PO_4^- + 2F^- \rightarrow Pb_{10}(PO_4)_6F_2(c) + 12H^+ \quad (2)$$

As the initial pH of aqueous Pb solution increased to 2.5 - 6.0, the final equilibrium pH also increased to near neutral range (6.6 - 7.0). This higher pH

Table 19. X-ray diffractin maxima of pyromorphite-type compounds and a comparision of the effect of carbonate substitition into apatite structure on d-spacing.

Pyromorphite-Type Compound	d-spacing (112, 211), Å									
		Initial pH of Aqueous Pb Solution								
	JCPDS	1.14	1.94	2.71	3.62	4.38	5.11	6.01	7.17	10.69	12.10
$Pb_{10}(PO_4)_6F_2$	2.92	2.93	2.93								
$Pb_{10}(PO_4)_6(F,OH)_2$				2.95	2.95	2.95	2.95				
$Pb_{10}(PO_4)_6(OH)_2$	2.97									2.97	2.97
$Pb_{10}(PO_4,CO_3)_6(F,OH)_2$								2.92	2.91		
Synthetic Apatite											
$Ca_{10}(PO_4)_6(OH)_2$	2.81										
$Ca_{10}(PO_4)_6F_2$	2.80										
$Ca_{10}(PO_4)_3(CO_3)_3(OH)_2$	2.78										

resulted in an increase of the activity of OH^-, resulting in the formation of hydroxyl fluoropyromorphite:

$$Ca_{10}(PO_4)_{6-x}(CO_3)_xF_{2-y}(OH)_y(c) + (12 - x + y)H^+ \rightarrow 10Ca^{2+} + (6 - x)H_2PO_4^- + xHCO_3^- + (2 - y)F^- + yH_2O \quad (3)$$

$$10Pb^{2+} + 6H_2PO_4^- + 2(F^-,OH^-) \rightarrow Pb_{10}(PO_4)_6(F,OH)_2(c) + 12H^+ \quad (4)$$

Although the dissolved carbonate occurred as HCO_3^- in Eq. (3), lead carbonate compounds, such as cerussite ($PbCO_3$) and hydrocerussite, were not formed because of their high solubility in this pH range (Lindsay, 1979). Rickard and Nriagu (1978) stated that cerussite is very common in the aqueous environments adjacent to lead-zinc-limestone ore deposits, which are characterized by high dissolved Pb, high carbonate ions, and relatively low pH. The chemical conditions in the experiments discussed above satisfy the aqueous Pb and pH requirements, but the aqueous mineral apatite systems are not highly carbonated compared to a limestone system. Nevertheless, hydrocerussite can be expected under conditions of high dissolved Pb, high pH, and low carbonate (Rickard and Nriagu, 1978). Such requirements for the precipitation of hydrocerrusite were easily met when the initial pH of the aqueous Pb solution was slightly above 7.0, which resulted in the equilibrium pH slightly above 10.0. Thus, the interaction of mineral apatite with aqueous Pb under these conditions was dominated by the formation of hydrocerrusite, with minor amounts of carbonate hydroxyl fluoropyromorphite (Figure 30):

$$Ca_{10}(PO_4)_{6-x}(CO_3)_xF_{2-y}(OH)_y(c) + (6 + y)H^+ \rightarrow 10Ca^{2+} + (6 - x)HPO_4^{2-} + xHCO_3^- + (2 - y)F^- + yH_2O \quad (5)$$

$$3PbOH^+ + 2HCO_3^- + 2H_2O \rightarrow Pb_3(CO_3)_2(OH)_2(c) + 4H^+ \quad (6)$$

$$10Pb^{2+} + 6(HPO_4^{2-},HCO_3^-) + 2(F^-,OH^+) \rightarrow Pb_{10}(PO_4,CO_3)_6(F,OH)_2(c) + 6H^+ \quad (7)$$

At pH slightly above 7.0 both Pb^{2+} and $PbOH^+$ contribute significantly to total lead in solution. Therefore, for simplicity, the species of dissolved Pb are presented generically as shown in Equations. (6) and (7). Although dissolved carbonate is presented as HCO_3^- in Equation (5), the amounts of HCO_3^- and CO_3^{2-} were actually about equal in the final pH of slightly above 10. Thus, the activity of carbonate ions in Equation (7) was higher than that in Equations (2) and (4) and the driving force for carbonate incorporation into pyromorphite sites increased. This may explain the precipitation of carbonate hydroxyl fluoropyromorphite. However, according to Lindsay (1979), fluoropyromorphite is more soluble than lead carbonate under alkaline condition, thus the carbonate hydroxyl fluoropyromorphite present in the solid

residues might eventually be transformed into hydrocerrusite if the reactions were allowed to proceed long enough.

When the initial pH of aqueous Pb solutions were between 10.7 and 12.1, their corresponding final pH did not change much, ranging from 10.7 to 11.9 after 24-h equilibration. The XRD patterns in Figure 29 indicated that new solid phases, including hydrocerussite, hydroxypyromorphite, and lead oxide fluoride, were formed as shown below:

$$Ca_{10}(PO_4)_{6-x}(CO_3)_xF_{2-y}(OH)_y(c) + (6 - x + y)H^+ \rightarrow 10Ca^{2+} + (6 - x)HPO_4^{2-} + xCO_3^{2-} + (2 - y)F^- + yH_2O \quad (8)$$

$$3Pb(OH)_3^- + 2CO_3^{2-} \rightarrow Pb_3(CO_3)_2(OH)_2(c) + OH^- \quad (9)$$

$$10Pb(OH)_3^- + 6HPO_4^{2-} \rightarrow Pb_{10}(PO_4)_6(OH)_2(c) + 6H_2O + 22OH^- \quad (10)$$

$$2Pb(OH)_3^- + 2F^- \rightarrow Pb_2OF_2(c) + H_2O + OH^- \quad (11)$$

The solubility of apatite minerals is highly pH dependent with lower solubilities at higher pH (e.g., Christoffersen and Christoffersen, 1982; Kanabo and Gilkes, 1987). The "blank" tests in this study also indicated that the amount of the apatite powder dissolved decreased dramatically above initial pH 10.0, resulting in a substantial drop in dissolved phosphate, carbonate and fluoride anions in the system. These suggested that the anions might be required to combine with dissolved Pb individually as shown in Equations (9), (10), and (11) because of oversupply of Pb in the system. In alkaline solutions, hydrocerussite is less soluble than fluoropyromorphite but slightly more soluble than hydroxypyromorphite (Lindsay, 1979). In addition, the activity of OH^- must be substantially higher than that of F^- supplied by the limited dissolution of the apatite, which resulted in the formation of hydroxypyromorphite instead of fluoropyromorphite. Although the solubility of hydrocerussite is slightly higher than that of hydroxypyromorphite, the shortage of phosphate ions from the limited dissolution of apatite and the oversupply of aqueous Pb in the system resulted in the precipitation of hydrocerussite as well as lead oxide fluoride. The lead oxide fluoride may be eventually converted into hydroxypyromorphite or hydrocerussite providing the continuous supply of phosphate and carbonate from the dissolution of mineral apatite, because lead oxide is thermodynamically much more soluble (Lindsay, 1979).

The reactions present above can be used to explain the relationship of the pH curves of the blank and aqueous Pb (Figure 29). In the blank curve, Equations (1), (3), and (5) contributed to an increase in final pH when initial pH was low but a decrease of final pH when initial pH was alkaline. The latter may be due to the consumption of OH^- from the formation of calcium hydroxide after the dissolution of the apatite. When aqueous Pb was present in solution, the precipitation would free either some H^+ (Eqs. 2, 4, 6, and 7) under acidic initial pH or some OH^- (Eqs. 9 - 11) under alkaline initial pH

condition, resulting in the final pH increase in the aqueous Pb system lower than that in the blank under acidic condition, but higher under alkaline condition (Figure 29).

In addition to the XRD results shown in Figure 30, the formation of new precipitates was supported by the examination of selected reacted solid residues under SEM. Scattered needle- or rod-shaped crystals, presumably fluoropyromorphite, were observed in the sample obtained from the reaction at very acidic condition (Figure 31). Similar crystals were reported by Ma et al. (1995). However, no obvious differences were detected under SEM between the unreacted apatite powder and those reacted with aqueous Pb at higher pH conditions (data not shown here), although the XRD data in Figure 30 indicated the presence of pyromorphite-type phases. This variation in the occurrence of the pyromorphite-type solids under SEM may support the conclusion obtained from the XRD data that the crystallinity of the solids decreased with the increase in pH. Another possible interpretation for the variable presence of the pyromorphite-type compound is that at less acidic solutions their phases were formed as a thin coating on apatite particles instead of scattered needle-like crystals.

From the above discussion, it appears that the precipitation of variable solid phases in the interaction of aqueous Pb with the mineral apatite has an excellent correspondence to thermodynamic predictions such as Lindsay (1979). His thermodynamic calculation suggested that pyromorphite-type compounds should be the most insoluble phases under acidic to neutral conditions while Pb carbonates and oxides should be less soluble than fluoropyromorphite under alkaline conditions. Such predictive relationships are what we observe in our study. Thus, the removal of aqueous Pb from solution primarily results from the formation of variable Pb compounds depending on solution pH and available anions.

Although the precipitation of variable Pb solid phases acted as the primary mechanism in the removal of aqueous Pb from solution, other sorption processes (e.g., ion exchange, adsorption, and surface complexation) cannot be excluded as possible attenuation mechanisms for aqueous Pb with apatite, in particular, at neutral to alkaline conditions. Previous studies have suggested ion exchange and adsorption as sorption processes in the experiments of aqueous Pb with synthetic hydroxyapatite (e.g., Suzuki et al., 1982, 1984; Miyake et al., 1986; Takeuchi et al., 1988; Takeuchi and Arai, 1990). Additionally, Ma et al. (1995) found that significant amounts of aqueous Pb were removed from solutions with no new solid phase identified by XRD and SEM after some mineral apatite samples from certain localities were reacted with aqueous Pb. They attributed these Pb removals to the formation of poorly crystalline or noncrystalline solid phases, cation substitution (or ion exchange), and adsorption. Our study shows that the precipitation of crystalline new phosphate and/or carbonate

Figure 31. SEM Micrographs of North Carolina Apatite Before (A) and After Interaction With Aqueous Pb Solution of pH 1.14 (B).

solid phases is the primary mechanism for the attenuation of aqueous Pb in the presence of mineral apatite, but it is unknown to what extent other mechanisms may be involved.

6.2.1.2 CADMIUM

The effect of pH on the sorption of aqueous Cd onto the mineral apatite is substantially different from those of aqueous Pb (Figure 28), but is very similar to Cd sorption onto calcite and clay minerals (e.g., Elliott et al., 1986; Zachara et al., 1991; Yong and Phadungchewit, 1992), which was characterized by increasing Cd sorption with increasing pH. The capacity of Cd removal in the presence of the mineral apatite varies substantially, ranging from 55 - 148 mg of Cd/g of apatite and representing 37% to nearly 100% removal of Cd from solution. The sorption curves of Cd show two jumps and two plateaus (Figure 28). The first abrupt increase of Cd sorption onto apatite occurred at Cd solution pH from 1 to 2, and, comparing to the second jump, it was a slight increase in the sorption capacity of apatite, representing a 10% (or about 15 mg of Cd/g of apatite) increase. When the pH of Cd solution increased from 2 to 7, the removal capacity of apatite powder remained at approximately 50% or 70 mg of Cd/g of apatite. However, as the Cd solution pH increased to 8 and above, its removal capacity substantially increased to 130 - 147.5 mg of Cd/g of apatite, representing 90% to almost 100% removal of aqueous Cd (Figure 28B).

Selected XRD patterns of the reaction products from the interaction of the apatite powder with aqueous Cd are shown in Figure 32. No crystalline cadmium phosphates were detected as reported by Xu et al. (1994) and Ma et al. (1994b) in their studies of synthetic hydroxyapatite reacted with Cd solution. Nevertheless, otavite ($CdCO_3$) and cadmium hydroxide [$Cd(OH)_2$] were formed in this study:

$$Cd^{2+} + HCO_3^- \text{---> } CdCO_3(c) + H^+ \qquad (12)$$

$$Cd^{2+} + 2H_2O \text{---> } Cd(OH)_2(c) + H^+ \qquad (13)$$

The XRD data can interpret the Cd sorption curve shown in Figure 28. The XRD analysis indicated the presence of otavite present in all of the reacted solid residues at variable initial pH except for pH 1.15 (final pH 3.4). At this low pH, otavite is too soluble (Lindsay, 1979), resulting in a lower removal of Cd from solution in the sorption curve (Figure 28). With the increase of Cd solution pH to 2 and above, otavite was precipitated. But the intensity of its XRD peak was low and remained the same as the initial pH ranged from 2 to below 8, , suggesting a small amount of otavite was formed. This may explain the first plateau observed in the sorption curve. Further increase of solution pH to 8.0 and above generated a significant increase of XRD

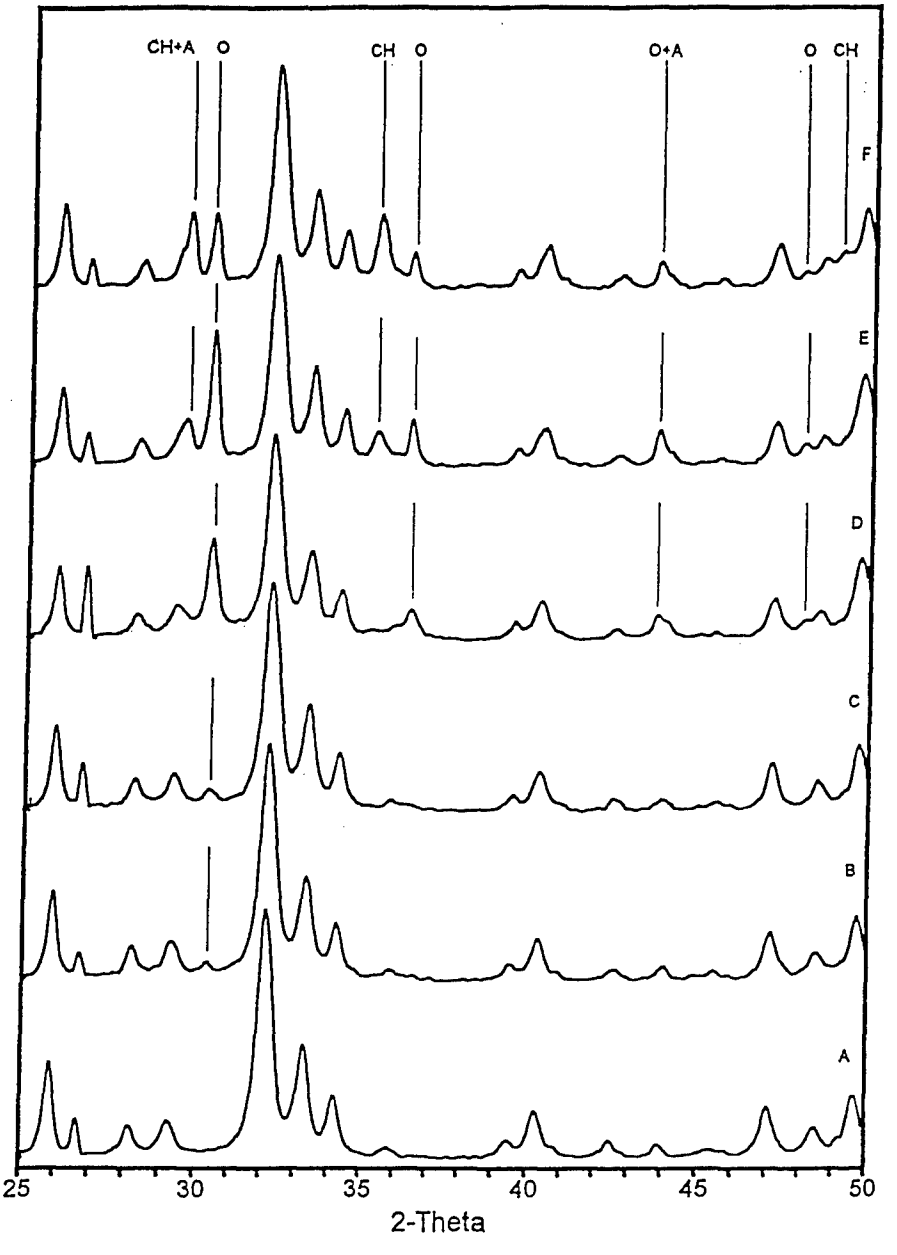

Figure 32. XRD Patterns of North Carolina Apatite Before (A) and After Interaction With Aqueous Cd Solutions of pH 5.13 (B), 6.80 (C), 8.02 (D), 10.47 (E), and 12.23 (F). Peak Labels: O=Otavite; CH=Cadmium Hydroxide.

intensity of otavite, with the strongest at pH approximately 10. This, coupled with the occurrence of cadmium hydroxide at very alkaline solutions (with its strongest peaks at initial pH 12), could account for the significant increase of Cd removal from solution, resulting in the second plateau of the sorption curve.

The dissolution of the mineral apatite powder may supply the carbonate required for the precipitation of otavite. When the Cd solution was acidic, the final pH after 24-h reaction was below 6.2, suggesting the dissolved carbonate mainly occurred as $H_2CO_3^0$ as described in Equation (1), resulting in a low activity of carbonate ion. This may be one of the factors for the limited amount of otavite formed in the reaction under acidic condition. Another factor regulating the amount of otavite precipitated is its relatively high solubility at low pH.

The theoretical solubility diagram (Lindsay, 1979) predicted that cadmium phosphate [$Cd_3(PO_4)_2$] should be less soluble than otavite under acidic conditions, and such relationship reverses under alkaline conditions. However, cadmium phosphate was not identified as expected in our XRD analysis. In our experiments, otavite and crystalline cadmium hydroxide precipitated and dictated the concentrations of aqueous Cd in solution at very low levels under alkaline conditions. The thermodynamic modeling and experimental studies by Rai et al. (1991a, b) also suggested that otavite and crystalline cadmium hydroxide have very low solubility products under alkaline conditions.

Due to the difficulty of quantitative determination of solid phases from a XRD pattern, the exact amounts of newly-formed otavite and cadmium hydroxide are not known, but can be estimated by using the sorption data. Assuming that when the pH of aqueous Cd increased from 1.15 to 2.0, the 15 mg of Cd/g of apatite increase of Cd removal was derived from the formation of otavite, then the otavite formed would account for about 2.3 wt% of the solid residue. On the other hand, if accepting 1 wt% as the detection limit of XRD, an increase of removal capacity of 7.8 mg of Cd/g of apatite was needed to observe the XRD peaks of otavite. Because in the presence of apatite, the total Cd removal capacity was about 70 mg of Cd/g of apatite when the initial pH of Cd solutions ranged from 2 to 7, the formation of otavite should account for about 11.1 - 21.4% of the total Cd removed. It is even more difficult to determine how much of the Cd removed is attributable to the formation of otavite or cadmium hydroxide when the solution pH ranged from 8.0 to 12. If assuming that (1) at initial pH below 2.0, all the Cd removed was due to mechanisms other than the formation of new solid(s); and (2) with the initial pH increase above 2.0 all the Cd removal increases resulted from the formation of octavite and/or cadmium hydroxide, then the maximum Cd removed by the formation of these two solids was approximately 62% of the total Cd lost from solution. However, it is unknown how much of the overall Cd removal is attributable to the formation of each of these two new solid phases. The XRD peak

intensities of otavite and cadmium hydroxide shown in Figure 32 suggest that the amount of these solids formed in the system increased substantially when the initial pH increased to above 8.0.

From the above discussion, it appears that in addition to precipitation of solid phases, other sorption mechanisms were also involved in the removal of Cd from solution in the presence of the mineral apatite. Jeanjean et al. (1994) studied the structural modification of the products from the interaction of synthetic hydroxyapatite with Cd^{2+} solution. They concluded that Cd^{2+} ions were sorbed by exchanged with Ca^{2+} and Na^{+} ions in the lattice of the apatite. The Cd^{2+} ions exchanged with Ca^{2+} preferentially occupy Ca(II) sites while the concentration of Ca(I) remains unchanged. In an investigation of calcium-cadmium hydroxyapatite coprecipitation, however, Nounah et al. (1992) suggested that Cd^{2+} are mainly located in Ca(II) sites but are also found in Ca(I) sites. Many other studies also preferred ion exchange process as the main mechanism in the sorption of Cd into apatite (Suzuki et al., 1981; Takeuchi et al., 1988; Takeuchi and Arai, 1990; Middelburg and Comans, 1991). However, Xu et al. (1994) suggested that surface complexation and Ca-Cd hydroxyapatite coprecipitation were the primary processes in the uptake of Cd in the presence of synthetic apatite while ion-exchange and solid diffusion might be secondary processes. Dalas and Koutsoukos (1989) also argued that the removal of Cd cannot be explained by simple adsorption mechanism and assumed that the coprecipitation of a surface Ca-Cd phase and surface diffusion may be involved.

6.2.1.3 ZINC

In the SSST, the overall sorption behavior of aqueous Zn in the presence of apatite was similar to that of aqueous Cd, with minor differences (Figure 28). One of the differences occurred at the initial pH increase from 1.0 to 2.0. In the Cd tests, the sorption capacity increased with initial pH, while in the Zn tests, the sorption capacity decreased approximately from 52 mg (37% sorbed) to 39 mg (27% sorbed) of Zn/g of apatite with the increase of initial pH. As the initial pH of aqueous Zn further increased from 2.0 to 6.20, the sorption capacity did not change significantly and was lower than that of Cd. A substantial increase of sorption capacity (143 mg/g) took place when the initial pH was above 7.0, resulting in nearly all of the aqueous Zn being removed from solution.

In a study of the interaction of aqueous Zn with hydroxyapatite, Misra and Bowen (1981) reported the formation of hopeite [$Zn_3(PO_4)_2 \cdot 4H_2O$] and tarbuttite [$Zn_2(OH)PO_4$]. Figure 33 shows selected XRD patterns of the solid residues from the interaction of the apatite powder with aqueous Zn at variable initial pH. Although no tarbuttite could be detected, hopeite was identified in the solid residues from the reaction at very low initial pH (in particular, 1.0 - 2.0). The dissolution of the apatite

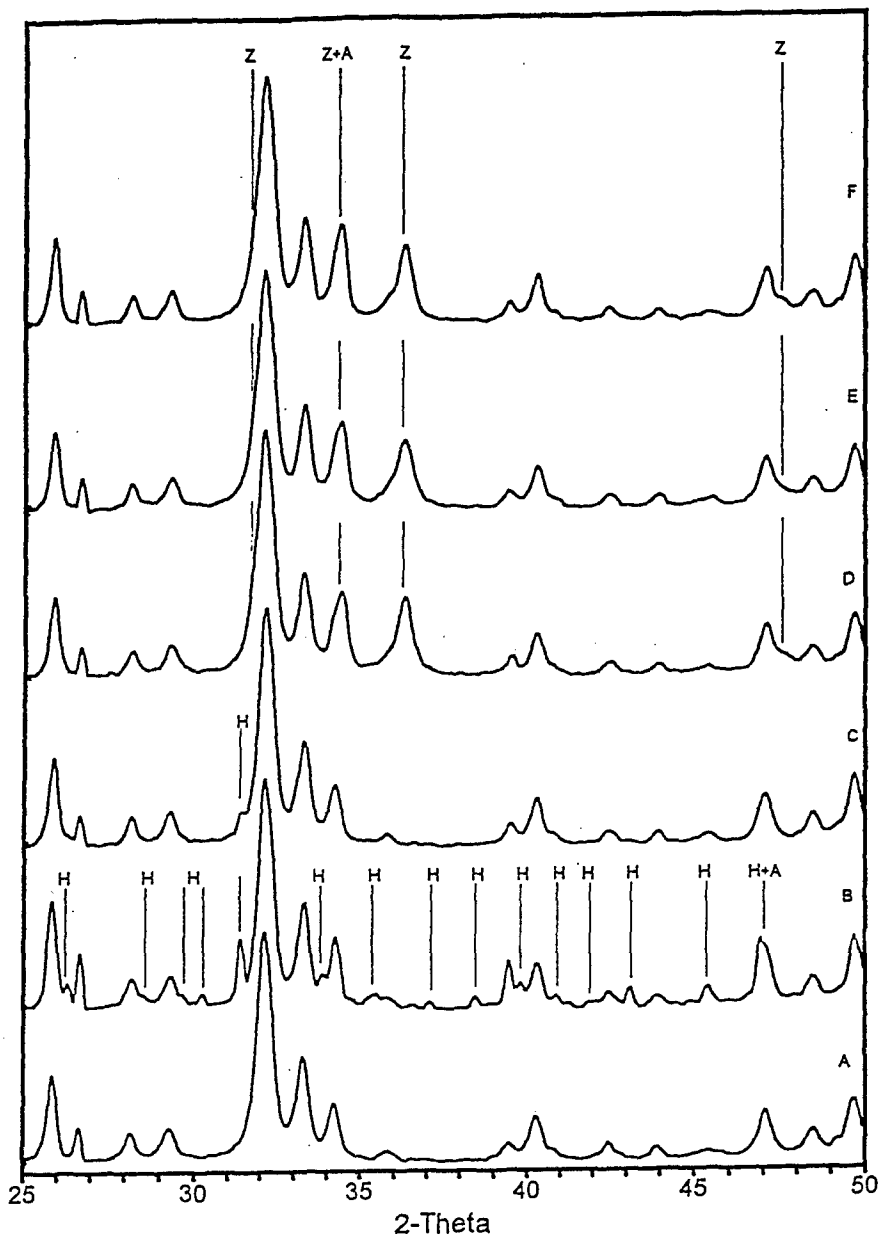

Figure 33 XRD Patterns of North Carolina Apatite Before (A) and After Interaction With Aqueous Zn Solutions of pH 1.15 (B), 2.03 (C), 8.12 (D), 10.45 (E), and 12.04 (F). Peak Labels: H=Hopeite; Z=Zincite.

powder (Eq. 1) supplied dissolved phosphate to the aqueous Zn solution, which was followed by the formation of hopeite:

$$3Zn^{2+} + 2H_2PO_4^- + 4H_2O \text{ ---> } Zn_3(PO_4)_2 \bullet 4H_2O(c) + 4H^+ \quad (14)$$

The XRD peaks of hopeite decreased with initial pH increase. SEM examination of the solid residues also indicated the formation of hopeite after the reaction (Figure 34). At the initial pH range of 3.10 - 7.10, no crystalline compound besides the original apatite could be identified. The decrease of Zn removal from solutions at initial pH above 2.0 may partially be interpreted by the absence of or substantially lower (<1%) occurrence of hopeite as a reaction product. If this is true, then the formation of hopeite at initial pH1.15 would account for approximately 25% of total Zn sorbed.

When the initial pH was increased to above 8.0, zincite (ZnO) was detected in the XRD patterns (Figure 33):

$$Zn(OH)_2^0 \text{ ---> } ZnO + H_2O \quad (15)$$

The theoretical solubility diagram (Lindsay, 1979) suggested that hopeite should be much less soluble than zincite and zinc carbonate (smithsonite, $ZnCO_3$) at acidic conditions while zincite should be less soluble than hopeite and smithsonite in an apatite system at alkaline conditions. Our experimental data confirm this thermodynamic prediction. Additionally, in a study of the interaction of aqueous metals with calcite, Zachara et al. (1993) concluded that Zn carbonate was not as easily precipitated as Cd carbonate did. Similar to the argument for Cd, if all the additional Zn removal capacity under alkaline conditions resulted from the formation of zincite, this would account for approximately 72% of total Zn removed.

Like the interaction of apatite minerals with aqueous Cd, ion exchange has also been proposed as an important mechanism in the removal of Zn from solution (Suzuki et al., 1981; Ingram et al., 1992). Also, Xu et al. (1994) suggested that the dominant sorption processes involving Zn^{2+} interaction with hydroxyapatite surfaces was surface complexation with HAP surface functional groups such as ≡POH and ≡CaOH, and coprecipitation of Zn with Ca into the apatite structure.

6.3 MSST OF HEAVY METALS WITH APATITE

The XRD patterns of the solid residues obtained from the MSST are shown in Figure 35. The peak intensities of the crystalline compounds are weaker than those obtained from the SSST, suggesting that lesser amounts of each solid phase was

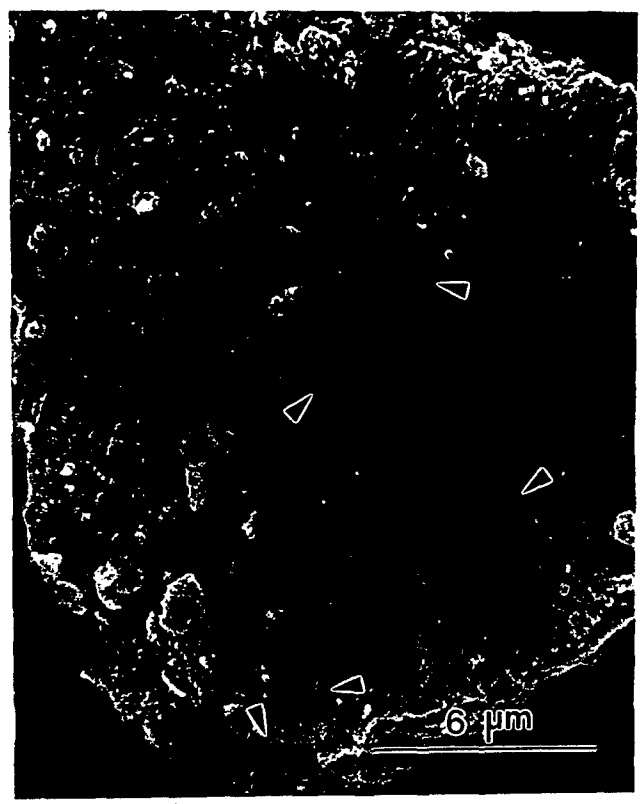

Figure 34. SEM Micrographs of North Carolina Apatite After Interaction With Aqueous Zn Solution of pH 1.15.

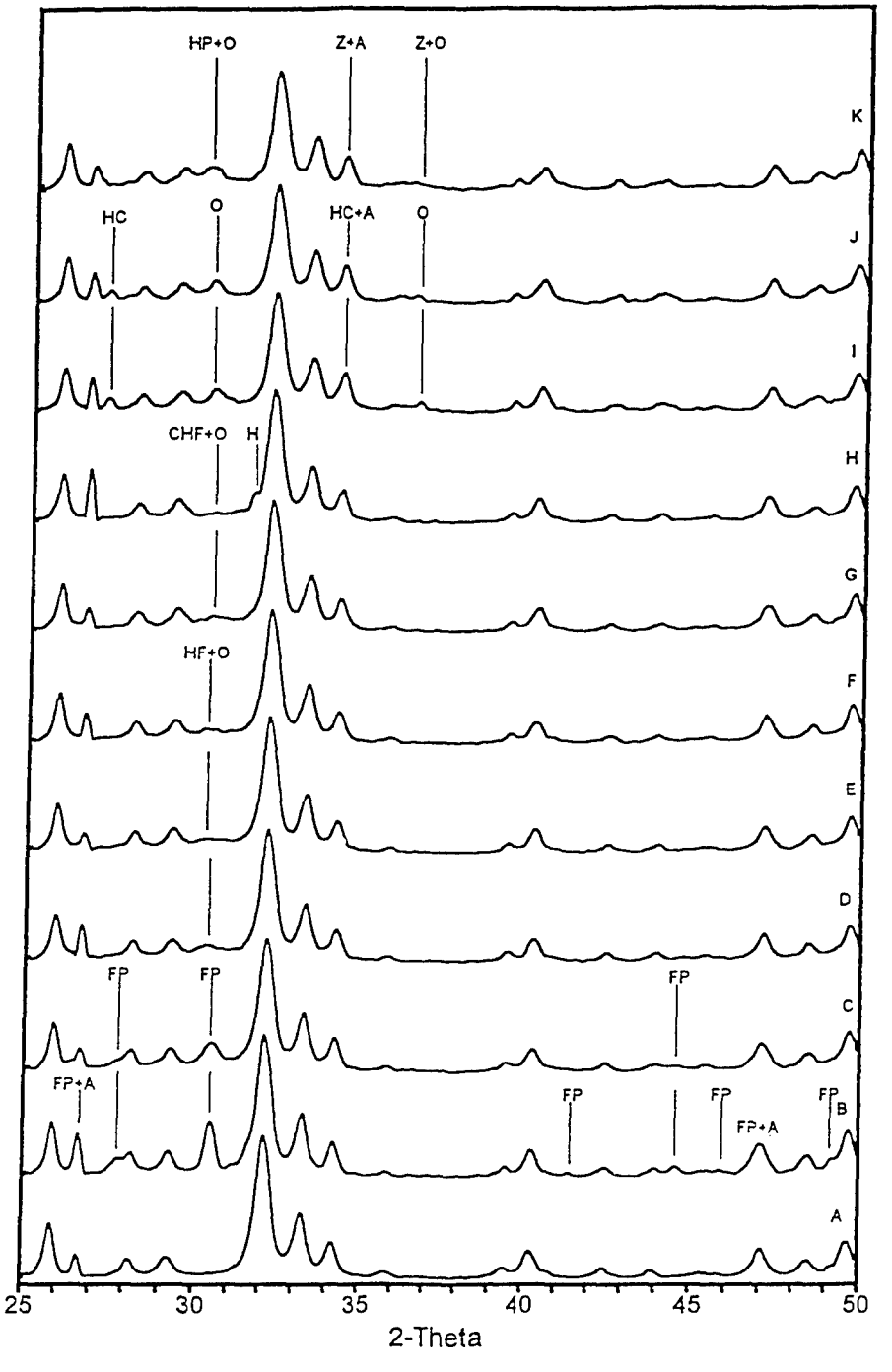

Figure 35. XRD Patterns of North Carolina Apatite Before (A) and After Interaction With Mixed Heavy Metal Solutions of pH 1.13 (B), 2.11 (C), 2.96 (D), 3.69 (E), 4.71 (F), 5.41 (G), 6.42 (H), 8.42 (I), 10.28 (J), 12.20 (K).

formed. The solid phases identified from the patterns are summarized in Table 20, with respect to pH range. Many of the solids found in the SSST were also formed in the MSST and no new solid phase (for instance, coprecipitate) can be identified solely based on the XRD data. Pyromorphite-type solids, hydrocerussite, otavite, and zincite were formed as expected. Hopeite was not formed at initial pH 1 - 2 as in the SSST (Figure 35). The absence of hopeite may result from the competition of Pb for phosphate ions or from the inhibition effect from aqueous Pb and/or Cd. Unexpectedly, hopeite did occur in the solid residue from the test at initial pH 6.4 (Figure 35), which can not be explained at present. The oxides and hydroxide of Pb and Cd which were recognized in the SSST could not be identified in the MSST.

Table 20. Summary of the new solid phases formed in the interaction of mineral apatite with mixed heavy metal solutions with respect to pH.

Initial pH	Final pH	New Solid Phase
1-2	3-5.8	Floropyromorphite
3.0-6.4	6.0-6.2	Hydroxyl Fluoropyromorphite Carbonate Hydroxyl Fluropoyromorphite Otavite Hopeite
8.4-12.2	8.8-12.0	Hydrocerussite Otavite Hydroxypyromorphite Zincite

In the MSST, the amount of each heavy metal applied was equivalent to one third of those applied in the SSST. Competitive sorption among the aqueous heavy metals is expected. Figure 36 shows the amounts of Pb, Cd, and Zn sorbed in the apatite with respect to variation of solution pH. Comparing the sorption curves for the MSST (Figure 36) and those for the SSST (Figure 28) suggests that with respect to the variation of initial pH the sorption behaviors of aqueous Pb are basically identical for both SSST and MSST. The aqueous Pb applied in both tests were nearly 100 percent removed for most of the initial pH values, suggesting that the removal of Pb was not affected by the presence of aqueous Cd and Zn in the current sorption experiments.

The overall sorption behaviors of aqueous Cd and Zn in the MSST were basically similar to those in the SSST, but with minor difference. For easy comparison, the sorption curves of Cd and Zn for both tests are re-graphed in Figure 37. The primary difference in the removal of Cd and Zn between SSST and MSST occurred at neutral

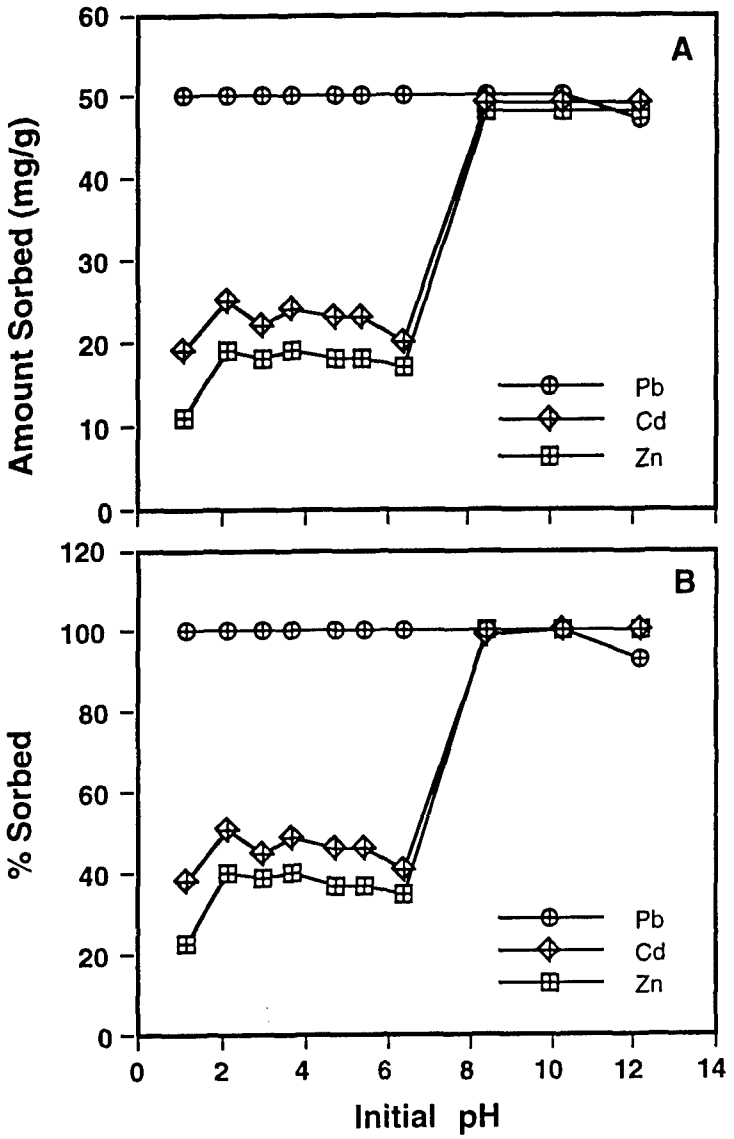

Figure36. Sorption of Heavy Metals in North Carolina Apatie With Respect to pH in MSST.

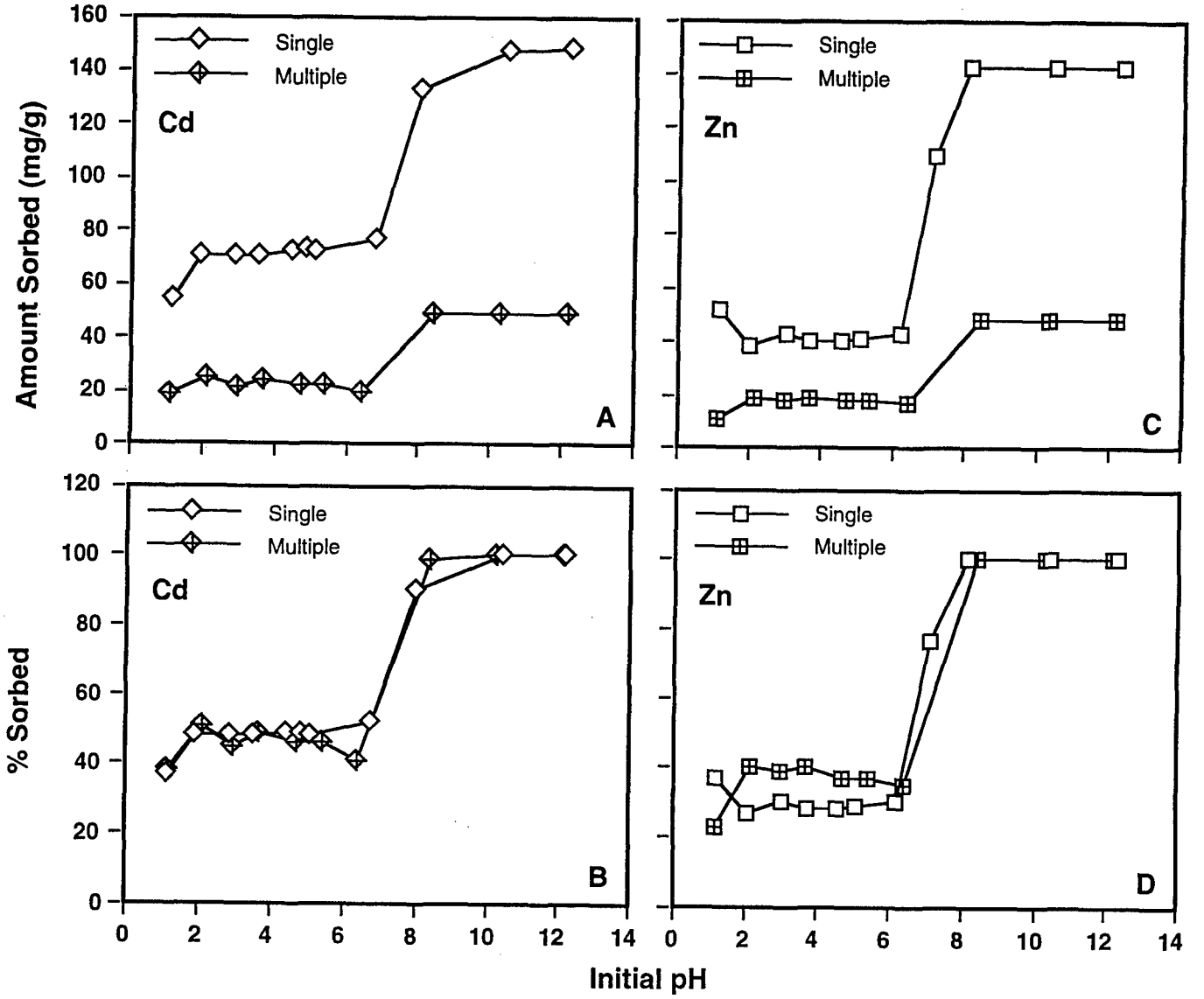

Figure 37. Comparison of Sorption of Aqueous Cd (A, B) and Zn (C,D) in North Carolina Apatite With Respect to pH in SSST and MSST.

to acidic initial pH. In the removal patterns for Cd at initial pH 2.0 - 6.5, the amount of Cd removed was slightly increased with pH in the SSST but slightly decreased with the increase of pH in the MSST (Figures 37A and 37B) although the effect is very small. Corresponding to the amount of individual heavy metal applied, the amount of Cd removed per gram of apatite in the MSST was about one third of that in the SSST, resulting in the similarity of the percentage of Cd removal patterns.

In the Zn sorption experiments, the amount of Zn removed per gram of apatite in the MSST was more than one third of that in the SSST when the initial pH ranged from 2.0 to 6.5, resulting in the higher percentage of Zn removal in the MSST than in the SSST. However, in this pH range the amounts of Zn removed slightly increased with pH in the SSST but slightly decreased with the increase of pH in the MSST (Figures 37C and 37D). This effect was similar to that of Cd as described above. But the important difference in the Cd and Zn sorptions is that with increase of initial pH from 1.0 to 2.0 the amount of Cd sorbed increased in both SSST and MSST (Figures 37A and 37B) while the amount of Zn sorbed increased in the MSST but decreased in the SSST (Figures 37C and 37D). This may be explained by the absence of hopeite precipitation at initial pH 1.0 in the MSST but its presence in the SSST.

From the XRD data and sorption information, it seems that the mechanism responsible for Pb removal from solution in the presence of mineral apatites remains basically unchanged in the presence of aqueous Cd and Zn. This is consistent with previous findings for synthetic hydroxyapatite system (Takeuchi and Arai, 1990; Ma et al., 1994b). In addition, the competitive effects among the heavy metals may alter the sorption behaviors of Cd and Zn to some extent. Here, the competitive effects may include competition for adsorption sites as well as competition for precipitation onto apatites. When the heavy metals were applied individually, they could precipitate as metal phosphates, carbonates, hydroxides, and oxides at their respective precipitation pH with competition solely between ions of the same metal (internal competition), and were in competition only with H^+ for adsorption sites. However, when the heavy metals were applied in their combination, there is internal competition, competition with H^+, and competition with each other for precipitation and for adsorption sites. In the MSST, the absence of hopeite at initial pH 1.1 might be the result of competition between Pb and Zn for precipitation, while the gradual decline of the amounts of Cd and Zn sorbed at initial pH ranging from 2.0 to 6.5 might be an example of the competition from Pb for adsorption sites as pH increase because the XRD patterns indicated that the pyromorphite-type solids formed decreased with the increase of pH. This may result in gradually more aqueous Pb available to compete with Cd and Zn for adsorption sites.

6.4 SELECTIVITY OF HEAVY METALS SORPTION ON APATITE

With a quick comparison of the sorption curves displayed in Figures 28B and 36B, some insight into the selectivity or preferential sorption of the mineral apatite for the species of heavy metals tested can be detected. The selectivity order of heavy metal sorption onto the apatite was dependent upon the pH of the solutions applied. For the initial pH values of less than 7.0, the selectivity order appears to be Pb >> Cd > Zn. For the pH values ranging from 7.0 to 10.0 in the SSST, Cd and Zn are reversed in terms of preferential sorption, resulting in the selectivity order of Pb > Zn > Cd. The selectivity order becomes Zn ≈ Cd > Pb at the initial pH above 10.0 in the SSST and above 8.0 in the MSST. The selectivity orders obtained in this study are summarized in Table 21, with a comparison to the selectivity orders of heavy metals in soils and other minerals reported in the literature. This comparison indicates that among Pb, Cd, and Zn, Pb always has the highest preferential to be sorbed under most circumstances while the selectivity order of Cd and Zn can be varied depending on the type of adsorbents and the chemical conditions, e.g. pH.

Table 21. Sorption selectivity of heavy metals in different materials

Material	Selectivity Order	Reference
Mineral apatite	Pb>>Cd>Zn	This study
Mineral apatite	Pb>Zn ≥Cd	This study
Mineral appatite	Zn≈Cd>Pb	This study
Al oxides	Cu>Pb>Zn>Cd	Kinniburgh et al.(1976)
Fe oxides	Pb>Cu>Zn>Cd	Benjamin & Leckie(1981)
Goethite	Cu>Pb>Zn>Cd	Forbes et al.(1974)
Kaolinite clay	Pb>Ca>Cu>Mg>Zn>Cd	Farrah & Pickering(1977a,b)
Illite clay	Pb>Cu>Zn>Ca>Cd>Mg	Farrah & Pickering(1977a,b)
Montmorillonite clay	Ca>Pb>Cu>Mg>Cd>Zn	Farrah & Pickering(1977a,b)
Mineral soils	Pb>Cu>Zn>Cd	Elliott et al.(1986)
Mineral soils w/20-40g org/kg	Pb>Cu>Cd>Zn	Elliott et al.(1986)

It has been discussed in previous sections that the removal of heavy metals from solutions is related to the formation of solid phases and the occurrence of other sorption processes at different initial pH in this study. The preferential formation of different solid phases and the relationship between ionic radii and the pK of metal hydrolysis product and sorption processes may have significant impact on the selectivity orders observed in this study. LeGeros (1981) and others indicated that ionic radii strongly affects the uptake of trace elements into apatite mineral phases. In

general, cations with ionic radii larger than Ca^{2+}, e.g., Pb^{2+}, may be incorporated into the apatite structure preferentially over those with smaller radii, e.g., Cd^{2+} and Zn^{2+}. In a study of the sorption of heavy metals by soils, Elliott et al. (1986) suggested that there is a correlation between ionic size and sorption selectivity. The ease of sorption or the strength with which cations of equal charge are held is, in general, inversely proportional to the unhydrated ionic radii (Bohn et al., 1971). This implies that the order of selectivity can be predicted based on unhydrated radii as: Pb (1.20 Å) > Cd (0.97 Å) > Zn (0.74 Å).

On the other hand, aqueous heavy metals hydrolyze at high pH levels. This hydrolysis will result in a suite of soluble metal complexes and may lead to precipitation of metal hydroxides (Lindsay, 1979; Stumm and Morgan, 1981). Under this circumstance, the sorption affinity of heavy metals can then be related to the pK of the first hydrolysis product of the metal cations (Forbes et al., 1974), where K is the equilibrium constant for the following reaction (Elliott et al., 1986):

$$M^{2+}(aq) + nH_2O \text{ ---> } M(OH)_n^{2-n} + nH^+ \qquad (16)$$

Ranking the pK values of Pb, Cd, and Zn in an ascending order as done by Baes and Messmer (1976) and Elliott et al. (1986) will result in a predicted selectivity order as follows: Pb (6.2) > Zn (9.0) > Cd (10.1). Apparently, the selectivity orders found in this study correspond closely to the selectivity orders of heavy metal retention predicted based on ionic size and the pK of the first hydrolysis product of the metals.

6.5 CONCLUSIONS

These sorption experiments indicate that the removal of aqueous Pb from solutions was nearly pH-independent while the reduction of aqueous Cd and Zn concentrations in solutions was pH-dependent. The removal capacities were about 151 mg of Pb, 55-148 mg of Cd, and 39-143 mg of Zn per gram of apatite, which represented that 99.9% Pb, 37-99.9% Cd, and 27-99.9% Zn applied were removed from solutions.

The current study also suggests that a change in pH leads to a corresponding change of the dominant sorption mechanism of heavy metals in the apatite and of new solid reaction products. The sorption of aqueous Pb was primarily through a process of the dissolution of the apatite followed by the precipitation of pyromorphite-type minerals under acidic conditions or of hydrocerussite and lead oxide fluoride under highly alkaline conditions. Otavite and cadmium hydroxide, and zincite were formed in the Cd and Zn systems, respectively, but mostly under alkaline condition, while hopeite might only occur under very acidic conditions. This suggests that alternative sorption mechanisms other than the precipitation of the crystalline phases were important in reducing Cd and Zn concentrations in the presence of apatite. The alternative mechanisms might include ion exchange, adsorption, absorption,

complexation, coprecipitation and precipitation of amorphous solids.

The competition and interference among aqueous metals had little effect on the retention of Pb but had some effect on Cd and Zn. The selectivity order of heavy metal sorption onto the apatite were also pH-dependent. At solution pH below 7, the selectivity order obtained was Pb > Cd > Zn; but it was Pb > Zn > Cd or Zn ≈ Cd > Pb at higher solution pH. This behavior was consistent with the order of ionic size and the pK of the first hydrolysis product of the metals.

7.0 REFERENCES

Altschuler, Z.S. 1980. The geochemistry of trace elements in marine phosphorites, part I. characteristic abundances and enrichment. Soc. Econ. Paleontol. Mineral. Spec. Publ. 29, p. 19-30.

Baes, C.F. and Messmer, R.E. 1976. The Hydrolysis of Cations. John Wiley & Sons, New York.

Baham, J. and Sposito, G. 1986. Proton and metal complexation by water-soluble ligands extracted from anaerobically digested sewage sludge. J. Environ. Qual., v. 15, p. 239-244.

Beckwith, R. S. 1964. "Sorbed phosphate at standard supernatant concentration as an estimate of the phosphate needs of soils," *Aust. J. Exp. Agr. and An Hus.* 5:52-58.

Benjamin, M.M. and Leckie, J.O. 1981. Multiple-site adsorption of Cd, Zn and Pb on amorphous iron oxyhydroxide. Journal of Colloid and Interface Science, v. 79, p. 209-221.

Bero, B.N. 1994. Characterization of lead contaminated soils and evaluation of vacuuming and X-ray fluorescence techniques for sampling carpeted surfaces. University of Idaho PhD thesis, 366 p.

Bohn, M.D.A., Posner, D.M. and Quirk, J.P. 1971. Soil Chemistry. John Wiley & Sons, New York.

Chien, S.H. and Hammond, L.L. 1978. "A comparison of various laboratory methods for predicting the agronomic potential of phosphate rock for direct application," *Soil Sci. Soc. Am. J.*, 42, 935-939.

Chien, S.H. and Black, C.A. 1976. Free energy of formation of carbonate apatites in some phosphate rocks. Soil Sci. Soc. Am. J., v. 40, p. 234-239.

Chien, S.H., Clayton, W.R. and McClellan, G.H. 1980. Kinetics of dissolution of phosphate rocks in soils. Soil Sci. Soc. Am. J., v. 44, p. 260-264.
Christensen, P.D., S. J. Toth, and F. E. Bear. 1951. *Soil Sci Soc Am Proc* 15:279-282.

Christoffersen, J. and Christoffersen, M.R. 1982. "Kinetics of dissolution of calcium hydroxyapatite V. The acidity constant for the hydrogen phosphate surface complex," *Journal of Crystal Growth,* 57, 21-26.

Conca, J. L. and J. V. Wright. 1992. "Diffusion and flow in gravel, soil, and whole rock," *Applied Hydrogeology* 1:5-24.

Conca, J. L., X. Chen, and J. V. Wright. 1994. "Flow experiments demonstrate the efficacy of apatite in the remediation of metal-contaminated soil," *American Geophysical Union Annual Meeting Abstracts* (in press).

Conca, J. L. and J. V. Wright. 1990. "Diffusion coefficients in gravel under unsaturated conditions," *Water Resources Research* 26:1055-1066.

Dalas, E. and Koutsoukos, P.G. 1989. Crystallization of hydroxyapatite from aqueous solutions in the presence of cadmium. J. Chem. Soc., Faraday Trans 1, v. 85, p. 3159-3164.

Davis, J.A., Fuller, C.C. and Cook, A.D. 1987. A model for trace metal sorption processes at the calcite surface: Adsorption of Cd^{2+} and subsequent solid solution formation. Geochimica et Cosmochimica Acta, v. 51, p. 1477-1490.

Davis, A., M. V. Ruby, and P. D. Bergstrom. 1992. "Bioavailability of arsenic and lead in soils from the Butte, Montana, Mining District," *Environmental Science and Technology*, 26: 461-468.

Drever, J.I. 1988. The Geochemistry of Natural Waters. Prentice Hall, New Jersey.

Eisenbud, M. 1987. *Environmental Radioactivity*, third edition, Academic Press, San Diego, pp. 125-127, 149-152.

Elliott, H.A., Liberati, M.R. and Huang, C.P. 1986. Competitive adsorption of heavy metals by soils. J. Enriron. Qual., v. 15, p. 214-219.

Farrah, H. and Pickering, W.F. 1979. pH effects in the adsorption of heavy metals ion by clays. Chemical Geology, v. 25, p. 317-326.

Farrah, H. and Pickering, W.F. 1977a. Influence of clay-solute interactions on aqueous heavy metal ion levels. Water, Air, and Soil Pollution, v. 8, p. 189-197.

Farrah, H. and Pickering, W.F. 1977b. The sorption of lead and cadmium species by clay minerals. Australian Journal of Chemistry, v. 30, p. 1417-1422.

Forbes, E.A., Posner, A.M. and Quirk, J.P. 1974. The specific adsorption of inorganic Hg(II) species and Co(III) complex ions on geothite. Journal of Colloid and Interface Science, v. 49, p. 403-409.

Förstner, U. and M. Kersten. 1988. "Assessment of metal mobility in dredged material and mine waste by pore water chemistry and solid speciation." In *Chemistry and Biology of Solid Waste, Dredged Material and Mine Tailings*, W. Salomons and U. Förstner, eds. Springer-Verlag, Berlin, Heidelberg, pp. 214-237.

Galehouse, J. S. 1971. "Sedimentation Analysis." In *Procedures in Sedimentary Petrology*, R. E. Carver, ed. Wiley-Interscience, New York, pp. 69-94.

Geochem Software, Inc. 1994. "Mac MINTEQ-A2: Aqueous Geochemistry for the Macintosh." Published by Geochem Software, Inc. Reston, VA.

Gibbs, R.J. 1971. X-ray diffraction mounts. *In*: Procedures in Sedimentary Petrology, R. E. Carver (ed.), Wiley-Interscience, New York, pp. 531-539.

Harter, R.D. 1983. Effect of soil pH on adsorption of lead, copper, zinc, and nickel. Soil Sci. Soc. Am. L., v. 47, pp. 47-51.

Howard, J. L. and Sova, J. E. 1993. "Sequential extraction analysis of lead in Michigan roadside soils: mobilization in the vadose zone by deicing salts," *Journal of Soil Contamination* 2: 361-378.

Ingram, G.S., Horay, C.P. and Stead, W.J. 1992. Interaction of zinc with dental mineral. Caries Res., v. 26, p. 248-253.

Ingram, R. L. 1971. "Sieve Analysis." In *Procedures in Sedimentary Petrology*, R. E. Carver, ed. Wiley-Interscience, New York, pp. 49-68.

Jeanjean, J., Vincent, U. and Fedoroft, M. 1994. Structural modiification of calcium hydroxyapatite induced by sorption of cadmium ions. Journal of Solid State Chemistry, v. 108, p. 68-72.

Kanabo, I.A.K. and Gilkes, R.J. 1987. The role of soil pH in the dissolution of phosphate rock fertilizers. Fertilizer Research, v. 12, p. 165-174.

Kinniburgh, D.G., Jackson, M.L. and Syers, J.K. 1976. Adsorption of alkaline earth, transition and heavy metal cations by hydrous oxide gels of iron and aluminium. Soil Sci. Soc. Am. J., v. 40, p. 796-799.

Kuo, S. and Baker, A.S. 1980. Sorption of copper, zinc, and cadmium by some acid soils. Soil Sci. Soc. Am. J., v. 44, p. 969-974.

LeGeros, R.Z. 1981. Apatites in biological systems. Prog. Crystal Growth Charact., v. 4, p. 1-45.

LeGeros, R.Z. and LeGeros, J.P. 1984. Phosphate minerals in human tissues. *In:* Phosphate Minerals. Nriagu, J.O. and Moore, P.B. (eds.). Springer-Verlag, Berlin, p. 351-385.

Lehr, J. R. and G. H. McClellan. 1972. "A revised laboratory reactivity scale for evaluating phosphate rocks for direct application," Bull. Y-43, TVA, Muscle Shoals, Ala.

Lichte, F.E. et. al. 1987. "Determination of the rare-earth elements in geological materials by inductively coupled plasma mass spectrometry," *Analytical Chemistry*, 59:1150-1157.

Lindsay, W. L. 1979. *Chemical Equilibria in Soils.* John Wiley & Sons. New York.

Lucas, R. E. and B. D. Knezek. 1972. In *Micronutrients in Agriculture*, J. J. Mortvedt, P. M. Giordano, and W. L. Lindsay, eds. Soil Sci Soc Am Inc., Madison, WI., pp. 265-288.

Ma, Q.Y., Logan, T.J. and Traina, S.J.. 1995. Pb immobilization from aqueous solutions and contaminated soils using phosphate rocks. Environ. Sci. Technol., v. 29(4), p. 1118-1126.

Ma, Q.Y., Logan, T.J., Traina, S.J. and Ryan, J.A. 1994a. Effects of NO_3^-, Cl^-, F^-, SO_4^{-2}, and CO_3^{-2} on Pb^{2+} immobilization by hydroxyapatite. Environ. Sci. Technol., v. 28(3), p. 408-418.

Ma, Q.Y., Traina, S.J., Logan, T.J. and Ryan, J.A. 1994b. Effects of aqueous Al, Cd, Cu, Fe(II), Ni, and Zn on Pb immobilization by hydroxyapatite. Environ. Sci. Technol., v. 28(7), p. 1219-1228.

Ma, Q. Y., Traina, S. J., and T. J. Logan. 1993. "In situ lead immobilization by apatite," *Environ. Sci. Technol.* 27: 1803-1810.

Malone, G. A. and D. E. Lundquist. 1994. "A survey of technical aspects of site remediation: stabilization and solidification," *Waste Management* 14: 67-73.

McBride, M.B. and Blasiak, J.J. 1979. Zinc and copper solubility as a function of pH in an acidic soil. Soil Sci. Soc. Am. J., v. 43, p. 866-870.

McClellan, G.H. and Lehr, J.R. 1969. Crystal chemical investigation of natural apatites. Amer. Mineral., v. 54, p. 1379-1391.

McClellan, G.H. 1980. Mineralogy of carbonate fluorapatites. J. geol. Soc. London, v. 137, p. 675-681.

McConnell, D. 1973. Apatites: Its crystal chemistry, mineralogy, utilization, and geologic and biologic occurrences. Springer-Verlag, Berlin.

Middelburg, J.J. and Comans, R.N.J. 1991. Sorption of cadmium on hydroapatite. Chemical Geology, v. 90, p. 45-53.

Misra, D.N. and Bowen, R.L. 1981. Interaction of zinc ions with hydroxyapatite. In: Adsorption from Aqueous Solutions. Tewari, P.H. (ed.). Plenum, New York, p. 179-192.

Miyake, M., Ishigaki, K. and Suzuki, T. 1986. Structure refinements of Pb^{2+} ion-exchanged apatites by X-ray powder pattern-fitting. Journal of Solid State Chemistry, v. 61, p. 230-235.

Moody, T. E., J. V. Wright, E. Wyse, X. Chen, and J. Leather, 1994. "Sorption/desorption geochemistry of apatite and phosphate minerals in metal-contaminated soils," *American Geophysical Union Annual Meeting Abstracts* (in press).

Moody, T.E. and Wright, J. 1995. Adsorption isotherms: North Carolina apatite induced precipitation of lead, zinc, manganese and cadmium from the Bunker Hill 4000 soil. Technical Report BHI-00197, Bechtel Hanford, Inc., Richland, WA, 21p.

NBS (National Bureau of Standards), Wagman et al. (1968, 1969, 1971), and Parker et al. (1971)

Nimmo, J. R. and K. C. Akstin. 1988. "Hydraulic conductivity of a sandy soil at low water content after compaction by various methods," *Soil Sci. Soc. Amer. Journal* 52:303-310.

Nimmo, J. R., D. A. Stonestrom, and K. C. Akstin. 1994. "The feasibility of recharge rate determination using the steady-state centrifuge method," *Soil Sci. Soc. Amer. Journal* 58:49-56.

Nimmo, J. R., J. Rubin, and D. P. Hammermeister. 1987 "Unsaturated flow in a centrifugal field: measurement of hydraulic conductivity and testing of Darcy's Law," *Water Resources Research* 23:124-134.

Nimmo, J. R. and K. A. Mello. 1991. "Centrifugal techniques for measuring saturated hydraulic conductivity," *Water Resources Research* 27:1263-1269.

Nounah, A., Lacout, J.L. and Savariault, J.M. 1992. Localization of cadmium in cadmium-containing hydroxyl- and fluorapatites. Journal of Alloys and Compounds, v. 188, p. 141-146.

Nriagu, J. O. 1972. "Lead orthophosphates, I. Solubility and hydrolysis of secondary lead orthophosphate." *Inorg. Chem.* 11(10): 2499-2503.

Nriagu, J. O. 1973. "Lead orthophosphates, II. Stability of chloropyromorphite at 25°C," *Geochim. et Cosmochim. Acta* 37:367-377.

Nriagu, J.O. 1973b. Lead orthophosphates - III. Stability of fluoropyromorphite and bromopyromorphite at 25°C. Geochimica et Cosmochimica Acta, v. 37, p. 1735-1743.
Nriagu, J. O. 1973. "Solubility equilibrium constant of hopeite," *Geochim. et Cosmochim. Acta* 37:2357-2361.

Nriagu, J. O. 1974. "Lead orthophosphates, IV. Formation and stability in the environment," *Geochim. et Cosmochim. Acta* 38:887-898.

Nriagu, J.O. 1984. Formation and stability of base metal phosphates in soils and sediments. *In:* Phosphate Minerals. Nriagu, J.O. and Moore, P.B. (eds.). Springer-Verlag, Berlin, p. 318-329.

Page, A.L. et al., 1982. "Methods of Soil Analysis." Agronomy 9, Part 2, pp. 167-179.

Peters, R.W. and Shem, L. 1992. Adsorption/desorption characteristics of lead on various types of soil. Environmental Progress, v. 11(3), p. 234-240.

Phillips, S. J. 1995. Private communication.

PNL-7-40.48. Procedures and quality control for energy dispersive X-ray fluorescence spectroscopy using the BFP approach with the Kevex 0810A system (Rev. 1, 1990).

PNL-ALO-211.2. Determination of elements by inductively coupled argon plasma atomic emissions spectrometry (Rev. 0, 1993).

PNL-ALO-212.1. Determination of inorganic anions by ion chromatography (Rev. 1, 1994).

PNL-ALO-382.1. Solutions analysis: carbon (Rev.0, 1993).

PTI Environmental Services. 1994. "Bioavailability of Lead."
Rai, D., Felmy, A.R. and Moore, D.A. 1991b. Thermodynamic model for aqueous Cd^{2+}-CO_3^{2-} ionic interactions in high-ionic-strength carbonate solutions, and the solubility product of crystalline $CdCO_3$. Journal of Solution Chemistry, v. 20, p. 1169-1187.

Rai, D., Felmy, A.R. and Szelmeczka, R.W. 1991a. Hydrolysis constants and ion-interaction parameters for Cd(II) in zero to high concentrations of NaOH-KOH, and the solubility product of crystalline $Cd(OH)_2$. Journal of Solution Chemistry, v. 20, p. 375-390.

Rickard, D.T. and Nriagu, J.O. 1978. Aqueous environmental chemistry of lead. *In:* The Biogeochemistry of Lead in the Environment. Nriagu, J.O. (ed.). Elsevier/North-Holland Biomedical Press, p. 219-284.

Ruby, M. V., Davis, A. and A. Nicholson. 1994. "In situ formation of lead phosphates in soils as a method to immobilize lead," *Environ. Sci. Technol.* 28: 646-654.

Ruby, M. V., A. Davis, J. H. Kempton, J. W. Drexler, and P. D. Bergstrom, 1992. "Lead bioavailability: dissolution kinetics under simulated gastric conditions," *Environmental Science and Technology* 26: 461-468.

Russell, M. B., and L. A Richards. 1938. "The determination of soil moisture energy relations by centrifugation," *Soil Science Society of America Proceedings* 3:65-69.

Sanchez, C. and E. J. Kamprath. 1959. *Soil Science Society of America Proceedings* 23:302-304.

Santillan-Medrano, J. and Jurinak, J.J. 1975. The chemistry of lead and cadmium in soil: solid phase formation. Soil Sci. Soc. Am. Proc., v. 39, p. 851-856.

Silviera, D.J. and Sommers, L.E. 1977. "Extractability of copper, zinc, cadmium, and lead in soils incubated with sewage sludge," *Journal of Environmental Quality* 6: 47-52.

Sims, R.C. 1990. Soil remediation techniques at uncontrolled hazardous waste sites, a critical review. J. Air Waste Manage. Assoc., v. 40(5), p. 704-732.

Sposito, G. 1986. Distinguishing adsorption from surface precipitation. *In:* Geochemical Processes at Mineral Surfaces. p. 217-228.

Sposito, G. 1989. *The Chemistry of Soils.* Oxford University Press, New York.

Stanforth, R. and Chowdhury, A. 1994. In-situ stabilization of lead-contaminated soil. *In:* Proceedings of Federal Environmental Restoration III and Waste Minimization II Conference, New Orleans, LA, April 27, 1994.

Stanforth, R. and A. Chowdhury. 1994. "In-situ stabilization of lead-contaminated soil," presented at the Federal Environmental Restoration III and Waste Minimization II Conference, New Orleans, LA.

Starkey, H. C., P. D. Blackmon, and P. L. Hauff. 1984. "The routine mineralogical analysis of clay-bearing samples," *U.S. Geol. Survey Bull.*, p. 1563.

Stumm, W. and Morgan, J.J. 1981. Aquatic Chemistry. John Wiley & Sons, New York.

Suzuki, T., Hatsushika, T. and Hayakawa, Y. 1981. Synthetic hydoxyapatites employed as inorganic cation-exchangers. J. Chem. Soc., Faraday Trans. 1, v. 77, p. 1059-1062.

Suzuki, T., Hatsushika, T. and Miyake, M. 1982. Synthetic hydoxyapatites as inorganic cation exchangers, part 2. J. Chem. Soc., Faraday Trans. 1, v. 78, p. 3605-3611.

Suzuki, T., Ishigaki, K. and Miyake, M. 1984. Synthetic hydoxyapatites as inorganic cation exchangers, part 3.-Exchange characteristics of lead ions (Pb^{2+}). J. Chem. Soc., Faraday Trans. 1, v. 80, p. 3157-3165.

Suzuki, T., Ishigaki, K. and Ayuzawa, N. 1985. Removal of toxic Pb^{2+} ions by synthetic hydroxyapatites. Chem. Eng. Commun., v. 34, p. 143-151.

Takeuchi, Y. and Arai, H. 1990. Removal of coexisting Pb^{2+}, Cu^{2+} and Cd^{2+} ions from water by addition of hydroxyapatite powder. Journal of Chemical Engineering of Japan, v. 23(1), p. 75-80.

Takeuchi, Y., Suzuki, T., and Arai, H. 1988. A study of equilibrium and mass transfer in processes for removal of heavy-metal ions by hydroxyapatite. Journal of Chemical Engineering of Japan, v. 21(1), p. 98-100.

Tennessee Valley Authority. 1976. *New Developments in Fertilizer Technology: 11th Demonstration, Oct. 5-6, 1976.* TVA National Fertilizer Development Center, Muscle Shoals, AL, pp. 70-74.

U.S. Environmental Protection Agency. 1989. "IWT/GeoCon in situ solidification/stabilization: applications analysis report." EPA report number EPA-540-A5-89-004.

United States Environmental Protection Agency: 1976, National Interim Primary Drinking Water Regulations. *EPA570/9-76-003*, Office of Water Supply.

Vieillard, P. and Tardy, Y. 1984. Thermochemical properties of phosphates. *In:* Phosphate Minerals. Nriagu, J.O. and Moore, P.B. (eds.). Springer-Verlag, Berlin, p. 171-198.

Weast, R. C. 1983. *CRC Handbook of Chemistry and Physics*, 64th edition. CRC Press, Boca Raton.

Weir, A. H., E. C. Ormerod, and I. M. I. El Mansey. 1975. "Clay mineralogy of sediments of the western Nile delta," *Clay Minerals* 10:369-386.

Wright, J. 1990. "Conodont apatite: Structure and geochemistry," In: *Skeletal Biomineralization: Patterns, Processes and Evolutionary Trends*, J. Carter, ed. Van Nostrand Reinhold, New York, pp. 445-459.

Wright, J., Schrader, H. and Holser, W.T. 1987. Paleoredox variations in ancient oceans recorded by rare earth elements in fossil apatite. Geochimica et Cosmochimica Acta, v. 51, p. 631-644.

Wright, J. V. and L. M. Peurrung. 1994. "In situ immobilization of metals, lanthanides and actinides in apatite minerals." *American Geophysical Union Annual Meeting Abstracts* (in press).

Wright, J., J. L. Conca, and X. Chen. 1994. *Hydrostratigraphy and Recharge Distributions from Direct Measurements of Hydraulic Conductivity Using the UFA™ Method*, PNL Technical Report PNL-9424, Pacific Northwest Laboratory, Richland, WA, p. 150.

Wright, J. V., H. Schrader, and W. T. Holser. 1987. "Paleoredox variations in ancient oceans recorded by rare earth elements in fossil apatite," *Geoch. et Cosmochem. Acta* 51:631-644.

Xu, Y., Schwartz, F.W. and Traina, S.J. 1994. Sorption of Zn^{2+} and Cd^{2+} on hydroxyapatite surfaces. Environ. Sci. Technol., v. 28(8), p. 1472-1480.

Xu, Y. and Schwartz, F.W. 1994. Lead immobilization by hydroxyapatite in aqueous solutions. Journal of Contaminant Hydrology, v. 15, p. 187-206.

Yong, R.N. and Phadungchewit, Y. 1993. pH influence on selectivity and retention of heavy metals in some clay soils. Can. Geotech. J., v. 30, p. 821-833.

Zachara, J.M., Cowan, C.E. and Resch, C.T. 1993. Metal cation/anion adsorption on calcium carbonate: Implications to metal ion concentrations in groundwater. *In*: Metals in Groundwater. Allen, H.E., Perdue, E.M. and Brown, D.S. (eds.). Lewis Publishers, Chelsea, MI, p. 37-71.

Zachara, J.M., Cowan, C.E. and Resch, C.T. 1991. Adsorption of divalent metallic cations on calcite. Geochimica et Cosmochimica Acta, v. 55, p. 1549-1562.

APPENDIX

MILESTONE ONE REPORT: JUNE 1994

CHARACTERIZATION OF SOILS, APATITES, AND GROUNDWATER

A.1.0 INTRODUCTION

The objective of this project is to develop and demonstrate that phosphatic solutions and slurries will react with lead, other heavy metals including lanthanides and actinides, in contaminated soils and cause the precipitation of metal-substituted apatite minerals. Metals sequestered in apatites have great durability and leach resistance that significantly exceeds other chemically stabilized waste forms because the apatite mineral structure is very stable over a wide range of environmental conditions for geologically-long time periods. This is applied research that will lead to advanced technology development that can be implemented to remediate tetraethyl lead (TEL) sludge contaminated soils and groundwater at Keesler Air Force Base (AFB) as well as metal and radiologically contaminated soils at other DoD, DOE, or industrial sites where metal contamination of soils and groundwater is a pervasive problem.

Results of Phase One activities are included in this report. In Phase One the goal was to establish the chemical and mineralogical baseline for soils, waters, and phosphatic materials that would subsequently be used in leaching-retardation and sorption-desorption studies from contaminated sites. Chemical analyses of the cationic and anionic compositions and soil and metal mineral speciation were performed on contaminated soils from the following sites: 1) Keesler AFB,Mississippi, a tetraethyl lead (TEL) sludge pit; 2) Keesler AFB, a lead and zinc contaminated landfill; 3) three soils with varying levels of metal contamination from Bunker Hill Mine, Idaho; and 4) two Montana soils with varying levels of metal contamination that serve as National Institute of Standards and Technology (NIST) chemical standards. Chemical analyses were also made on water downgradient from the TEL sludge pit at Keesler AFB. Chemical and mineralogical analyses of several types of phosphatic materials including synthetic hydroxylapatite, natural carbonate fluorapatite from phosphorites, fish and shark teeth and fish cannery wastes are also reported. The data from the chemical and mineralogical speciation studies were used in the geochemical code MINTEQ to determine the stability relationships of soil minerals under varying conditions.

The methodologies used for each type of analytical procedure and the results of each group of analyses are detailed in the following sections of the report.

Scientific Contributors:
James L. Conca, Ph.D., Associate Scientist, WSU Tri-Cities
Xiaobing Chen, Ph.D., AWU-NW Postdoctoral Fellow
James M. Leather, Ph.D., AWU-NW Postdoctoral Fellow
T.E. Moody, Ph.D., Senior Research Scientist, WHC

A.2.0 METHODOLOGY

A.2.1 ELEMENTAL ANALYSIS

Elemental contents were determined by a series of methods depending on the sample type and particular element of interest. X-ray fluorescence (XRF) analyses on powder mounts following standard PNL procedure PNL-7-40.48 (Rev. 1) were used for total elemental analysis. For separate cation analyses, major and trace metals were determined by Inductively Coupled Argon Emission Spectrometer (ICP) on a Jarrell-Ash Model 975 following standard PNL procedure PNL-ALO-211.2 (Rev. 0). Major anion contents were determined by ion chromatography (IC) on a Dionex Series 4000i following standard PNL procedure PNL-ALO-212.1 (Rev. 1). For both ICP and IC, elements were put into solution using a nitric acid leach. Total and organic carbon contents were determined by Xertex-Dohrmann Model DC-80 Carbon Analyzer, with inorganic carbon content calculated from the difference (PNL-ALO-382.1 (Rev.0)). The analytical errors associated with the various techniques are estimated to be ±10% of the reported values.

Input data for the execution of the computer program was acquired from a complete metal and ligand analysis of saturation extracts (Page, et. al, 1982). The computer program used was MacMINTEQ-A2, acquired from Geochem Software, 1994. Metal concentrations on the extract was accomplished by ICP analysis, and anions by IC analysis (PNL-AL0-211.2 Rev. 0, and PNL-ALO-212 Rev. 1).

A.2.2 MINERALOGY

Mineralogical information was obtained by utilizing X-ray diffraction and electron microprobe techniques. X-ray diffraction (XRD) analyses were employed to characterize the mineralogy of bulk soil samples and were done for clay-sized (smaller than 2 μm), and silt- and sand-sized (larger than 2 μm) fractions. The different grain-sized fractions of each sample were separated by following the procedures proposed by Ingram (1971) and Galehouse (1971). Oriented samples of the smaller than 2 μm fraction were prepared for XRD analysis by pipetting clay suspension into a beaker containing a glass slide. When the beaker was placed in an oven at 40°C, the water evaporated and the clays settled onto the slide. XRD analyses were performed using a Siemen 500 diffractometer operated at 35 kV and 30 mA using CuKa radiation. Data were collected in a step scanning mode using a 0.02° step and a count time of 0.5 seconds per step. The scanning range of 2° angle is from 2° to 34° for oriented clay samples and from 10° to 50° for randomly oriented powders of the coarser than 2 μm fraction of the samples. Each oriented clay sample was made into an air-dried, ethylene glycolated mount, heat treated to 375°C and 550°C, and analyzed (Starkey et al. 1984). The compositions of the larger than 2 μm fractions were estimated by combining XRD data with information gathered through visual inspection using optical

microscopy. Semi-quantitative estimations of clay minerals were determined by a method modified from Weir et al. (1975), in which clay mineral XRD intensities (I) are normalized to variations in crystallinity as follows:

$I_{kaolinite}/2.5 + I_{illite} + I_{smectite} + I_{chlorite}/2.0 = <2\ \mu m$ fraction

If any non-clay minerals were detected in the smaller than 2 μm fraction XRD scans, estimates of their relative weight percent were subtracted from the weight percent smaller than 2 μm fraction prior to the clay mineral normalization. The estimated accuracy for these techniques is ±10% to 50% depending on the particular mineral.

For the examination of the Keesler and Bunker Hill samples with electron microprobe, a small portion of each sample was mounted on a piece of conducting double sided tape with an area of about 1 cm^2. The samples were then carbon coated to provide the necessary conducting surface. Preliminary investigation of the samples was done with a Cameca Camebax Microprobe equipped with an energy dispersive spectrometer (EDS) and three wavelength dispersive spectrometers (WDS). The X-ray spectrometers were used to analyze the elements present in the samples, in which the WDS have a better sensitivity for the detection of trace elements, and a better resolution for separation of interfering elements, for example sulfur and lead. The machine was operated at a beam accelerating voltage of 20 kv, and a beam current of 12 nA. To find Pb-bearing particles, a WDS spectrometer was positioned on the Pb peak position with the audio signal turned on. Then, the electron beam in point mode was traversed across the sample until Pb was detected. Generally, the WDS was used to determine the presence of P, S, and Cl, the EDS was used to acquire an EDS spectrum, and Back-scattered electron mode (BSE) was used to examine the morphology of the particles.

A.3.0 RESULTS

This Milestone Report provides characterization data on samples to be utilized in this project. In addition to Kessler AFB samples, a number of mining soils are also included. Due to the relatively low Pb concentrations in the Keesler soils, the highly Pb contaminated mining soils are included in the project to demonstrate the utility of apatite based remediation over a large range of soil Pb contaminations.

A.3.1 PRELIMINARY SOILS DATA

A.3.1.1 ELEMENTAL ANALYSIS

Table A1 contains the data on elemental concentrations for the Keesler AFB

samples. Concentrations for cation data are determined by ICP/ES, anion data by IC, and carbon data by carbon analyzer. The three listed samples show a range in Pb concentration from less than 10 to slightly greater than 100 mg kg^{-1}. Table A2 contains elemental data from XRF analysis of three Bunker Hill mining soils (with Pb from 1000 to 4000 mg kg^{-1}) and one Keesler soil (a duplicate from Table A1a). XRF analysis was chosen to characterize the elemental contents in the mining soils because of concerns that acid leaching might not provide total Pb elemental contents due to the variable Pb mineralogy in mining soils. The comparable data for Keesler HA7-8 given in Tables A1a and A2 show this is not a problem for the much lower Pb contents and consistent mineralogy present in the Keesler soils.

Tables A3 and A4 show the elemental contents for NIST standard reference material (SRM) mining soils SRM 2710 and SRM 2711. These samples are included in the project to provide an extremely well characterized set of mining soils with high Pb contents (from 1000 to 5000 mg kg^{-1}). The multiple analytical methods used to obtain this chemical characterization data are given in Table A5. Tables A3, A4, and A5 are taken directly from the NIST Certificate of Analysis for these soils.

A.3.2 MINERALOGY

A.3.2.1 KEESLER SOILS

Tables A6 and A7 contain information on the mineralogy of the Keesler bulk soil samples. Quartz dominates the mineralogical composition of the soils. Very small amounts of rock fragments and clay minerals occur in the samples. In addition, calcite from shell fragments is also present in the sample of HA7-8. The clay minerals present in the Keesler soils are vermiculite, illite, and kaolinite. Minor hematite also occurs.

Figures A1 to A4 show X-ray spectra obtained from 2 Keesler soil samples (HA7-8 and HA7-15). Another 2 Keesler soil samples were also examined with electron microprobe. However, no Pb-bearing particle was detected because of low total Pb concentration in the samples. Most of the particles examined were small, commonly surrounded by other particles. Therefore, it is believed that most of the spectra are probably not only of the Pb-bearing materials, but of the underlying and adjacent materials as well, which is suggested by most of the spectra exhibiting very large Si $K\alpha$ peaks.

The spectra shown in Figures A1 and A2 were taken from the Keesler sample HA7-8. The spectrum #1 was from an area of Pb detectability of about 10 microns across, occurring on a quartz or feldspar grain, which is very high in Mn. Other metals include Zn, Fe, Ca, and Al. No P or Cl were detected. Note that the background is low in the low energy portion (left side) of the spectrum, and the Pb $M\alpha$ peak is missing. It is believed that this is because the secondary X-ray was partially blocked by another

particle. Pb, Ti, Fe, Ca, and Al are present in the spectrum #2, in which minor S, P, and Cl were detected. In the spectrum #3 and #4, Pb is the only heavy metal occurring. Both P and Cl are present in small amounts in the spectrum #3. The Cl peak position is on the side of the Pb Mα peak, and in EDS is not visible in small amounts. In this case the Cl peak was only detected by WDS. The high lead concentration in the spectrum #4 is also shown in Figure A11A as small bright areas, in which the lead is attached to the surface of a quartz grain that is much larger than the field of view. Minor P and S were detected in the spectrum #4. Heavy metals Pb, Zn, Mn, Fe, and Ti are high in concentration in the spectrum #5. They are associated with high concentration of P. As for the spectrum #5, the spectrum #6 contains major Zn, in addition to Pb. Ti and Fe are also present. Minor P and Cl were detected.

Figures A3 and A4 show the spectra obtained from the Keesler soil HA7-15. Although ICP/MS whole sample analysis was only 166 mg kg^{-1} (ppm) of Pb, several areas of high Pb concentration were found. Only minor Pb was observed in the spectrum #1 and #2, in which the difference is that the spectrum #2 contains significant P in proportion to Pb. High concentration of Pb is shown in the spectrum #3 and #4. There is high Cl in the spectrum #3, which also contains minor Zn, Fe, Cu, and Ti. However, no associated P or Cl occurs in the spectrum #4.

A.3.2.2 BUNKER HILL SOILS

Sulfur was common in the Bunker Hill soils. In the EDS spectrum, the S Kα and Pb Mα peaks overlap, but they are resolved nicely using WDS. Thus the presence or absence of S was determined using WDS.

The spectra obtained from Bunker Hill 1000 are shown in Figures A5 and A6. Pb is associated with Fe, without other heavy metals present. The spectrum #1 was from a 15 micron irregularly shaped particle with a hollow middle. It contains major S, perhaps more than required to form PbS. A small amount of P was also detected. No Cl was observed. However, low S present in the spectrum #2 and #3 as well as several other particles. The spectrum #4 was taken from a 2 micron lenticular grain with no P, S, or Cl, in which Pb is the only major element detected; Al, Si, and Fe were minor compared to Pb in this spectrum.

Figures A7 and A8 shows the spectra of Bunker Hill 2000, in which Pb is always associated with Fe, with minor other heavy metals such as Zn, Mn, and Ti in some grains. In the spectrum #1, major S was present, but sulfur concentrations about half as great were detected in the immediate vicinity without associated Pb. No Cl or P were detected. A 50-60 micron grain of the spectrum #2, mostly Fe, with major S

(more than required for PbS), some P, and no Cl, are shown in Figure A11B. The Fe in this grain may be in the form of FeS_x. The spectrum #3 is from a 20 micron area on an alumina silicate, with some P, no S or Cl. The spectrum #4 was obtained from a 15 micron grain, probably PbS.

Figures A9 and A10 contain the spectra of the Bunker Hill 4000 (BH4). Heavy metal association is similar to Bunker Hill 2000. The spectrum #1 is from a 15 micron grain, with very high S, which is more than required for PbS, thus it is suspected FeS_x also present. Pb dominate the spectrum #2, with minor S, Al, Fe, and S. The spectrum #3 is obtained from a 10 micron grain, with S present in about the right proportion for PbS, without P or Cl present. No S, P, or Cl occur in the spectrum #4, which is a 25 micron grain. It is probably PbO_x.

A.3.2.3 NIST STANDARD REFERENCE MATERIAL

Table A8 is a list of the Pb-bearing minerals occurring in the NIST standard reference material (SRM) mining soils SRM2710 and SRM2711. Additional data is being obtained to allow quantification of the data and determination of the relative amounts of the various minerals.

A.3.3 PRELIMINARY APATITE DATA

Tables A9, A10, and A11 contain characterization data on the apatite samples that have been selected for use in the project. The hydroxyapatite (Tribasic Calcium Phosphate, TCP) is a reagent grade laboratory-precipitated powder with few impurities (Table A9). SRM 120b Florida Phosphate Rock is a naturally occurring apatite that serves as a NIST chemical standard (Table A10). It has therefore been ground into a fine powder and well mixed to provide homogeneous sample aliquots. The North Carolina Apatite is an unprocessed (not acidified or ground) natural sample commercially available from Texasgulf Inc. as a fertilizer supplement for soils (Table A11). The Florida and North Carolina apatite samples are both carbonate fluorapatites obtained from naturally occurring marine deposits and therefore contain additional impurities that will affect the amount of phosphate available for dissolution. Table A12 contains ICP/ES data on these three samples along with some biogenic apatites for comparison. The biogenic apatites are included in this study since it is expected that fishery wastes would be readily available as less costly apatite sources, but they also contain many impurities and the amount of available phosphate is correspondingly lower.

A.3.4 PRELIMINARY WATERS DATA

Table A11 contains information on the waters used in this study. Concentrations for cation data are determined by ICP/ES, anion data by IC, and carbon data by carbon analyzer. Data from a laboratory synthetic groundwater to be used in leach studies is shown to be comparable to the naturally occurring groundwater at Keesler AFB. Additional studies will also utilize distilled and nanopure filtered water that is below detection limits for Pb and other heavy metals.

A.3.5 PRELIMINARY MODELING DATA

A.3.5.1 GEOCHEMICAL THERMODYNAMIC SPECIATION

In order to gain knowledge about the nature of lead complexation and to determine how much PO_4 is needed to complex the groundwater available lead in the Keesler soils, a geochemical thermodynamic speciation computer program was implemented.

The natural soil system has a solid phase and a solution phase. When chemical equilibrium is assumed to exist between the soil solution and the associated solid phases of the soil, one can elicit important information about solid phase formations by using thermodynamic calculations performed in geochemical thermodynamic speciation programs. Specifically, this computer program is used to examine the precipitation of a selected metal, i.e., lead, induced by the application of a specific phosphate compound.

Saturation Indices (determined from MINTEQ-A2) for the following Keesler soils exemplify the lead containing minerals that may be present. The saturation index is defined as

Ion Activity Product/Solubility Product

and is a thermodynamic indication of mineral dissolution or formation. Values < 0 indicate that the mineral is undersaturated with respect t the equilibrium concentration, and values > 0 indicate saturation with respect to the equilibrium concentration. The higher the number, the greater the probability of precipitation.

Keesler soil HA 7-8 :

Mineral	Saturation Index	
PbCrO4	0.197	
Cerrusite	0.537	
Hydroxypyromorphite		0.742
$Pb_3 (PO_4)_2$		0.982
Hercynite	2.347	
Plumbgummite	8.458	
Chloropyromorphyte		11.612

Keesler soil HA 7-12:

Mineral	Saturation Index	
Plumbgummite	8.458	
Chloropyromorphyte		11.612

Keesler soil HA 7-15:

Mineral	Saturation Index
Plumbgummite	5.637

Table A1a. Elemental Contents for Keesler AFB Soil Samples

Sample ID # >>>		Detection	94-04579	94-03086	94-03087
Sample ID >>>>		Limit	HA-7-8	HA-7-12	HA-7-15
Type or Form of Sample >>>>>			dry	dry	dry
Aluminum	Al	0.005	2680	4990	5560
Boron	B	0.02	31.8	99.4	104
Barium	Ba	0.0005	57.9	32	33
Calcium	Ca	0.01	3110	48	252
Cadmium	Cd	0.001	1.8	3.3	1.4
Cobalt	Co	0.001	< 1	4.9	3.3
Chromium	Cr	0.002		16.9	10.6
Copper	Cu	0.0005	31	1.8	4.8
Iron	Fe	0.005	3270	3990	1370
Potassium	K	0.2	< 210	250	170
Lithium	Li	0.003	< 3	2.5	1.9
Magnesium	Mg	0.005	273	239	194
Manganese	Mn	0.0005	463	51	27
Sodium	Na	0.05	55.6	112	112
Nickel	Ni	0.003	< 3	2.8	3.1
Phosphorus	P	0.03	287	34	71
Lead	Pb	0.005	119	3.4	3
Selenium	Se	0.01	< 10	14	31
Silicon	Si	0.01	191	860	700
Tin	Sn	0.015	< 10	26	14
Strontium	Sr	0.0005	9.7	2.4	43
Titanium	Ti	0.001	60.7	1980	1300
Zinc	Zn	0.003	16.4	17	12
Zirconium	Zr	0.001	< 1	5.9	8
Dilution Factor			106	155	100

*note: All amounts are in ppm

Table A1b. Elemental Contents for Keesler AFB soil samples (anions)

Sample ID # >>>		94-04579	94-03086	94-03087
Sample ID >>>>		HA-7-8	HA-7-12	HA-7-15
Sample Form >>>		dry	dry	dry
Flourine	F			
Chlorine	Cl	<4	16.3	43.7
Nitrate	NO3	59	29.3	91.7
Sulfate	SO4	15	204	588
Organic	C	0.49	109	953
Inorganic	C	0.4	21	53
Total	C	0.89	130	1006

Table A2. XRF Data for Bunker Hill (BH) and Keesler AFB Samples

Sample>>>	BH 1000		BH 2000		BH 4000		HA7-8	
		%		%		%		%
	ppm solid	oxide	ppm solid	oxide	ppm solid	oxide	ppm solid	oxide
Na AA	7000	0.94	9900	1.33	10300	1.39	1300	0.18
Mg AA	6634	1.1	6031	1	5307	0.88	603	0.1
Al AA	72600	13.72	70000	13.23	79000	14.93	2360	0.45
Si AA	313000	66.96	296000	63.32	293000	62.68	417000	89.21
Al xrf	76100	14.38	84400	15.95	93200	17.61	2900	0.55
Si xrf	301000	64.39	287000	61.4	304000	65.03	426000	91.13
P xrf	2330	0.53	3020	0.69	2670	0.61	1070	0.25
S xrf	0	0	430	0.11	0	0	300	0.08
Cl xrf	430	0.04	919	0.09	1860	0.19	0	0
K xrf	22900	2.76	23200	2.79	26800	3.23	568	0.07
Ca xrf	4490	0.63	7110	0.99	4930	0.69	6410	0.9
Ti xrf	4340	0.72	4320	0.72	4440	0.74	1011	0.17
V xrf	91	0.01	76	0.01	115	0.02	10	0
Cr xrf	33	0	36	0.01	38	0.01	30	0
Mn xrf	777	0.1	1167	0.15	1031	0.13	66	0.01
Fe xrf	31700	4.53	35900	5.13	38800	5.55	4180	0.6
Ni xrf	22	0	23	0	25	0	6	0
Cu xrf	40	0.01	69	0.01	119	0.01	27	0
Zn xrf	257	0.03	1171	0.15	1087	0.14	186	0.02
Ga xrf	11	0	6	0	0	0	2	0
Se xrf	0	0	0	0	0	0	0	0
Pb xrf	1157	0.13	2000	0.23	4170	0.48	142	0.02
Rb xrf	115	0.01	121	0.02	137	0.02	3	0
Sr xrf	79	0.01	146	0.02	120	0.01	16	0
Y xrf	27	0	32	0	31	0	3	0
Zr xrf	335	0.05	320	0.04	314	0.04	179	0.02
Nb xrf	13	0	14	0	15	0	4	0
Mo xrf	0	0	0	0	2	0	0	0
Ru xrf	0	0	0	0	0	0	0	0
Rh xrf	0	0	0	0	0	0	0	0
Pd xrf	0	0	0	0	0	0	0	0
Ag xrf	0	0	0	0	0	0	0	0
Cd xrf	12	0	0	0	17	0	0	0
Sn xrf	0	0	15	0	0	0	0	0
Sb xrf	27	0	24	0	72	0.01	0	0
Te xrf	0	0	20	0	0	0	0	0
Cs xrf	0	0	0	0	0	0	0	0
Ba xrf	664	0.07	823	0.09	808	0.09	94	0.01
La xrf	89	0.01	70	0.01	66	0.01	0	0
Ce xrf	62	0.01	62	0.01	95	0.01	0	0
LOI Wt %		7.49		7.92		7.25		3.97
Wt.% total		99.9		98.09		99.12		96.05
xrf		97.99		98.89		104.16		98.08

Table A3. Elemental Contents for NIST SRM 2710

Certified Values

Element	wt. %	Element	µg/g
Aluminum	6.44 ± 0.08	Antimony	38.4 ± 3.0
Calcium	1.25 ± 0.03	Arsenic	626 ± 38
Iron	3.38 ± 0.10	Barium	707 ± 51
Magnesium	0.853 ± 0.042	Cadmium	21.8 ± 0.2
Manganese	1.01 ± 0.04	Copper	2950 ± 130
Phosphorus	0.106 ± 0.015	Lead	5532 ± 80
Potassium	2.11 ± 0.11	Mercury	32.6 ± 1.8
Silicon	28.97 ± 0.18	Nickel	14.3 ± 1.0
Sodium	1.14 ± 0.06	Silver	35.3 ± 1.5
Sulfur	0.240 ± 0.006	Vanadium	76.6 ± 2.3
Titanium	0.283 ± 0.010	Zinc	6952 ± 91

Noncertified Values: Noncertified values, shown in parentheses, are provided for information only. An element concentration value may not be certified if a bias is suspected in one or more of the methods used for certification, or if two independent methods are not available. Certified values for some of these elements will eventually be provided in a revised certificate when more data is available.

Noncertified Values

Element	wt.%	Element	µg/g
Carbon	(3)	Bromine	(6)
		Cerium	(57)
		Cesium	(107)
		Chromium	(39)
		Cobalt	(10)
		Dysprosium	(5.4)
		Europium	(1)
		Gallium	(34)
		Gold	(0.6)
		Hafnium	(3.2)
		Holmium	(0.6)
		Indium	(5.1)
		Lanthanum	(34)
		Molybdenum	(19)
		Neodymium	(23)
		Rubidium	(120)
		Samarium	(7.8)
		Scandium	(8.7)
		Strontium	(240)
		Thallium	(1.3)
		Thorium	(13)
		Tungsten	(93)
		Uranium	(25)
		Ytterbium	(1.3)
		Yttrium	(23)

Table A4. Elemental Contents for NIST SRM 2711

Certified Values

Element	wt. %		Element	µg/g	
Aluminum	6.53	± 0.09	Antimony	19.4	± 1.8
Calcium	2.88	± 0.08	Arsenic	105	± 8
Iron	2.89	± 0.06	Barium	726	± 38
Magnesium	1.05	± 0.03	Cadmium	41.70	± 0.25
Phosphorus	0.086	± 0.007	Copper	114	± 2
Potassium	2.45	± 0.08	Lead	1162	± 31
Silicon	30.44	± 0.19	Manganese	638	± 28
Sodium	1.14	± 0.03	Mercury	6.25	± 0.19
Sulfur	0.042	± 0.001	Nickel	20.6	± 1.1
Titanium	0.306	± 0.023	Selenium	1.52	± 0.14
			Silver	4.63	± 0.39
			Strontium	245.3	± 0.7
			Thallium	2.47	± 0.15
			Vanadium	81.6	± 2.9
			Zinc	350.4	± 4.8

Noncertified Values: Noncertified values, shown in parentheses, are provided for information only. An element concentration value may not be certified, if a bias is suspected in one or more of the methods used for certification, or if two independent methods are not available. Certified values for some of these elements will eventually be provided in a revised certificate when more data is available.

Noncertified Values

Element	wt. %	Element	µg/g
Carbon	(2)	Bromine	(5)
		Cerium	(69)
		Cesium	(6.1)
		Chromium	(47)
		Cobalt	(10)
		Dysprosium	(5.6)
		Europium	(1.1)
		Gallium	(15)
		Gold	(.03)
		Hafnium	(7.3)
		Holmium	(1)
		Indium	(1.1)
		Iodine	(3)
		Lanthanum	(40)
		Molybdenum	(1.6)
		Neodymium	(31)
		Rubidium	(110)
		Samarium	(5.9)
		Scandium	(9)
		Thorium	(14)
		Tungsten	(3)
		Uranium	(2.6)
		Ytterbium	(2.7)
		Yttrium	(25)
		Zirconium	(230)

Table A5. Analytical Methods for Tables A3 and A4

Element	Certification Methods *	Element	Certification Methods *
Ag	ID ICPMS; RNAA; INAA	Mo	ID ICPMS
Al	XRF1; XRF2; DCP; ICP	Na	INAA; FAES
As	RNAA; HYD AAS; ICP; INAA	Nd	ICP
Au	INAA; FAAS	Ni	ID ICPMS; ETAAS; INAA
Ba	XRF2; FAES	P	DCP; COLOR; XRF1; XRF2
Br	INAA	Pb	ID TIMS; POLAR; ICP
C	COUL	Rb	INAA
Ca	XRF1; XRF2; DCP	S	ID TIMS
Cd	ID ICPMS; RNAA	Sb	RNAA; ETAAS
Ce	INAA; ICP	Sc	INAA; ICP
Co	INAA; ETAAS; ICP	Si	XRF1; XRF2; GRAV
Cr	INAA; DCP; ICP	Sm	INAA
Cs	INAA	Sr	ID TIMS; INAA; ICP
Cu	RNAA; FAES; ICP	Th	ID TIMS; INAA; ICP
Dy	INAA	Ti	XRF1; XRF2; DCP
Eu	INAA	Tl	ID TIMS; LEAFS
Fe	XRF1; XRF2; DCP; INAA; ICP	U	ID TIMS; INAA
Ga	INAA; ICP	V	INAA; ICP
Hf	INAA	W	INAA
Hg	CVAAS	Y	ICP
Ho	INAA	Yb	INAA
In	INAA	Zn	ID TIMS; ICP; INAA; POLAR
K	XRF1; XRF2; FAES; ICP		
La	INAA; ICP		
Mg	XRF1; ICP		
Mn	INAA; DCP; XRF2		

*Methods in bold were used to corroborate certification methods or to provide information values.

COLOR - Colorimetry; lithium metaborate fusion.
COUL - Combustion coulometry.
CVAAS - Cold vapor atomic absorption spectrometry.
DCP - Direct current plasma atomic emission spectrometry; lithium metaborate fusion.
ETAAS - Electrothermal atomic absorption spectrometry; mixed acid digestion.
FAAS - Flame atomic absorption spectrometry; mixed acid digestion except for Au, leached with $HBr\text{-}Br_2$.
FAES - Flame atomic emission spectrometry; mixed acid digestion.
GRAV - Gravimetry; sodium carbonate fusion.
HYD AAS - Hydride generation atomic absorption spectrometry.
ICP - Inductively coupled plasma atomic emission spectrometry; mixed acid digestion.
ID ICPMS - Isotope dilution inductively coupled plasma mass spectrometry; mixed acid digestion.
ID TIMS - Isotope dilution thermal ionization mass spectrometry; mixed acid digestion.
INAA - Instrumental neutron activation analysis.
LEAFS - Laser enhanced atomic fluorescence spectrometry; mixed acid digestion.
POLAR - Polarography.
RNAA - Radiochemical neutron activation analysis; mixed acid digestion.
XRF1 - Wavelength dispersive x-ray fluorescence on fused borate discs.
XRF2 - Wavelength dispersive x-ray fluorescence spectrometry on pressed powder.

Table A6. Mineralogical Composition of Keesler bulk soil samples

Sample ID >>>>	HA7-8	HA7-11	HA7-12	HA7-13	HA7-14	HA7-15
Quartz	96.57	98.6	99	97.7	97.38	97.18
Rock fragments	0.38	0.57	0.22	0.7	1.9	0.68
Calcite	1.81	0	0	0	0	0
Clay	1.01	0.97	0.72	1.96	1.46	2.29
Total	99.77	100.14	99.94	100.36	100.74	100.15

Table A7. Clay-size minerals occurring in Keesler soil samples.

Mineral >>>>>>	Vermiculite	Illite	Kaolinite	Quartz	Hematite
HA7-8 Percentage in < 2 um fraction	13	9	6	65	7
percentage in whole sample	0.14	0.09	0.06	0.65	0.07
HA7-11 percentage in < 2 um fraction	69	1	6	23	0.5
percentage in whole sample	0.67	0.01	0.06	0.23	0.01
HA7-12 percentage in < 2 um fraction	71	2	7	21	NA
percentage in whole sample	0.51	0.01	0.05	0.15	NA
HA7-13 percentage in < 2 um fraction	3	8	3	82	5
percentage in whole sample	0.06	0.15	0.05	1.6	0.09
HA7-14 percentage in < 2 um fraction	14	8	7	65	7
percentage in whole sample	0.2	0.11	0.1	0.95	0.1
HA7-15 percentage in < 2 um fraction	21	4	3	69	3
percentage in whole sample	0.48	0.09	0.07	1.57	0.07

Table A8. List of the lead-bearing minerals occurring in the samples of NIST standard reference material (SRM) mining soil SRM2710 and SRM2711.

Anglesite
Mn-Pb oxide
$PbSiO_4$
Fe-Pb oxide
Fe-Pb sulfate
Pb phosphate
Pb organic material
Galena

Table A9. Reported Analysis for Reagent Grade Synthetic Apatite

CALCIUM PHOSPHATE TRIBASIC **CERTIFIED**
Precipitated powder

Hydroxylapatite
Approx. $Ca_{10}(OH)_2(PO_4)_6$

Product Specifications
Actual Lot Analysis is reported on label.

Insolube in dilute HCl	≤0.010%
Dibasic or Free CaO	To pass test
Chloride	≤0.010%
Sulfate	≤0.02%
Ammonia	≤0.02%
Arsenic	≤1ppm
Barium	≤0.01%
Heavy Metals (as Pb)	≤0.002%
Iron	≤0.005%
Magnesium	≤0.20%
Soluble Salts	≤1.5%

Table A10. Reported Analysis for Florida Phosphate Rock

U. S. Department of Commerce
Peter G. Peterson

National Bureau of Standards
Certificate of Analysis
Standard Reference Material 120b
Phosphate Rock
(Florida)

This standard is a finely powdered material intended for use in checking chemical methods of analysis and in calibration with optical emission and x-ray spectrometric methods of analysis.

Percent by Weight

ANALYST[a]	P_2O_5	CaO	SiO_2	F	Soluble Fe_2O_3	Soluble Al_2O_3	MgO	Na_2O	MnO	K_2O		TiO_2	CO_2	CdO
1	34.51[a]	49.42[b]	4.70[c]	3.82[d]	1.10[e]	1.09[f,g]	0.29[h]	0.33[f]	0.032[i]	0.12[f,j]	--	0.15[k]	--	0.002[l]
2	34.51[m]	49.35[m]	4.73[n]	3.79[m]	1.10[h]	1.07[h]	.28[h]	.36[h]	.031[h]	.12[j]	0.09[o]	--	2.76[p]	.002[h]
3	34.66[n]	49.38[m]	4.67[q]	3.83	1.09[h]	1.07[h]	.30	.36[h]	.032[h]	.12[j]	.090[o]	.15	2.79	.002[h]
4	34.67[r]	49.47[m]	4.69[q]	3.81[s]	1.13[h]	1.04[h]	.28[h]	.35[h]	.032[h]	--	.087[o]	.15[k]	2.78[p]	.003[h]
5	34.57	49.32[m]	4.63[q]	3.86	1.06[h]	1.05[h]	.25[h]	.34[h]	--	--	.005[o]	--	2.83	--
6	34.48[m]	49.45[m]	--	3.92[s]	1.14[m]	1.07[t]	--	--	--	--	--	--	--	--
Average	34.57	49.40	4.68	3.84	1.10	1.06	0.28	0.35	0.032	0.12	0.090	0.15	2.79	0.002

[a] Phosphorus precipitated with magnesia mixture, ignited and weighed as $Mg_2P_2O_7$.

[b] Calcium precipitated as oxalate, ignited and weighed as CaO.

[c] Sample fused with Na_2CO_3, silica precipitated with ZnO and dehydrated with HCl. Traces of SiO_2 recovered by H_2SO_4 dehydration.

[d] Fluorine distilled into NaOH solution and precipitated as lead chlorofluoride. Chloride is precipitated with excess $AgNO_3$ and excess $AgNO_3$ is titrated with standard KCNS solution.

[e] $SnCl_2$ reduction – $K_2Cr_2O_7$ titration.

[f] Flame emission spectrometry with repetitive optical scanning.

[g] A value of 1.13 percent was obtained for total Al_2O_3 by gravimetry.

[h] Atomic absorption spectrometry.

[i] KIO_4 spectrophotometric method.

[j] Sample digested with mixed acids for 1 hour. Determination completed by atomic absorption spectrometry.

[k] H_2O_2 spectrophotometric method.

[l] Polarographic method.

[m] Volumetric method.

[n] Gravimetric method.

[o] Sample digested with dilute HCl or aqua regia for 15 minutes. Determination completed by atomic absorption spectrometry.

[p] CO_2 absorbed and weighed.

[q] Dehydration with $HClO_4$ in presence of boric acid.

[r] Molybdovanadophosphate spectrophotometric method.

[s] Distillation – titration with standard thorium nitrate solution.

[t] Aluminum precipitated with 8 hydroxyquinoline and weighed.

Washington, D.C. 20234
July 31, 1972

J. Paul Cali, Chief
Office of Standard Reference Materials

Table A11. Reported Analysis for North Carolina Natural Phosphate

Texasgulf

North Carolina Natural Phosphate (NCNP)

30% P_2O_5 - For Use As A Fertilizer In Acid Soil

NCNP is a natural source of Phosphorus and Calcium derived from marine sediments. NCNP has not been subjected to acidulation or grinding.

Typical Analysis - (dry basis)

Component	Typical Percent
Total Phosphorus, as P	13.2
Total Phosphorus, as P_2O_5	30.3
Calcium, as CaO	48.8
Magnesium, as MgO	0.6
Total Sulphur, as S	1.3
Total Carbon, as C	3.1
Zinc, as Zn	313 ppm
Boron, as B	95 ppm
Molybdenum, as Mo	45 ppm
Copper, as Cu	13 ppm

Soluble Phosphorus	% of total P
–in Water	0
–in Neutral Ammonium Citrate	13
–in 2% Citric Acid	37
–in 2% Formic Acid	72
–in HNO_3/HCl	100

Physical Characteristics

Screen Analysis (Tyler)	Sieve Opening	%
Passing 14 mesh	1.190 mm	100
Passing 35 mesh	0.420 mm	97
Passing 65 mesh	0.210 mm	49
Passing 100 mesh	0.149 mm	19
Passing 200 mesh	0.074 mm	1
Surface Area (B.E.T.)	22 m^2/mg	

Bulk Density	
Loose	1.44 g/cm^3 (90 lbs/ft^3)
Tamped	1.60 g/cm^3 (100 lbs/ft^3)

Color	Brownish Black

Table A13a. ICP Data for Synthetic and Keesler Groundwaters

Sample ID # >>>		Detection	94-03084	94-03085
Sample ID >>>>		Limit	HVS Water	Keesler H2O
Type or Form of Sample >>>>>			aqueous	aqueous
Aluminum	Al	0.005	< 0.09	0.02
Boron	B	0.02	< 0.3	
Barium	Ba	0.0005		0.01
Calcium	Ca	0.01	16	16.2
Cadmium	Cd	0.001		
Cobalt	Co	0.001		
Chromium	Cr	0.002		
Copper	Cu	0.0005		
Iron	Fe	0.005		
Potassium	K	0.2	12	1.5
Lithium	Li	0.003		
Magnesium	Mg	0.005	6.75	1.3
Manganese	Mn	0.0005		
Sodium	Na	0.05	20.6	11.1
Nickel	Ni	0.003		
Phosphorus	P	0.03	4.2	
Lead	Pb	0.005	< 0.08	< 0.007
Selenium	Se	0.01		
Silicon	Si	0.01	0.99	3.2
Tin	Sn	0.015		
Strontium	Sr	0.0005	0.086	0.057
Titanium	Ti	0.001		
Zinc	Zn	0.003		0.008
Zirconium	Zr	0.001		
Dilution Factor			1.7	1.02x

*note: All amounts are in ppm

Table A13b. ICP Data for Synthetic and Keesler Groundwaters (Anions)

Sample ID # >>>		94-03084	94-03085
Sample ID >>>>		HVS Water	Keesler H2O
pH		7.73	8.22
Flourine	F		
Chlorine	Cl	22	13
Nitrate	NO3	10.7	<0.1
Sulfate	SO4	38	11.2
Organic	C	0.67	4.65
Inorganic	C	7.09	17.5
Total	C	7.76	22.2

Table A12. ICP Data for Apatite Samples

Sample ID # >>>		Detection	94-4580	94-4581	94-4582	94-3090	94-3088	94-3089
Sample ID >>>>		Limit	Florida	N. Carolina	Tribasic	Fish	Shark	Fish
Type or Form of Sample >>>>>			apatite	apatite	CaHPO4	Bits (misc.)	Teeth Sheath	Bone
Aluminum	Al	0.005	7980	2480	35.5	62	268	
Boron	B	0.02	5820	1880		20	727	46
Barium	Ba	0.0005	63.9	42.8	< 3		4	
Calcium	Ca	0.01	364000	359000	392000	168000	313000	205000
Cadmium	Cd	0.001	26.4	50.8	< 6			
Cobalt	Co	0.001				23		
Chromium	Cr	0.002	71	135	20			
Copper	Cu	0.0005						
Iron	Fe	0.005	7600	4420	331	20	40	
Potassium	K	0.2				2000		
Lithium	Li	0.003						
Magnesium	Mg	0.005	1770	2950	2560	2420	2400	3400
Manganese	Mn	0.0005	257	62	15	7	6	8
Sodium	Na	0.05	6770	832	140	2930	10100	3080
Nickel	Ni	0.003						
Phosphorus	P	0.03	160000	140000	177000	85400	160000	105000
Lead	Pb	0.005	< 80	47	< 60		< 28	
Selenium	Se	0.01						
Silicon	Si	0.01	7630	8390	1520	170	6400	250
Tin	Sn	0.015						
Strontium	Sr	0.0005	7390	2430	145	452	1640	530
Titanium	Ti	0.001	418	360	< 6			
Zinc	Zn	0.003	121	362	< 2	76	462	105
Zirconium	Zr	0.001	100	34	< 6			
Dilution Factor			803	638	596	246	393	433

*note: All amounts are in ppm

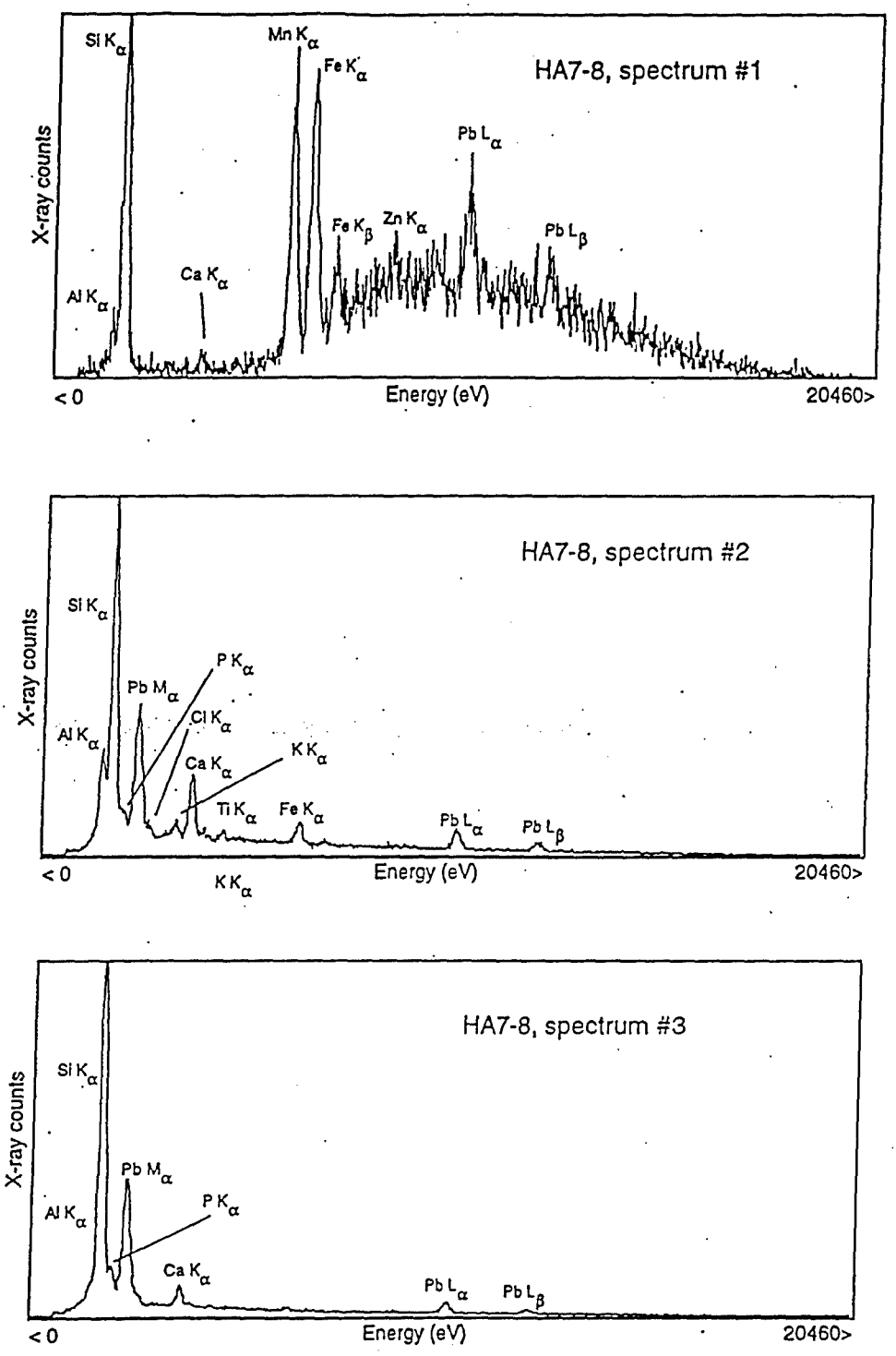

Figure A1. **X-ray Energy Dispersive Spectra for Keesler AFB Soil Sample HA7-8.**

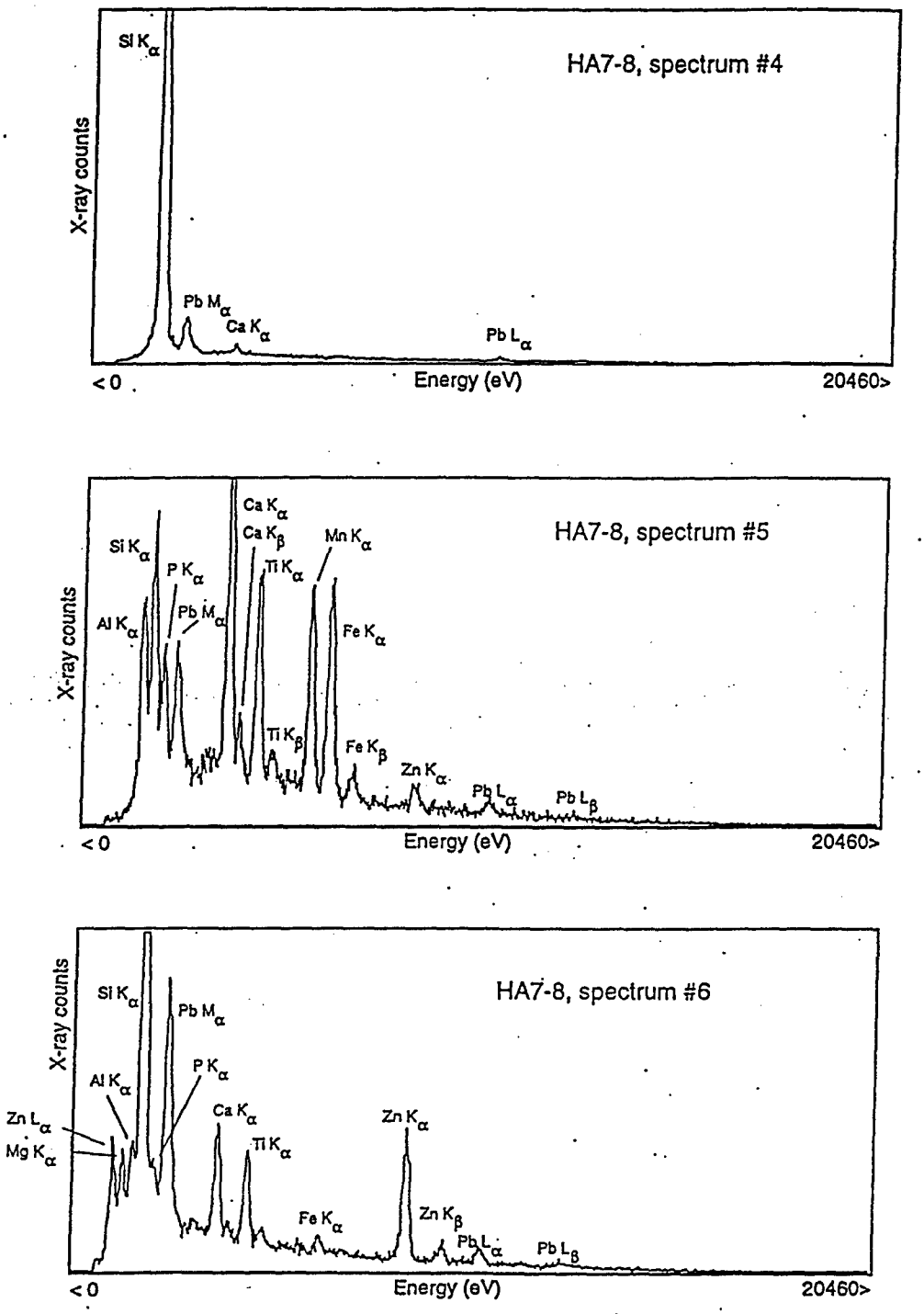

Figure A2. **X-ray Energy Dispersive Spectra for Keesler AFB Soil Sample HA7-8.**

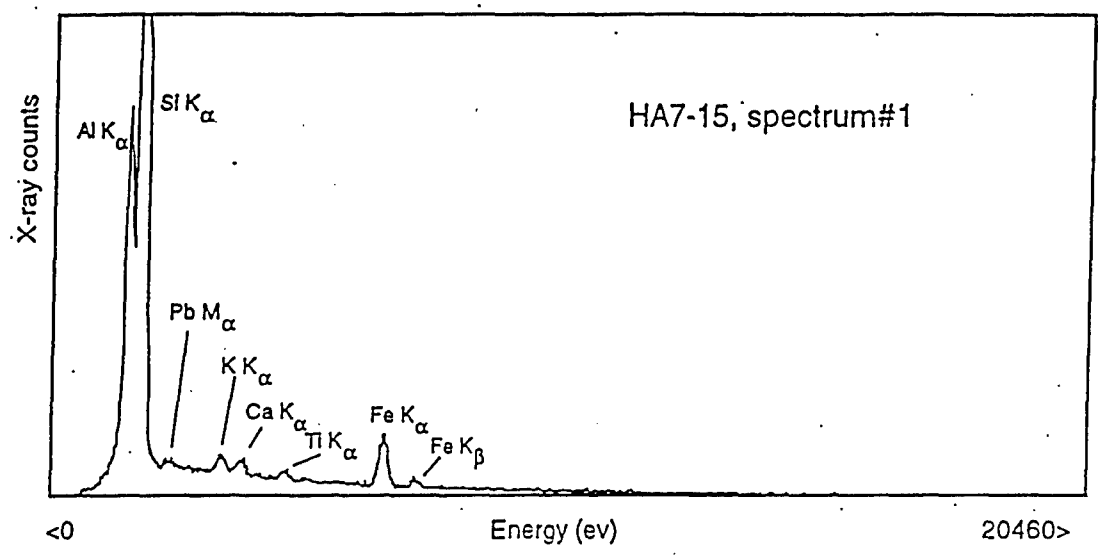

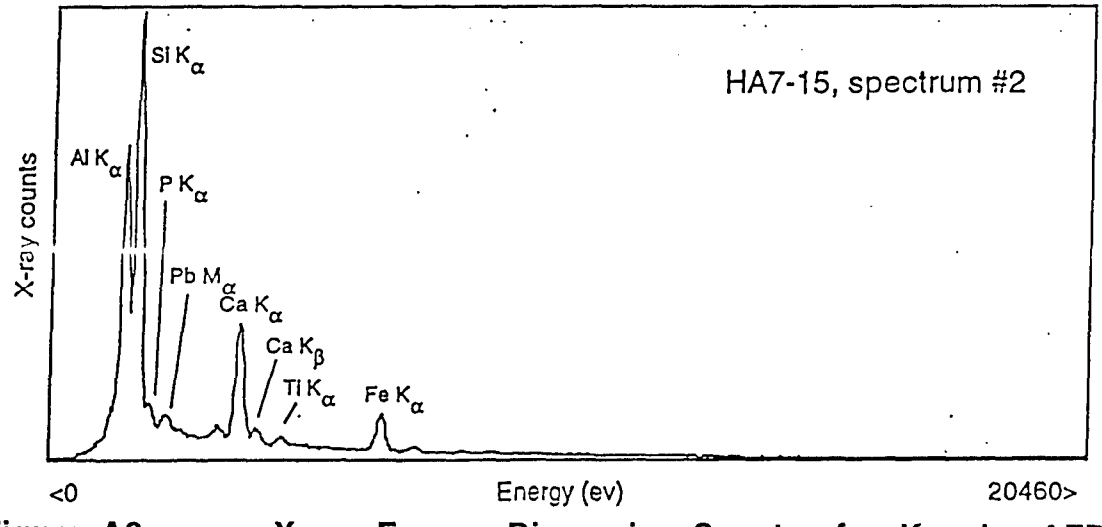

Figure A3. **X-ray Energy Dispersive Spectra for Keesler AFB Soil Sample HA7-15.**

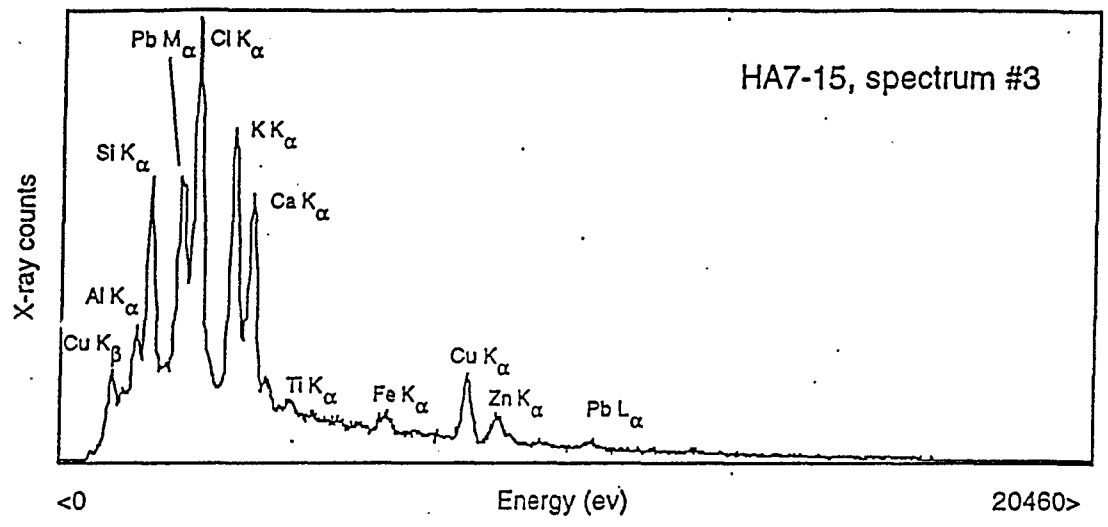

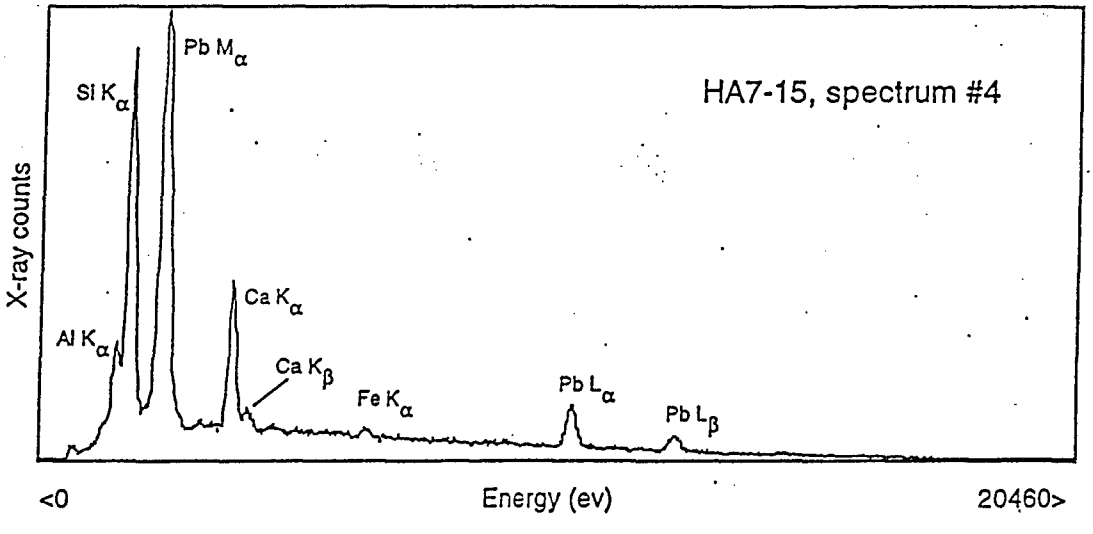

Figure A4. **X-ray Energy Dispersive Spectra for Keesler AFB Soil Sample HA7-15.**

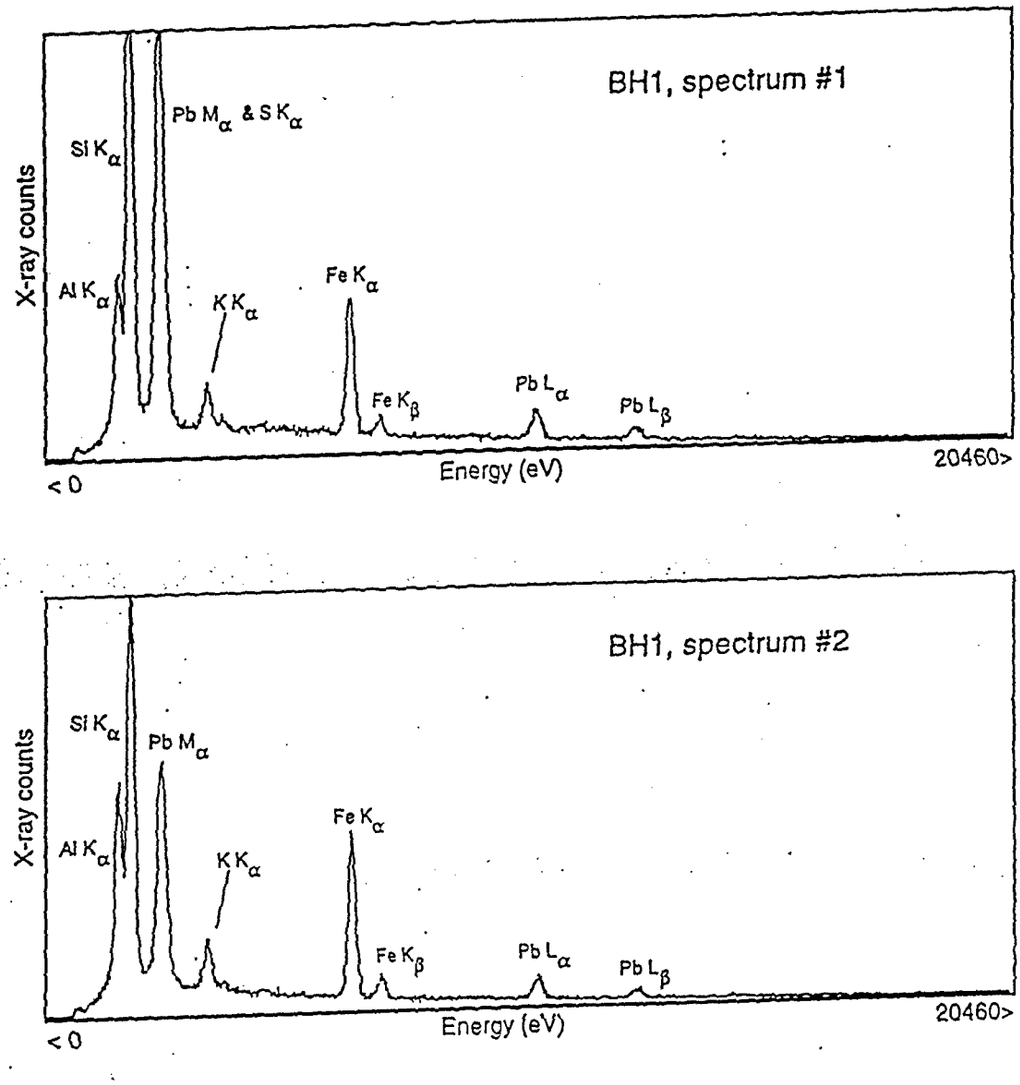

Figure A5. **X-ray Energy Dispersive Spectra *for Bunker Hill 1000* (BH1) mining soil.**

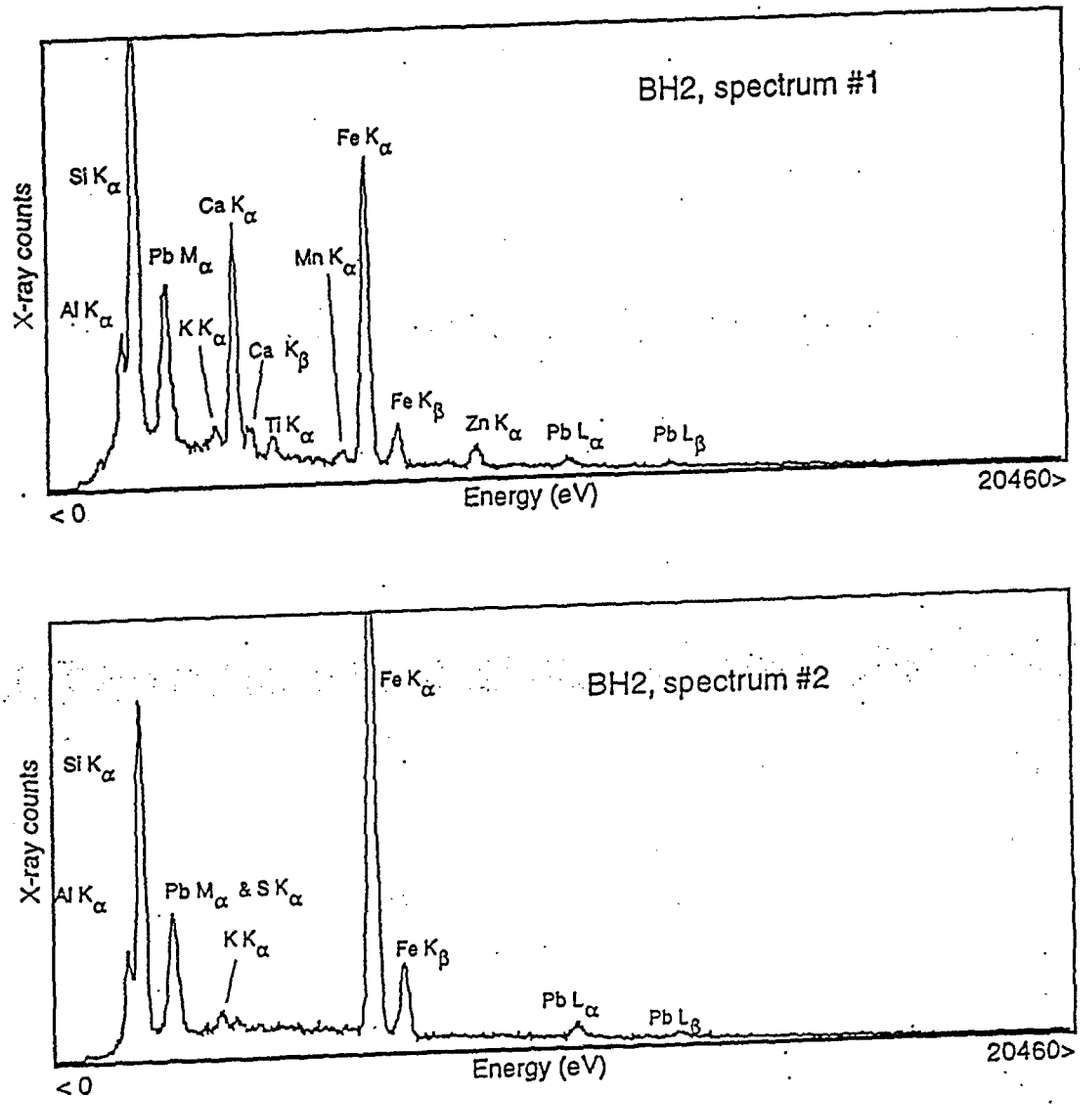

Figure A6. **X-ray Energy Dispersive Spectra for Bunker Hill 1000 (BH1) mining soil.**

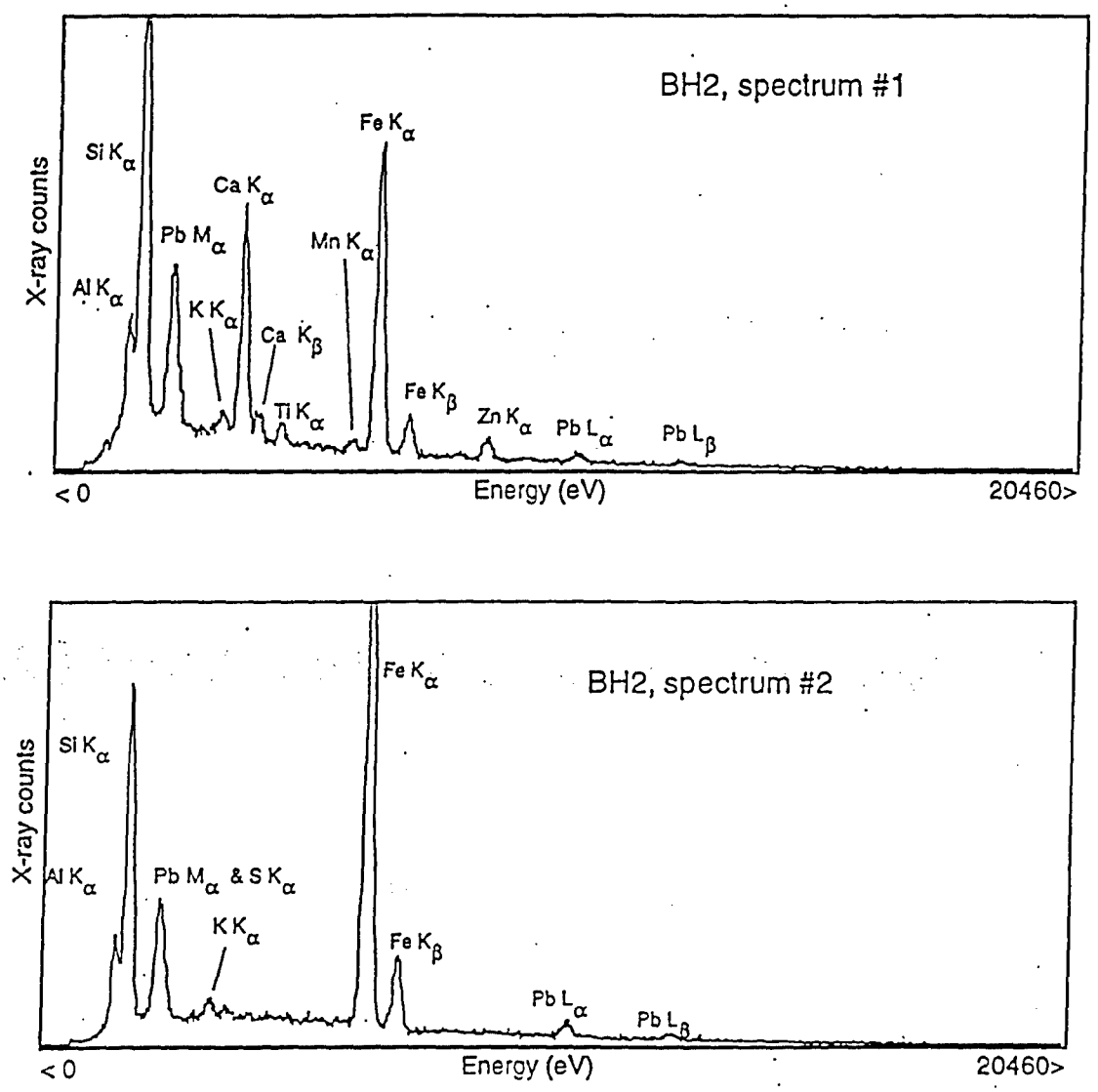

Figure A7. **X-ray Energy Dispersive Spectra for Bunker Hill 2000 (BH2) mining soil.**

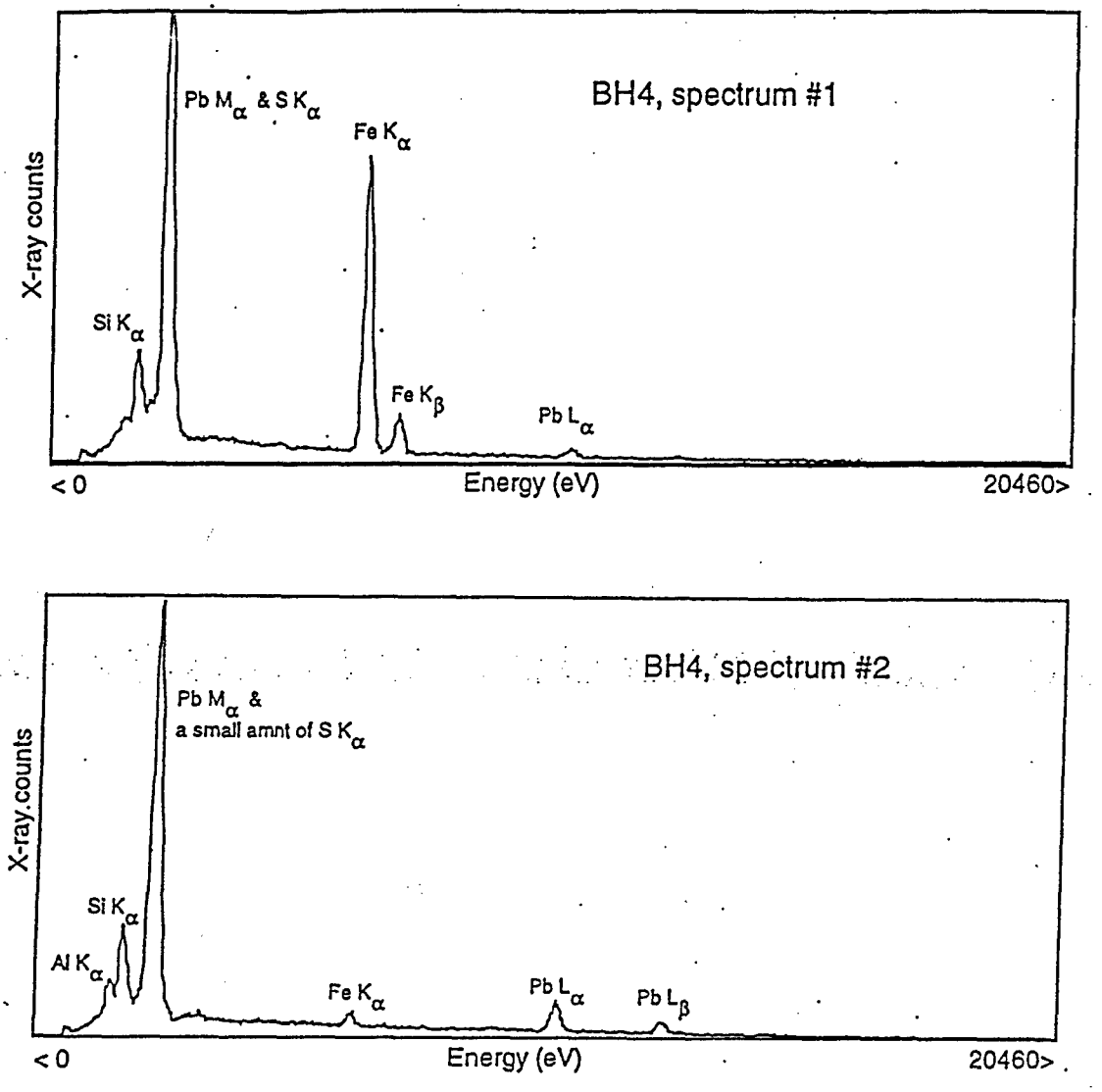

Figure A8. **X-ray Energy Dispersive Spectra for Bunker Hill 2000 (BH2) mining soil.**

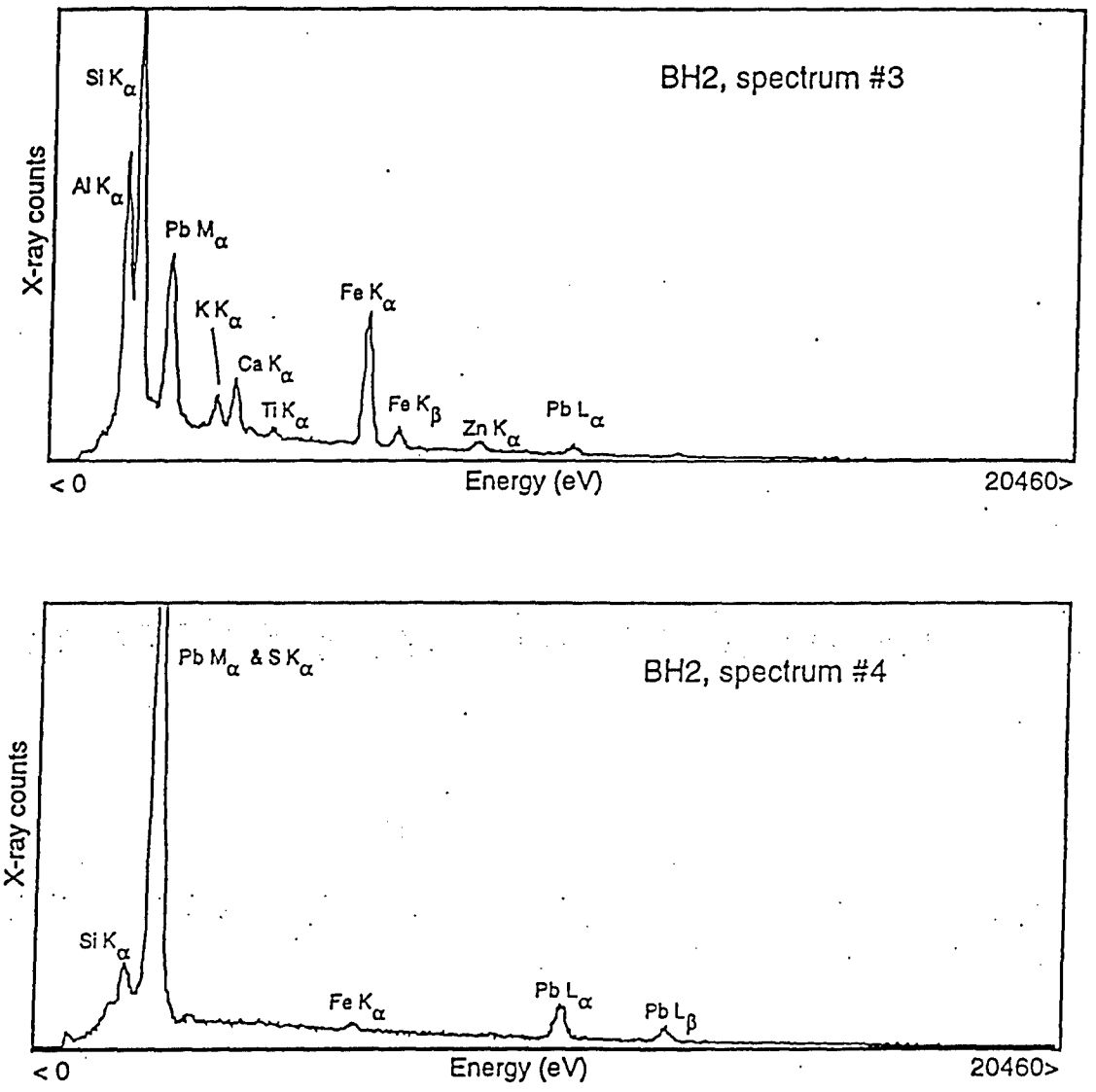

Figure A9. **X-ray Energy Dispersive Spectra for Bunker Hill 4000 (BH4) mining soil.**

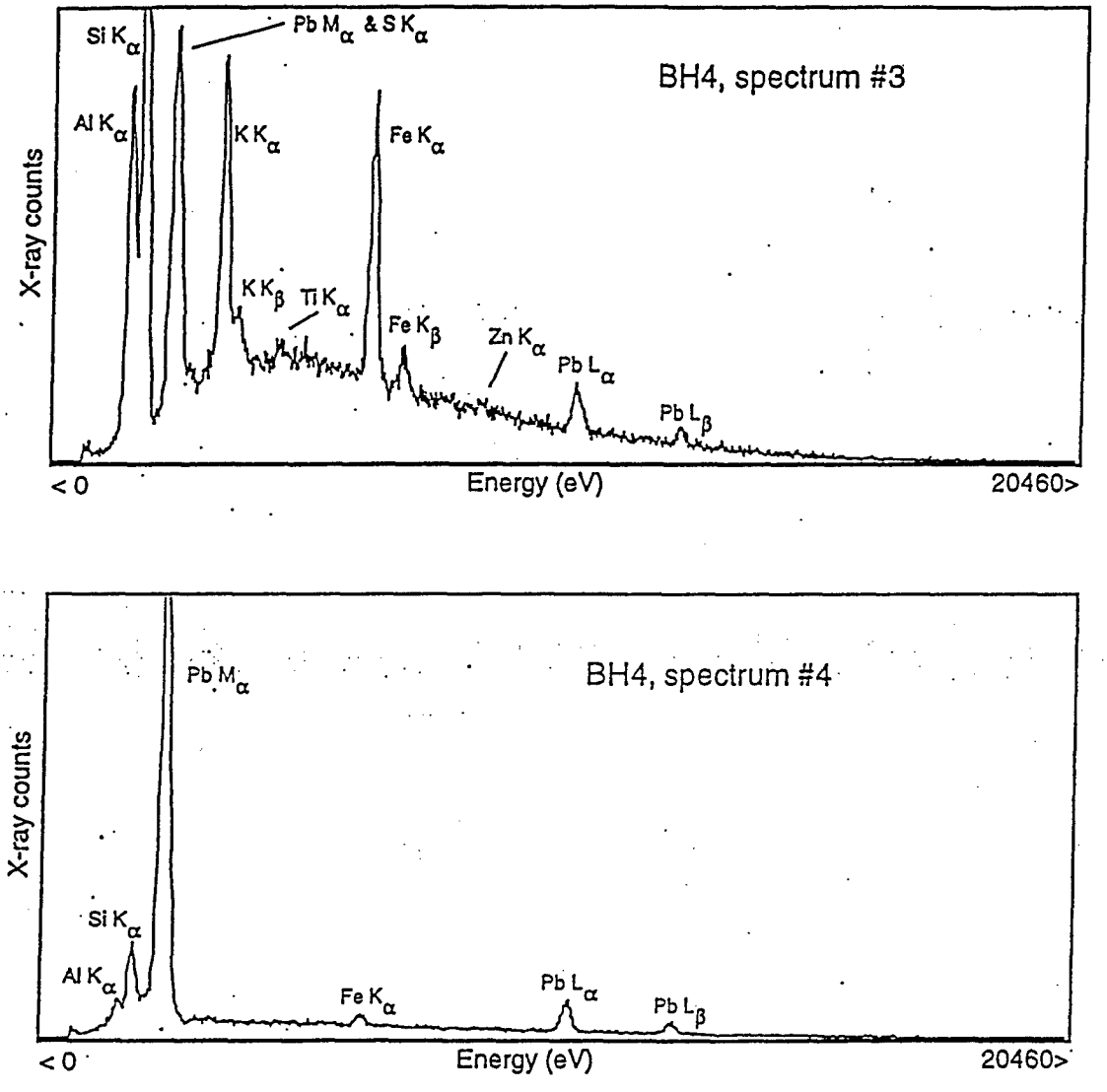

Figure A10. X-ray Energy Dispersive Spectra for Bunker Hill 4000 (BH4) mining soil.

A

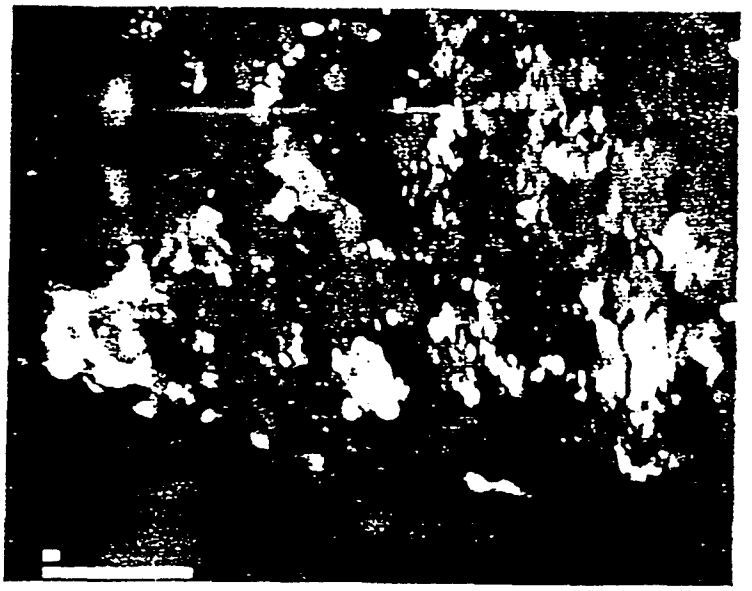

B

Figure A11. Back Scattered Electron (BSE) Photos of Pb-bearing Grains. (A) HA7-8, Spectrum #4. (B) Bunker Hill 2000 (BH2), spectrum #2. The Longer Scale Bar = 10 microns.